AN INVESTIGATION OF HYDRAULIC SELECTION IN ACTIVATED SLUDGE AND ITS EFFECTS ON FLOC CHARACTERISTIC, SETTLING VELOCITY, AND MICROBIAL COMMUNITY

by

Rudy Alexander Maltos

A thesis submitted to the Faculty and the Board of Trustees of the Colorado School of Mines in partial fulfillment of the requirements of the degree of Doctor of Philosophy
(Civil and Environmental Engineering).

Golden, CO

Date: _____

Signed: _____
Rudy A. Maltos

Signed: _____
Dr. Tzahi Y. Cath
Thesis Advisor

Golden, CO

Date: _____

Signed: _____
Dr. Junko Munakata-Marr
Professor and Department Head
Department of Civil and Environmental Engineering

ABSTRACT

Wastewater facilities in urban communities are quickly approaching their maximum treatment capacity due to increased influent wastewater flows. Thus, expansion is needed, but facilities located in urban settings may not have access to additional land for development. The major bottleneck of these traditional facilities tends to be the secondary clarifiers, which often span 100 ft in diameter each, and are responsible for the solid-liquid separation process, allowing the dispersed microbial community known as activated sludge (AS) to separate from the effluent via gravity. The AS that settles to the bottom of the clarifier is then collected and partially returned to the start of the wastewater treatment process, and the effluent is disinfected and released to the environment. If the overflow rate, the vertical flow velocity of water in the clarifier, is higher than the settling velocity of the AS, the AS will not completely separate from the effluent and a fraction escapes to the disinfection basin, leading to higher consumption of chlorine, formation of carcinogenic disinfection byproducts, and a potential discharge permit violation. Lower overflow rate in the secondary clarifier reduces the risk of AS washout, but it also increases the hydraulic retention time and reduces the treatment capacity of the facility.

The settling velocity of the AS (the rate at which the AS separates itself from the effluent) determines the maximum overflow rate of the clarifier; fast settling sludge allows the overflow rate and treatment capacity to increase. However, the majority of wastewater facilities experience slow settling velocity of less than 10 m/h due to the current operation practices of AS treatment trains and the wasting methods used to control AS concentration. Technology such as membrane bioreactors promise to deliver fast and effective physical separation, but would require major capital investments and alterations to the treatment train. In addition, membranes do not resolve the core problem of the AS process, the accumulation of poor settling floc.

Aerobic granular sludge (AGS) is a dense community of microorganisms with an anaerobic core and aerobic outer layer. This unique structure allows denitrifying and phosphorus accumulating organisms to grow in the core while nitrifying and heterotrophic microorganisms thrive on the outer layers, resulting in improved nutrient removal abilities compared to conventional AS. AGS also has enhanced settling characteristics due to its circular shape and high density, settling at a rate between 15 and 60 m/h. However, AGS has not been adopted by wastewater facilities due to an 18 ft reactor height requirement, this height allows for the stratification and separation of slow settling floc.

Thus, the objective of the research described in this dissertation was to develop a new AS wasting system through rapid prototyping and bench scale testing. The developed technology, aka the hydraulic selector, was long-term tested at the pilot scale in sequencing batch reactors, which were able to increase AS settling velocity above 10 m/h and maintain constant nitrification and carbon removal throughout the experiments. Subsequently, the feasibility of developing AGS when combining hydraulic selection technology with traditional wasting practices was tested for 238-days. The effects of the hydraulic selector on the AS microbiome and the communities present in various floc diameter ranges were evaluated over

time using 16S-rRNA gene and 18S-rRNA gene. Abundance of filamentous bacteria, phosphorus accumulating bacteria, ammonia-oxidizing bacteria, and nitrite-oxidizing bacteria were also quantified in both hydraulic selector discharge and AGS. Lastly, computational fluid dynamics were used to quantify and visually express the velocity flow field and separation of poor settling solids under turbulent conditions. This model may influence future selector geometry and selector operation to maximize the removal of poorly settling floc.

TABLE OF CONTENTS

ABSTRACT iii
LIST OF FIGURES ix
LIST OF TABLES xiii
LIST OF ABBREVIATIONS xiv
ACKNOWLEDGEMENTS xv
DEDICATION xvi
CHAPTER 1 INTRODUCTION 1
1.1 Problem statement and significance 1
1.2 Objectives and scope of work 2
1.3 Structure of dissertation 3
1.3.1 Hydraulic selector development and comparison to traditional aerobic granular technology 3
1.3.2 Reducing solid retention time through hydraulic selection for the development of aerobic granular sludge 5
1.3.3 Evaluating the activated sludge microbial community under environmental pressures induced by hydraulic selection and feast/famine conditions 7
1.3.4 The development of a computational fluid dynamic model for the optimization of poor settling floc removal and evaluation of turbulence on floc separation 8
1.4 References 8
CHAPTER 2 ENHANCEMENT OF ACTIVATED SLUDGE WASTEWATER TREAMENT WITH HYDRAUILC SELECTION 11
2.1 Abstract 11
2.2 Introduction 11
2.3 Materials and methods 14
2.3.1 System configuration 14
2.3.2 Hydraulic selector design 15
2.3.3 Influent wastewater characteristics 15
2.3.4 Operating conditions 15
2.3.5 Data acquisition 17
2.3.6 Analytical methods 17
2.3.6.1 Sludge volume index (SVI) 17
2.3.6.2 Chemical analysis 17
2.3.6.3 Floc characterization 17
2.4 Results and discussion 18
2.4.1 AGS development and characteristics 18
2.4.1.1 Sludge settling velocity 20
2.4.1.2 Floc diameter 22

2.4.1.3 Zeta potential 23
2.4.1.4 Phase contrast 24
2.4.2 Nutrient removal 25
2.4.2.1 sCOD removal 26
2.4.2.2 Nitrogen Removal 27
2.4.2.3 Decant biosolids 30
2.5 Conclusion 31
2.6 References 32
CHAPTER 3 REDUCING SOLID RETENTION TIME THROUGH HYDRAULIC SELECTION FOR THE DEVELOPMENT OF AEROBIC GRANULAR SLUDGE 36
3.1 Abstract 36
3.2 Introduction 36
3.3 Material and methods 39
3.3.1 Pilot system configuration and operation 39
3.3.2 Influent wastewater characteristic 41
3.3.3 Hydraulic selector design 43
3.3.4 Data acquisition 43
3.3.5 Analytical methods 44
3.3.6 Floc characterization 44
3.3.6.1 Biomass-based floc diameter distribution 44
3.3.6.2 Volume based floc diameter distribution 44
3.3.6.3 Microscopy 45
3.4 Results and discussion 45
3.4.1 Activated sludge MLSS and SRT 45
3.4.2 Activated sludge settling velocity and hydraulic selector operation 47
3.4.3 Hydraulic selector optimization 51
3.4.4 Floc characteristic of activated sludge and hydraulic selector discharge 53
3.5 Conclusion 58
3.6 References 59
CHAPTER 4 SHIFTS IN ACTIVATED SLUDGE MICROBIOLOGY DUE TO FEAST/FAMINE CONDITIONS AND THE OPERATION OF A HYDRAULIC SELECTOR 62
4.1 Abstract 62
4.2 Introduction 62
4.3 Material and methods 65
4.3.1 Experimental setup and operation 65
4.3.2 Sample collection and physicochemical processing 66
4.3.3 DNA extraction, PCR and 16s/18s rRNA sequencing 67
4.3.4 Abundance analysis 68

4.3.5 Microscopy 68
4.4 Results and discussion 69
4.4.1 The development of AGS, AS settling velocity and hydraulic selector operating conditions 69
4.4.2 Activated sludge floc diameter and biomass distribution 69
4.4.3 Activated sludge imaging and physical transformation over time 71
4.4.4 Nutrient removal 75
4.4.5 Solids removal 78
4.4.6 DNA sequencing 79
4.4.6.1 Eukaryotes 79
4.4.6.2 16 rRNA sequencing 81
4.5 Conclusion 85
4.6 References 85
CHAPTER 5 THE DEVELOPMENT OF THE HYDRAULIC SELECTOR THROUGH COMPUTIONAL FLUID DYNAMICS 90
5.1 Abstract 90
5.2 Introduction 90
5.3 CFD and wastewater modeling 93
5.4 Materials and methods 94
5.4.1 Bioreactor and hydraulic selector geometry 94
5.4.2 Mixed particles simulation 94
5.4.3 Multiphase model 96
5.4.4 Viscous modeling 96
5.4.5 Mesh independence 97
5.4.6 Simulation setup - mixing, settling, and hydraulic selector operation ... 102
5.4.7 Boundary conditions 102
5.4.8 Experimental setup 102
5.5 Results and discussion 104
5.5.1 Bench scale result – particle distribution 104
5.5.2 Mixing and settling simulation 106
5.5.3 Hydraulic selector results 111
5.6 Conclusion 114
5.7 References 115
CHAPTER 6 CONCLUSION 118
6.1 Research synopsis 118
6.1.1 Enhancement of activated sludge wastewater treatment with hydraulic selection 118

6.1.2 Reducing solids retention time through hydraulic selection for the development of aerobic granular sludge 118
6.1.3 Shifts in activated sludge microbiology due to feast/famine conditions and the operations of a hydraulic selector 119
6.1.4 Development of the hydraulic selector through computational fluid dynamics 119
6.2 Future work 120
APPENDIX A 121

LIST OF FIGURES

Figure 1.1 A schematic of the hydraulic selector placed in a bioreactor. At an outflow of 1 L/min the velocity gradient developed around the selector removes a higher percentage of low-density floc. At an outflow of 3 L/min the velocity gradient developed by the selector is higher and higher density floc are removed 4

Figure 2.1 A schematic of the hydraulic selector placed in a bioreactor. At an outflow of 1 L/min the velocity gradient developed around the selector removes a higher percentage of low-density floc. At an outflow of 3 L/min the velocity gradient developed by the selector is higher and higher density floc are removed 13

Figure 2.2 A schematic of the pilot system. Raw wastewater was diverted from an on-campus student apartment complex and activated sludge from an onsite SBMBR was used as seed sludge for the bioreactor 14

Figure 2.3 A) mixed liquor suspended solids (MLSS) and biosolids removed by the hydraulic selector and B) sludge volume index (SVI) at 4 and 30 minutes. Changes in selector operating flow rates are shown in Figure 3 as a vertical line 18

Figure 2.4 AS settling velocities (orange), selector's entrance velocity (red), and minimum settling velocity (green) was measured or calcuated over the study period. Changes in selector outflow rate are identified by vertical lines. 21

Figure 2.5 Volume based cumulative distribution of AS floc diameter over the duration of the experiment. The mean floc diameter of the seed AS (day 0) was less than 62 µm. 22

Figure 2.6 Zeta potential measurements of the AS for 98 days of the experiment. The seed AS was highly negative resulting in repulsive electrostatic integration and poor settleability. With the production of positively charged EPS the zeta potential becomes more positive and settleability is improved. 23

Figure 2.7 Phase contrast photos of AS, pictures A, B, C, D, and H are gram stained, E, F and G are live samples 24

Figure 2.8 Influent sCOD and ammonia measured over the 120-day experiment. 25

Figure 2.9 Influent and effluent sCOD and percent sCOD removal measured over the 120-day experiment. 26

Figure 2.10 A) influent and effluent ammonia concentration and percent ammonia removal and B) influent sCOD and effluent nitrate concentration measured during the experiment 28

Figure 2.11 Online dissolved oxygen, ammonia, and nitrate probe data from a single fill, mix, and aeration phase cycle. 29

Figure 2.12 Bioreactor effluent (decant) TSS measured over the 120-day the experiment. .. 30

Figure 3.1 AS wasting conditions for SRT control..... 39

Figure 3.2 A flow diagram of the experimental system 40

Figure 3.3 A schematic of the hydraulic selector, all units are in centimeters. 41

Figure 3.4 Mixed liquor suspended solids (MLSS) and solid retention time (SRT) in the bioreactors as a function of time. 45

Figure 3.5 AS settling velocities for BR1 (no hydraulic selector), BR2 (traditional wasting and hydraulic selector), and BR3 (only hydraulic selector) over the study period. 48

Figure 3.6 A) Sludge volume index 30 and B) sludge volume index 5 for BR1 (blue diamonds), BR2 (red squares), and BR3 (green triangles) as a function of time over the duration of the study. 50

Figure 3.7 Optimizing HS operation for the removal of poor settling floc for BR3 on day 7 and day 43 by comparing the volume percentage floc diameter distribution of various HS operating conditions 52

Figure 3.8 Mean floc diameter of AS from BRs 1-3 as a function of time, measured via volume-based floc diameter distribution. Each sample was measured 3-5 times. 54

Figure 3.9 A) BR2 and B) BR3, AS MFD (blue diamonds), hydraulic selector discharge MFD (orange squares) and activated sludge settling velocity (green triangles) as a function of time over the duration of the study. 56

Figure 3.10 Phase contrast images of the AS from BRs 1-3 on days 14 and 130. Images take on day 14 used a 100x magnification and floc were outlined in red through ImageJ software. Images taken on day 130 used 40X magnification. 57

Figure 4.1 Biological sampling protocol for the three 66

Figure 4.2 AS settling velocity of the three BRs, as indicated by the blue diamonds, red squares, or green triangles, respectively. 69

Figure 4.3 Activated sludge floc diameter biomass distribution, separated into five floc diameter categories (A) Seed sludge from Denver Metro, (B) BRs 1-3 on day 105, and (C) BRs 1-3 on day 210. 70

Figure 4.4 Phase contrast images at 100x magnification of the Denver Metro Wastewater seed floc and activated sludge of BR 1-3 from day 14 to 41. 72

Figure 4.5 Phase contrast images of BR 1-3 at 40X magnification on days 59, 99, 124, 159, and 195 74

Figure 4.6 On day 224 floc >250 µm for BR2 and BR3 was suspended in DI water. Photos were taken using a Sony Alpha 6000, with a 16-50 mm zoom lens and 16 mm tube extender 75

Figure 4.7 A) influent sCOD and COD concentration (mg/L) as a function of time and B) effluent sCOD concentrations (mg/L) as a function of time. 76

Figure 4.8 A) Influent ammonia and BRs 1-3 effluent ammonia B) Effluent nitrate for BRs 1-3 and maximum nitrate concentration based on influent ammonia concentration 77

Figure 4.9 Influent and BRs effluent orthophosphate concentration over the duration of the study. 78

Figure 4.10 BR1 had a total of 10 decant TSS measurements while BR2 and BR3 had online TSS probes. 79

Figure 4.11 Heatmaps of the following eukaryotes: (A) Epistylis, (B) Telotrochidium, (C) Rhogostoma, (D) LKM11, and (E) Diplogasterida over the duration of the study. 81

Figure 4.12 Percentage of relative abundance of filamentous bacteria, PAOs, AOBs, and NOBs for BR2, BR2 hydraulic selector (S2), BR3, and BR3 hydraulic selector (S3). 82

Figure 4.13 Percentage of relative abundance of filamentous bacteria, PAOs, AOBs, and NOBs for BRs 1-3 on days 150 and 205 separated into four floc diameter categories, <250 µm, 250-500 µm, 500-1000 µm, and >1000 µm. 84

Figure 5.1 A secondary clarifier, traditional activated sludge (AS) wasting only occurs from the bottom of the clarifier, resulting in elimination of dense floc and accumulation of poor settling floc. 92

Figure 5.2 The selection process used for tradition AGS development. 92

Figure 5.3 (A) Reactor dimensions used in both CFD simulation and bench-scale experiments (B) The hydraulic selector dimensions, the same selector was used in both CFD simulation and bench-scale experiments, all units are in cm. 94

Figure 5.4 Three lines from each XY and YZ planes were used for mesh independence. .. 98

Figure 5.5 A tetrahedral structured mesh with the reactor water shown in gray and selector water in brown. (A) a sliced image of the reactor and selector, and (B) a zoomed in image of the selector 98

Figure 5.6 Water velocity profiles on the XY plane for Meshes 1-4 for the (A) Left, (B) Center, and (C) Right lines. 100

Figure 5.7 A) XY planes at three locations along the z-axis labeled top, middle, and bottom. (B) ZY planes with three locations along the x-axis labeled, positive, center, and negative. 101

Figure 5.8 The experimental setup, experiments were conducted at the Mines Park laboratory. 103

Figure 5.9 Particle distribution for bench scale experiments 104

Figure 5.10 Water velocity contours of the reactor and selector water. 107

Figure 5.11 Turbulent kinetic energy of water, contours on the left are slices from the ZY plane and contours on the right are slices from the XZ plane. 108

Figure 5.12 Volume fraction contours in the XZ and ZY planes 109

Figure 5.13 The average volume fraction of the 60 µm, 120 µm, and 220 µm particles after A) mixing and B) after settling 110

Figure 5.14 Velocity contours of the reactor and selector water on the XZ and YZ planes after operating the hydraulic selector at 2 L/min for 10 seconds 111

Figure 5.15 (A) The eddy viscosity and (B) the turbulent kinetic energy in the YZ plane after 10 second of hydraulic selector discharge at 2 L/min 112

Figure 5.16 Volume fraction distribution across XZ and YZ planes after operating the hydraulic selector at 2 L/min for 10 seconds 113

Figure 5.17 The distribution of the particle mass in the reactor after 10 second of selector operation at 2 L/min. The reactor water was split into three regions bottom, middle and top, each region approximately 1/3 of the reactor volume. 113

Figure 5.18 The particle composition for all hydraulic selector discharges (0.5, 1, and 2 L/min) after 10 second of operation. 114

LIST OF TABLES

Table 2.1 Average influent wastewater characteristics and concentrations 15

Table 2.2 Operation phase of the bioreactor during Stage 1,2, and 3 16

Table 3.1 The calculated F/M values of the BRs based on influent sCOD and BR MLVSS. Green highlighted cells represent F/M within the 0.1-0.2 range and red cell represent F/M values above or below the specified range 42

Table 3.2 Average influent wastewater parameters from the mixing tank (before carbon dosing) and PC decant (after carbon dosing) 42

Table 3.3 List of the four HS optimization scenarios tested on BR3 for day 42 52

Table 4.1 The study was conducted over five stages for a total of 238 days. Each stage had a unique HS operating condition, described by the settling time (prior to the hydraulic selection process) and hydraulic selector outflow. 65

Table 4.2 The operation of the three BRs was composed of 5 or 7 phases. Total cycle time was approximately 325 min and all BRs operated with a 30% exchange ratio ... 66

Table 4.3 PCR thermocycling conditions, a total of 22 cycles were required 67

Table 5.1 The particle diameter percentiles from a study conducted in Chapter 3, on day 42. Orange cells represent slow settling floc, yellow cells medium settling floc, and green cells fast settling floc 95

Table 5.2 A description of the particle characteristics and the volume fraction distribution used in the CFD model and bench scale experiments. 96

Table 5.3 Four meshes were developed and simulated. Each mesh varied in quantity of elements and quality of mesh. Mesh quality was determined by the element quality, aspect ratio and skewness 99

Table 5.4 Comparing water velocity profiles for meshes 1-4, on lines across the XY plane (left, center, and right) 100

Table 5.5 Comparing average volume fraction distribution for meshes 1-4, on various XY (top, middle, and bottom) and ZY (positive, center, negative) planes. 101

Table 5.6 Operating conditions of experiments. Settling time and hydraulic selector outflows were varied and effected the minimum settling velocity and total operation time 104

LIST OF ABBREVIATIONS

AGS	Aerobic granular sludge
AOB	Ammonia oxidizing bacteria
AS	Activated sludge
BR	Bioreactor
CAS	Conventional activated sludge
CFD	Computational fluid dynamics
COD	Chemical oxygen demand
EPS	Extracellular polymeric substance
F/M	Food to microorganism ratio
HRT	Hydraulic retention time
HS	Hydraulic selector
MFD	Mean floc diameter
MLSS	Mixed liquor suspended solids
MLVSS	Mixed liquor volatile suspended solids
N	Nitrogen
NOB	Nitrite oxidizing bacteria
OF	Outflow
P	Phosphorus
PAO	Phosphorus accumulating organisms
pCOD	particulate chemical oxygen demand
RAS	Return activated sludge
sCOD	Soluble chemical oxygen demand
SBR	Sequencing batch reactor
SND	Simultaneously nitrifying and denitrifying
SRT	Solid retention time
ST	Settling time
SVI	Sludge volume index
tCOD	total chemical oxygen demand
TKE	Turbulent kinetic energy
TSS	Total suspend solids
WRRFs	Water resource reclamation facilities

ACKNOWLEDGEMENTS

I would like to thank the National Science Foundation (NSF), specifically the engineering research center (ERC), Reinventing the Nation's Water Infrastructure (ReNUWIt) (NSF EEC-1028968) and the Colorado Higher Education Competitive Research Authority for funding and supporting my research and education at the Colorado School of Mines (Mines). I would also thank the Rocky Mountain section of the American Water Works Association (AWWA), WaterReuse Colorado, and the Edna Bailey Sussman Fund for their financial support in my research on improving solid/liquid separation process in activated sludge. I would also like to thank Kennedy Jenks Consultants for providing me technical support critical to the research of this dissertation.

I would like to thank my committee members: Dr. Gregory Bogin, Dr. Junko Munakata Marr, and Dr. John Spear, for their inspiration, patience, and guidance. Completion of this doctoral dissertation was made possible by my advisor Dr. Tzahi Cath and my mentor Dr. Ryan Holloway. Tzahi often found himself busy every hour of the day, but he always found time to visit me in the lab and always had time to review all my presentations and reports. Thank you Tzahi, for when I had doubt in myself you gave me courage and strength.

This dissertation is product of the community I found myself in at Mines. Thank you to Kate Newhart, Tayler Elwell, Mike Verse, and Tani Cath for the support you provided that kept the Mines Park Lab operational. Thank you to Kate Spangler, Nate Rothe, Estefani Bustos, Gary Vanzin, Johan Vanneste, Hooman Vatankhah, and Conner Murray for your technical expertise and friendship. Thank you to Sierra Fox, Miles, and Lux who always provided me a home away from away from home.

To my family, who always provided me with a strong foundation of love and support, thank you. Thank you, dad, mom, Cynthia, Yasmine, Adrian, Gus, Marcos, Jasmine, and to all my nieces and nephews. Being far from home was always difficult, thank you for giving me the strength to complete this long adventure. I hope I continue to make you proud.

DEDICATION

I would like to dedicate this work to Ryan Holloway, my mentor, research “father”, and friend. I met Ryan as an undergraduate student, at a time in my life when I was deciding to continue onto graduate school or pursue a career in consulting. Prior to meeting Ryan, I had worked in a modeling research lab; and while the work was interesting, I wanted to do applied research in a wet lab setting. For my junior summer I applied and was accepted into a National Science Foundation (NSF) research experience for undergraduate (REU) program sponsor by the Engineering Research Center (ERC) Reinventing the Urban Water Infrastructure (ReNUWIt). Being a first-generation Hispanic, I always felt out of place in academic settings; I was nervous and timid, and research seemed formal and had its own culture that I didn’t quite understand.

Ryan was assigned as my REU mentor at the Colorado School of Mines (Mines), and immediately upon my arrival, Ryan made me feel at home: he gave me a tour of the labs and introduced me to his colleagues, as if I was another graduate student. I soon realized that Ryan had befriended all his lab mates and research community. For Ryan, research did not require formalities, it was an opportunity to explore, discover, and ask question without fear. Ryan was always open about his mistakes, which removed my concerns of failure and allowed me to gain confidence in the lab. Ryan asked what type of research I was interested in and gave me the opportunity to work in a wet lab and eventually trusted me enough to conduct my own experiments. After the summer at Mines and seeing Ryan’s approach to research and community building, I felt confident and excited to apply to graduate school.

Ryan and I remained in contact, and a year later Ryan completed his PhD and I returned Mines to begin graduate school. As I completed my master’s work, Ryan approached me with a research idea that would eventually become the core of this dissertation. Ryan and I spoked several times a week about the development of the hydraulic selector technology, and soon after we began working on the hydraulic selector, Ryan was diagnosed with Stage 4 colon cancer. Ryan underwent many treatments, including years of chemotherapy, radiation, and many surgeries. Ryan was blessed to have his amazing wife and daughter always by his side. I expected Ryan to withdraw and become less involved in the research, but this never was the case, Ryan never missed a meeting, and was always there to provide me guidance. Ryan challenged me to become a better engineering and was essential for this entire dissertation.

After a four-year battle with cancer, Ryan passed away in the early morning on December 16, 2020. Ryan forever changed my life, he believed in me when I had so much self-doubt, and most important he showed me what a community of friends and scientist could achieve. With such a community, the definition of work becomes obscure, and it turns into a journey, or an adventure where we try to make each other and the world a better place, one small improvement at a time. This community continues to mourn the loss of our friend Ryan but we’re still here and we will continue to inspire the next generation of students, scientists, and engineers.

CHAPTER 1
INTRODUCTION

Conventional activated sludge (CAS) is a simple, robust, and low-cost wastewater treatment technology. Because of the operational and cost benefits of CAS, it is used by approximately 75% of water resource reclamation facilities (WRRFs) in the United States [1,2]. CAS systems are a critical component in wastewater treatment infrastructure, but additional improvements to the process are needed (e.g., nutrient removal, contaminants of emerging concern removal, and physical footprint reduction) to accommodate population growth and meet more stringent effluent discharge requirements. It is estimated that by 2032, 56 million additional customers (23% increase) will be using these WRRFs [3], many of which are already near their maximum treatment capacity. To serve these new customers, the US Environmental Protection Agency has estimated that $271B are needed to upgrade the existing wastewater infrastructure over the next 20 years [3].

1.1 Problem statement and significance

CAS systems are comprised of a bioreactor containing aerobic zones for biological removal of organic matter and nutrients, and a clarifier for physical solid-liquid separation. A portion of the activated sludge (AS) from the bottom of the clarifier is returned to the bioreactor and the remaining is wasted (commonly treated by anaerobic digestion). Clarifiers with poorly settling activated sludge usually have tall sludge blankets with lower biomass concentrations, resulting in higher return activated sludge (RAS) pumping rates, activated sludge with a higher water content pumped to the digesters, and higher suspended solids concentrations in the clarifier supernatant (effluent). Poorly settling activated sludge is characterized by a slow settling velocity—less than 5 m/h—and high sludge volume index at 30 minutes (SVI_{30}), commonly above 250 mL/g. To manage poorly settling activated sludge, the surface overflow rate (SOR) in the clarifier must be reduced, thus increasing the hydraulic retention time (HRT) in the WRRF [4] and requiring larger plant footprint. To eliminate the 'bottleneck' at WRRFs, expensive construction of additional clarifiers would be required, but may not be possible for landlocked treatment plants with no space for expansion. Yet, additional clarifiers do not resolve the core problem – accumulation of poorly settling activated sludge. Another solution might be the replacement of clarifiers with microfiltration or ultrafiltration membranes or retrofitting the entire CAS system with membrane bioreactors. However, this is an expensive undertaking that increases both the capital and operational costs of WRRFs.

WRRFs prefer to expand the life of current secondary clarifier infrastructure. This would require a reduced SVI. SVI is directly related to the secondary clarifier capacity; a 25% reduction in SVI is capable of increasing clarifier capacity, specifically surface overflow rate, by 50-75%, potentially eliminating the need for expansion. To improve sludge settleability and reduce SVI, a substantial change to sludge morphology and density would be required. This activated sludge transformation may be induced by hydraulic selection, defined as selectively removing unwanted floc (<100 µm) from a bioreactor by means

of hydrodynamic forces. Hydraulic selection in the secondary clarifier or bioreactor would increase the mean floc diameter of the activated sludge, thus, improve SVI and reduce the need for WRRF expansion.

1.2 Objectives and scope of work

The main goal of the study presented here is to demonstrate the feasibility and increase the efficiency of a newly developed hydraulic selection process, resulting in the removal of poorly settling floc with a diameter smaller than 100 µm and leading to the development of aerobic granules, regardless of reactor depth. The objectives that must be met to achieve this goal are as follows:

Objective I: Develop hydraulic selector technology through rapid prototyping and bench-scale testing. Operate the hydraulic selector in a long-term, pilot-scale, batch reactor experiment and ensure nitrification and carbon removal is consistent throughout the experiment. The success of the experiment will be evaluated through the improvements of sludge settling velocity measurements and nutrient removal percentage.

Objective II: Determine the feasibility of developing aerobic granular sludge when combining hydraulic selection with the traditional wasting mechanisms. Operate the hydraulic selector so that only 25-50% of the waste activated sludge is removed via the selector and the remaining waste activated sludge is discharged from the bottom of the bioreactor. Solid retention time (SRT) and food to microorganism ratio (F/M) will be maintained between 10 to 15 days and 0.10-0.20 gCOD/gVSS-d, respectively, to replicate typical CAS operating parameters. Periodically evaluate the hydraulic selector operation by comparing the floc diameter distribution of the activated sludge removed via the selector versus the activated sludge retained in the bioreactor.

Objective III: Evaluate how environmental stress induced by the hydraulic selector operation affects the activated sludge microbiome over time. Determine what microbial communities are selected for and removed by the hydraulic selector and how the remaining activated sludge community changes over time. Operate a bioreactor with and without hydraulic selection, collect samples of the activated sludge and selector discharge over time.

Objective IV: Quantify and visually express the velocity flow field and separation of poorly settling solids induced by the hydraulic selector through the development of a computational fluid dynamic model. Use a multiphase CFD model to influence the selector operation to maximize the removal of poor settling floc from the activated sludge.

1.3 Structure of dissertation

This dissertation builds, expands, and improves on the previous bench, pilot, and full-scale AGS research conducted by various researchers around the world. However, nearly all research efforts have focused on the impacts that influent wastewater characteristics and bioreactor operations have on AGS development – very few efforts have investigated how the selection process enables or enhances aerobic sludge granulation formation. Currently, the traditional selection process is dependent on reactor height and relies on the separation of floc according to their terminal velocity. The traditional selection process has not been widely adopted by WRRFs due to the reactor height requirements. Alternatively, hydrocyclones, used in the mining industry for particle separation in air and in slurries, have recently been adopted for the removal of poorly settling floc in AS. Hydrocyclones may be an effective selection process that can easily be integrated into current WRRFs infrastructure and are currently being tested at full-scale WRRFs. However, the main concern in hydrocyclone operation is the high shear force induced on the AS, which may lead to the deterioration of AGS. An alternate selection process was developed at the Colorado School of Mines to further study how the various degrees of environmental stress induced by hydraulic selection affect activated sludge settling characteristic and nutrient removal abilities. This dissertation is a collection of two journal articles and two manuscripts that are in preparation for submission that describe the different experiments, analyses, and models that were developed to analyze the hydraulic selector for the development of AGS. Chapter 2 is hydraulic selector proof of concept and comparison to traditional AGS technology that was published in the journal *Separation and Purification Technology* and is reprinted here (not requiring copyright permission). Chapter 3 is a manuscript that explores the possibilities of combining the hydraulic selector with traditional activated sludge wasting while maintaining a solid retention time <15 d and evaluates the effects on sludge settleability; results were submitted for publication in the journal *Separation and Purification Technology.* Chapter 4 quantifies and evaluates the impacts of the stress induced by hydraulic selection on the activated sludge microbial communities that remain in the bioreactor and compares microbiome diversity to a bioreactor operating with identical conditions without the hydraulic selector technology. Results from Chapter 4 are in preparation for submission to the journal *Frontiers in Microbiology.* Chapter 5 investigates the benefits of developing a computational fluid dynamic model that can calculate the hydraulic selector's sphere of influence and predicts the selector's ability to separate poorly settling floc across various scenarios such as sludge characteristics and sludge settling time prior to selector operation. This model may serve as a foothold for future full-scale simulations that would like to reduce the need for long term bench-scale experiments.

1.3.1 Hydraulic selector development and comparison to traditional aerobic granular technology

Improved activated sludge settling and secondary clarifier performance can be achieved by hydraulically selecting for and eliminating biosolids with poor settling properties. Hydraulic selection is defined as selectively removing unwanted floc from a bioreactor by means of hydrodynamic forces. A relatively new technology that implements hydraulic selection is AGS systems [5–8]. An AGS reactor is

commonly a batch process and operates like a sequencing batch reactor (SBR); while an SBR has fill, mix, aeration, settling, and decant phases, an AGS cycle is simply comprised of three phases, fill/decant, aeration, and settling. The development of AGS is attributed to both a feast/famine feeding regime and physical selection process. The feast occurs during the anaerobic phase when high substrate uptake is high, and famine follows during the aerobic phase when substrate concentration in the bioreactor is low. In the famine phase the microorganisms use their internal stored substrate to produce extracellular polymeric substance, allowing granulation to occur [9,10]. The selection process occurs through the stratification of activated sludge —this typically requires a reactor height of 5.5 m for full-scale systems or a depth-to-width (D:W) ratio higher than 2.5 for bench-scale systems. This specific height facilitates the stratification of fast and slow settling floc in the settling phase; in the decant/fill phase the slow settling floc are removed through the decant and fast settling floc accumulate and grow in the bioreactor. The selection process is further improved by decreasing the settling period before the decant phase over several months, thus increasing the settling velocity of the remaining floc. These systems are effective in producing fast settling granular sludge (ranging from 15 to 60 m/h), with an SVI_{30} below 60 mL/g, and an average floc diameter and density higher than 200 µm and 1.1 g/mL, respectively [8,11–14]. AGS systems have demonstrated improved wastewater treatment, but full-scale reactors must have a depth greater than 5.5 m and the start-up times are as long as 12 months [11,15]. The enhancement of solid settling is advantageous for all WRRFs, but the required expensive capital improvements make it difficult to be implemented. Thus, a technology that can be easily integrated into current CAS and SBR infrastructure and can achieve improved activated sludge settleability is needed. The selection and removal of poorly settling floc can be accomplished through the decanting of water containing the floc from the clarifier using a hydraulic selector device (Figure 1.1).

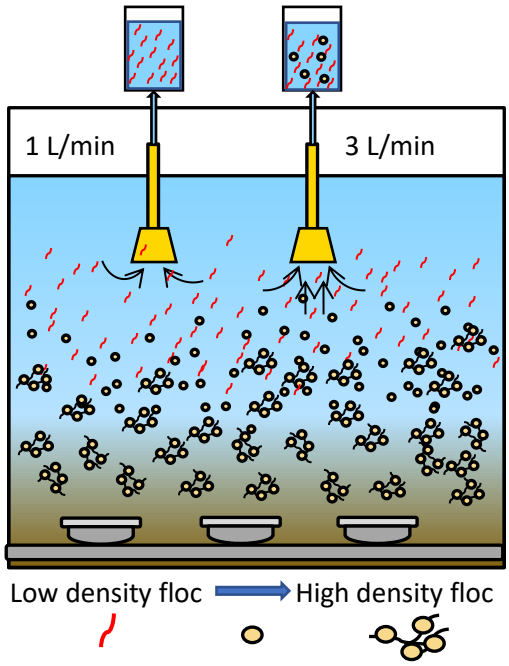

Figure 1.1 A schematic of the hydraulic selector placed in a bioreactor. At an outflow of 1 L/min the velocity

gradient developed around the selector removes a higher percentage of low-density floc. At an outflow of 3 L/min the velocity gradient developed by the selector is higher and higher density floc are removed.

The selector—a trough-like device—is placed in the bioreactor at an optimized depth below the water surface and at the level where poorly settling floc are at the highest concentration. By pumping water through the selector, a localized flow field develops ("selection pressure") that pulls poorly settling flocs from the supernatant. By changing the flowrate through the selector, the radius of influence can be increased or decreased. At lower flow rates the lighter flocs (having slower-settling velocities) are pulled into the hydraulic selector, and heavier flocs (having faster settling velocities) can escape the selector and are retained in the bioreactor.

The main objective of Chapter 2 was to investigate the performance and effectiveness of the hydraulic selector using a lab-scale SBR and compare the technology to a traditional AGS bench-scale reactor. Specifically, the chapter aims at understanding how increased velocity gradients developed by the hydraulic selector affects SVI_{30}, settling velocity, and nutrient removal abilities over time.

1.3.2 Reducing solid retention time through hydraulic selection for the development of aerobic granular sludge

AGS has been recognized as a next generation activated sludge treatment because it simultaneously nitrifies and denitrifies (SND), thereby allowing for 1) the development of phosphorus accumulating organisms (PAO), 2) resistance to spikes in nutrient loading, and 3) improved settleability properties [8,16,17]. Under appropriate oxic conditions, AGS can also remove ammonium via the nitrite pathway; this process requires approximately 25% less oxygen compared to CAS, and approximately 40% less electron donor for denitrification compared to nitrogen removal via nitrate [12]. Denitrifying PAOs, a desirable class of microorganisms present in AGS systems, use nitrite or nitrate as an electron acceptor to remove phosphorus, which utilizes carbon in the most effective manner and reduces the aeration requirement [8,13,18]. Lastly, the settling velocity of AGS ranges between 15 and 60 m/h, far faster than traditional activated sludge, which ranges from 1 to 10 m/h.

Despite the benefits to AGS, the development of granules has not been easily achieved. In the pursuit of the perfect operating conditions for AGS development and maintenance, numerous operation variables have been tested by many researchers at bench, pilot, and full-scale. Variables that have been tested over the last three decades include influent wastewater strength (chemical oxygen demand (COD), N, and P concentrations), aerobic to anoxic/anerobic ratio, bioreactor (BR) fill process/conditions, SRT, HRT, and required water temperature, to list a few [9,11,12,19,20]. However, the physical selection pressure required to develop AGS has not been tested as rigorously, relying on minimum settling velocity and, more recently, hydrocyclones for the separation of fast and poor settling floc [21].

Improved solid-liquid separation can still be achieved by targeting and eliminating floc with poor settling characteristics within the BRs. Recently, a pilot scale study conducted at the Colorado School of Mines (Mines) demonstrated that a new selection technology, the hydraulic selector, along with feast/famine

conditions could develop AGS [22]. While the previous hydraulic selector study was successful, two aspects of the research required further investigation. Specifically, we need to understand how the duration and operating conditions of the hydraulic selector impact activated sludge settling velocity and if the hydraulic selector could be combined with traditional activated sludge wasting to reduce SRT below 15 d. In our prior research, only one sudden increase in activated sludge settling velocity was observed, and by that time, four unique hydraulic selector operating conditions had been tested, which made it difficult to explore how each of the conditions influenced the changing settling velocity of the activated sludge.

Another aspect of the hydraulic selector operation that required additional insight is an understanding of the minimum amount of biomass that must be wasted through the hydraulic selector to achieve granulation. In our previous study wasting occurred solely through the hydraulic selector; however, this new wasting paradigm may pose a challenge to facilities with limited dewatering capacity. Wasting solely through the selectors removes a higher percentage of poorly settling floc compared to wasting from the bottom of a BR, but the hydraulic selector effluent has a low total suspended solids (TSS) concentration. Thus, the total volume discharged to the dewatering process will increase if the same SRT is maintained and will pose a problem to those facilities that cannot easily increase their dewatering throughput. If the dewatering volumes are maintained constant, as in our previous study, SRT will increase and will pose a new challenge. SRT values above 15 d increase the mixed liquor suspended solids (MLSS) beyond a necessary concentration. Then, the food to microorganism ratio (F/M) values begin to decline (assuming a facility has a relatively consistent influent sCOD), thereby resulting in granule instability and prevention of new granulation [23]. The kinetics of activated sludge with a high SRT are also less favorable (a decreased observed yield and increase in oxygen demand) [23]. Also, longer SRTs allow eukaryotic life to thrive; species such as nematodes destroy AGS and traditional floc, resulting in poor settling and high concentration of pin floc in the effluent [24–26]. Thus, there is a need to determine if the hydraulic selector can provide enough selection pressure to induce the development of AGS while operating at a reduced capacity.

Chapter 3 evaluates the hydraulic selector's impact on AGS development using a lab-scale SBR. Specifically, we investigated the impact of long-term hydraulic selector operating conditions on activated sludge settling characteristics and AGS development. We also evaluated the impact of a 10-15 d SRT on activated sludge settling characteristics using a combination of hydraulic selector and traditional wasting to achieve a target SRT. The results from this study can further increase our understanding on how selection pressure influences aerobic granulation and can assist in the transfer of this technology from batch reactor systems to a continuous flow CAS process.

1.3.3 Evaluating the activated sludge microbial community under environmental pressures induced by hydraulic selection and feast/famine conditions

Current wastewater treatment facilities have been configured and engineered to accumulate various helpful bacteria such as ammonia oxidizers, denitrifiers, and more recently phosphorus-accumulating organisms. Operational parameters that can vary the concentration of nutrient-removing bacteria include solids retention time, carbon concentration, dissolved oxygen concentration, and anaerobic/anoxic phases. In addition to nutrient removal these facilities are also responsible for complying with stringent effluent solids regulations. This results in facilities maximizing their solids capture in the secondary clarifier, leading to accumulation of slow settling floc and ultimately reducing clarifier capacity or surface overflow rate. Due to the current design of clarifiers, flocs that can settle quickly are removed from the treatment train at a higher rate than the slow settling flocs, thus propagating the attributes of the slow settling floc.

Floc that settles poorly may have a microbial composition dominated by filamentous bacteria that decrease the density of the floc structure or may lack the production of extracellular biopolymers that reduces electronegativity and results in a dense fast floc structure, or may simply not have a large enough diameter to settle quickly. These problems may be mitigated by maintaining a solid retention time less than 15 days and feast/famine conditions. Feast/famine conditions include a high-substrate anaerobic phase followed by a long aerobic phase. These conditions avoid low substrate conditions where filamentous bacteria traditionally outcompete bacteria with preferred nutrient removal abilities. However, these changes in bioreactor operation will not result in an activated sludge dominated by AGS due to the lack of hydraulic selection. The proposed hydraulic selection technology selects for and removes floc based on their respective settling velocity; this allows for the mean floc diameter to increase over time.

Previous AGS experiments have resulted in increased abundance of phosphorus-accumulating organisms, stalked ciliates, and ammonia-oxidizing archaea, but these shifts were observed when both extreme feast/famine and selection processes were applied. In Chapter 4, an in-depth study via 16S-RNA gene analysis is conducted to determine how feast/famine and hydraulic selection influence the microbial shifts in the AGS community. Understanding the hydraulic selection effects on the microbial community is important for the long-term operation of an activated sludge system. Chapter 4 also evaluates the shifts in AS microbiology caused by the operation of the hydraulic selector combined with traditional activated sludge wasting to control floc diameter and solid retention time. Flocs with a diameter <100 µm settle slowly while flocs >2000 µm suffer from carbon diffusion limitation and often deteriorate quickly. Chapters 2 and 3 demonstrate the hydraulic selector's ability to develop an activated sludge with a specific mean floc diameter. Various researchers have observed increasing settling velocities as AGS increases in diameter; thus, many researchers have focused on developing the largest granules possible. However, few studies have investigated how the microbiome of the floc changes with diameter. Thus, flocs in specific floc diameter ranges (<250 µm, 250-500 µm, 500-1000 µm, and >1000 µm) were sequenced using 16S-RNA to develop an understanding of how the microbial community in each floc diameter category changes over time.

1.3.4 The development of a computational fluid dynamic model for the optimization of poor settling floc removal and evaluation of turbulence on floc separation

The hydraulic selection process for a traditional AGS reactor is based on the minimum settling velocity of the activated sludge floc—this is the settling velocity required for a floc to pass the decant weir during the settling period. The minimum settling velocity of an AGS reactor can vary from 5 to 40 m/hr. The problems with the current wasting process are that high amounts of biomass are washed out during the start-up of the AGS reactor, this could violate a wastewater facilities' permit and require additional treatment. More importantly, the minimum reactor height for this separation technology is 5.5 m. Traditional reactor height varies between 3 and 4.5 m. The selection process in an AGS reactor begins after the mixing and aeration of activated sludge, once laminar conditions become dominant activated sludge floc begin to settle according to their terminal settling velocities, resulting in a stratified activated sludge blanket. This would not occur in a traditional reactor where turbulent or transitional conditions may still be present, making the extract of poor settling difficult to achieve and prevents an accumulation of AGS.

To date, only few studies have investigated a technology that selects and removes poor settling floc in traditional reactors. Additionally, no single study has combined the selection process with a CFD model to further enhance poor floc removal. Traditionally, CFD models in the wastewater community have focused on the development of a two phase, laminar, 2-D secondary clarifier model to improve activated sludge settling through baffling. Chapter 5 describes a four phase, turbulent, 3-D CFD model that was developed to provide an in depth understanding of the solid/liquid separation process created by the selector and inform how the geometry of the selector effects the settling trajectory of activated sludge. The CFD model can then be used to optimize the hydraulic selector operating conditions for the maximum removal of poorly settling floc. This would reduce the time required to improve activated sludge settling characteristics and minimize the volume discharged by the selector. From empirical bench top studies on the hydraulic selector, it was determined that the settling time prior to the selection, the selector outflow (pressure difference developed by the selector), and selector depth in the reactor were the most important factors that influence floc selection and removal. The CFD model developed in Chapter 5 investigates the effects of the settling time and hydraulic selector outflow.

1.4 References

[1] United States Environmental Protection Agency. Basic Information about Water Security, (n.d.). https://web.archive.org/web/20150906005124/http://water.epa.gov/infrastructure/watersecurity/basicinformation.cfm (accessed December 1, 2017).

[2] T. Sato, M. Qadir, S. Yamamoto, Global , regional , and country level need for data on wastewater generation , treatment , and use, Agric. Water Manag. 130 (2013) 1–13. https://doi.org/10.1016/j.agwat.2013.08.007.

[3] ASCE's 2017 Infrastructure Report Card, Conditions & Capacity, (2017).

www.infrastructurereportcard.org/wastewater/conditions-capacity/.

[4] G. Tchobanoglous, Wastewater Engineering Treatment and Resource Recovery, 5th ed., McGraw-Hill Education, United Kingdom, 2014.

[5] B. Ni, W. Xie, S. Liu, H. Yu, Y. Wang, G. Wang, X. Dai, Granulation of activated sludge in a pilot-scale sequencing batch reactor for the treatment of low-strength municipal wastewater, Water Res. 43 (2009) 751–761. https://doi.org/10.1016/j.watres.2008.11.009.

[6] J.H. Tay, S.F. Yang, Y. Liu, Hydraulic selection pressure-induced nitrifying granulation in sequencing batch reactors, Appl. Microbiol. Biotechnol. 59 (2002) 332–337. https://doi.org/10.1007/s00253-002-0996-6.

[7] H. Horn, C. Klarmann, K. Sørensen, T. Rocktäschel, P. Boisson, J. Ochoa, Influence of the granulation grade on the concentration of suspended solids in the effluent of a pilot scale sequencing batch reactor operated with aerobic granular sludge, Sep. Purif. Technol. 142 (2015) 234–241. https://doi.org/10.1016/j.seppur.2015.01.013.

[8] M. Pronk, M.K. De Kreuk, B. De Bruin, P. Kamminga, R. Kleerebezem, M.C.M. Van Loosdrecht, Full scale performance of the aerobic granular sludge process for sewage treatment, Water Res. 84 (2015) 207–217. https://doi.org/10.1016/j.watres.2015.07.011.

[9] B.S. McSwain, R.L. Irvine, P.A. Wilderer, The effect of intermittent feeding on aerobic granule structure, Water Sci. Technol. 49 (2004) 19–25. https://doi.org/10.2166/wst.2004.0794.

[10] M.K. de Kreuk, M.C.M. van Loosdrecht, Selection of slow growing organisms as a means for improving aerobic granular sludge stability, Water Sci. Technol. 49 (2004) 9–17. https://doi.org/10.2166/wst.2004.0792.

[11] R.D.G. Franca, H.M. Pinheiro, M.C.M. Van Loosdrecht, N.D. Lourenço, Stability of aerobic granules during long-term bioreactor operation, 36 (2018) 228–246. https://doi.org/10.1016/j.biotechadv.2017.11.005.

[12] Y. V Nancharaiah, G.K. Kumar, Bioresource Technology Aerobic granular sludge technology : Mechanisms of granulation and biotechnological applications, 247 (2018) 1128–1143. https://doi.org/10.1016/j.biortech.2017.09.131.

[13] M.K.D.K. Ã, M. Pronk, M.C.M. Van Loosdrecht, Formation of aerobic granules and conversion processes in an aerobic granular sludge reactor at moderate and low temperatures, 39 (2005) 4476–4484. https://doi.org/10.1016/j.watres.2005.08.031.

[14] M.K. De Kreuk, C. Uijterlinde, Aerobic granular sludge technology : an alternative to activated sludge, (2001) 1–7.

[15] T. Rocktäschel, C. Klarmann, B. Helmreich, J. Ochoa, P. Boisson, K.H. Sørensen, H. Horn, Comparison of two different anaerobic feeding strategies to establish a stable aerobic granulated sludge bed, Water Res. 47 (2013) 6423–6431. https://doi.org/10.1016/j.watres.2013.08.014.

[16] M. Winkler, C. Meunier, O. Henriet, J. Mahillon, M. Suarez-Ojeda, G. Del Moro, M. De

Sanctis, C. Di Iaconi, D. Weissbrodt, An integrative review of granular sludge for the biological removal of nutrients and recalcitrant organic matter from wastewater, Chem. Eng. J. 336 (n.d.) 489–502. https://doi.org/10.1016/j.cej.2017.12.026.

[17] M.K. De Kreuk, J.J. Heijnen, M.C.M. Van Loosdrecht, Simultaneous COD, nitrogen, and phosphate removal by aerobic granular sludge, Biotechnol. Bioeng. 90 (2005) 761–769. https://doi.org/10.1002/bit.20470.

[18] R. Pishgar, J.A. Dominic, Z. Sheng, J.H. Tay, Influence of operation mode and wastewater strength on aerobic granulation at pilot scale: Startup period, granular sludge characteristics, and effluent quality, Water Res. 160 (2019) 81–96. https://doi.org/10.1016/j.watres.2019.05.026.

[19] S.S. Adav, D. Lee, K. Show, J. Tay, Aerobic granular sludge : Recent advances, (2008) 411–423. https://doi.org/10.1016/j.biotechadv.2008.05.002.

[20] M.K.H. Winkler, R. Kleerebezem, W.O. Khunjar, B. de Bruin, M.C.M. van Loosdrecht, Evaluating the solid retention time of bacteria in flocculent and granular sludge, Water Res. 46 (2012) 4973–4980. https://doi.org/10.1016/j.watres.2012.06.027.

[21] I. Avila, D. Freedman, J. Johnston, B. Wisdom, J. McQuarrie, Inducing granulation within a full-scale activated sludge system to improve settling, Water Sci. Technol. (2021) 1–12. https://doi.org/10.2166/wst.2021.006.

[22] R.A. Maltos, R.W. Holloway, T.Y. Cath, Enhancement of activated sludge wastewater treatment with hydraulic selection, Sep. Purif. Technol. 250 (2020) 117214. https://doi.org/10.1016/j.seppur.2020.117214.

[23] C. P. Leslie Grady, Jr., Glen T. Daigger, Nancy G. Love, Biological Wastewater Treatment, 3rd ed., London, UK, IWA Publishing, 2011.

[24] P. Oliveira, M. Alliet, C. Coufort-Saudejaud, C. Frances, R. Nawaz, L.Y. Tan, H. Nisar, M.B. Khan, J. Zhang, G. Chen, Z. Jia, M.B. Khan, H. Nisar, C.A. Ng, K.H. Yeap, K.C. Lai, J.C. Costa, D.P. Mesquita, A.L. Amaral, M.B. Khan, H. Nisar, N.C. Aun, P.K. Lo, D. Eikelboom, Process Control of Activated Sludge Plants by Microscopic Investigation, Water Sci. Technol. 77 (2000) 2415–2425. https://www.iwapublishing.com/sites/default/files/ebooks/9781900222297.pdf.

[25] J.J. Bisogni, Relationships between biological solids retention time and settling characteristics of activated sludge, Water Res. 9 (1971) 753–763.

[26] E. Amanatidou, G. Samiotis, E. Trikoilidou, G. Pekridis, N. Taousanidis, Evaluating sedimentation problems in activated sludge treatment plants operating at complete sludge retention time, Water Res. 69 (2015) 20–29. https://doi.org/10.1016/j.watres.2014.10.061.

CHAPTER 2

ENHANCEMENT OF ACTIVATED SLUDGE WASTEWATER TREATMENT WITH HYDRAULIC SELECTION

Modified from a paper published in Separation and Purification Technology (Vol. 250 (2020) 117214).

Rudy A. Maltos[1], Ryan W. Holloway[2], Tzahi Y. Cath[1]*

2.1 Abstract

The slow settling rate of activated sludge (AS) in secondary clarifiers and batch reactors results in increased hydraulic retention time, AS with a higher water content pumped to the digesters, and higher suspended solids concentration in the clarified supernatant. Settling rates of AS can be improved through the removal of poor settling floc with a diameter less than 100 µm. Currently, the main technology used for the enhancement of AS settling is aerobic granular sludge reactors—very few of these reactors have been adopted into the United States market due to their cost and difficulty to integrate the technology into current wastewater treatment infrastructure. The objective of this study was to develop a technology that could enhance the settling properties of AS while maintaining nitrification/denitrification and that could easily be integrated into current wastewater treatment infrastructure. We have developed a hydraulic selection process that removes poor settling floc directly from the secondary clarifiers or batch reactors. The hydraulic selection process is a vacuum system that is suspended in the AS, the system then develops a unique pressure difference based on poor settling sludge density, floc diameter, and terminal settling velocity. The selection process captures and removes poor settling floc allowing the remaining floc to grow and increase the settling rate of AS. The hydraulic selection process was tested for 120 days in a 120 L batch reactor. Results from the experiment showed that the hydraulic selection process was successful, in 63 days the settling velocity increased from 0.2 to 20 m/hr, mean floc diameter increased from 62 to 430 µm, and sludge volume index decreased from 280 to 45 mL/g. Nitrification was maintained for nearly the entire duration of the experiments with the exception of a few days due to drastic changes in influent wastewater concentrations. Denitrification was only maintained for a limited period during the experiment due to an unfavorable carbon to nitrogen ratio.

2.2 Introduction

Conventional activated sludge (CAS) is a simple, robust, and low-cost wastewater treatment technology. Because of the operational and cost benefits of CAS it is used by approximately 75% of water resource reclamation facilities (WRRFs) in the United States [1,2]. CAS systems are a critical component in wastewater treatment infrastructure, but additional improvements to the process are needed (e.g., nutrients removal, contaminants of emerging concern removal, and physical footprint reduction) to accommodate population growth and meet more stringent effluent discharge requirements. It is estimated that by 2032, 56 million additional customers (23% increase) will be using these WRRFs [3], many of which are already at their maximum treatment capacity. To serve these new customers, the US Environmental

Protection Agency has estimated that $271B are needed to upgrade the existing wastewater infrastructure over the next 20 years [3].

CAS systems are comprised of a bioreactor containing aerobic zones for biological removal of organic matter and nutrients, and a clarifier for physical solid-liquid separation. A portion of the activated sludge (AS) from the bottom of the clarifier is returned to the bioreactor and the remaining is wasted (commonly treated by anaerobic digestion). Clarifiers with poorly settling AS usually have tall sludge blankets with lower biomass concentrations, resulting in higher return activated sludge (RAS) pumping rates, AS with a higher water content pumped to the digesters, and higher suspended solids concentrations in the clarifier supernatant (effluent). Poorly settling AS is characterized by a slow settling velocity—less than 5 m/h—and high sludge volume index at 30 minutes (SVI_{30}), commonly >250 mL/g. To manage poorly settling AS, the surface overflow rate (SOR) in the clarifier must be reduced, thus increasing the hydraulic retention time (HRT) in the WRRF [4] and requiring larger plant footprint. To eliminate the 'bottleneck' at WRRFs, expensive construction of additional clarifiers would be required, but may not be possible for landlocked treatment plants with no space for expansion. Yet, additional clarifiers do not resolve the core problem – accumulation of poorly settling AS. Another solution might be the replacement of clarifiers with microfiltration or ultrafiltration membranes or retrofitting the entire CAS system with membrane bioreactors. However, this is an expensive undertaking that increases both the capital and operational costs of WRRFs.

Improved AS settling and secondary clarifier performance can be achieved by hydraulically selecting for and eliminating biosolids with poor settling properties. Hydraulic selection is defined as selectively removing unwanted floc from a bioreactor by means of hydrodynamic forces. A relatively new technology that implements hydraulic selection is aerobic granular sludge (AGS) systems [5–8]. An AGS reactor is commonly a batch prosses and operates like a sequencing batch reactor (SBR); while an SBR has a fill, mix, aeration, settling, and decant phases, an AGS cycle is simply comprised of three phases, fill/decant, aeration, and settling. To enable the development of AGS at the bench scale, the reactors must have a depth-to-width (D:W) ratio higher than 2.5. This specific ratio facilitates the stratification of fast and slow settling floc in the settling phase, in the decant/fill phase the slow settling floc are removed through the decant and fast settling floc accumulate and grow in the bioreactor. The selection process is further improved by decreasing the settling period before the decant phase over several months, thus increasing the settling velocity of the remaining floc. These systems are effective in producing fast settling granular sludge (ranging from 15 to 60 m/h), with an SVI_{30} below 60 mL/g, and an average floc diameter and density higher than 200 μm and 1.1 g/mL, respectively [8–12]. AGS systems have demonstrated improved wastewater treatment, but full-scale reactors have to have a depth greater than 5.5 m and the start-up times as long as 12 months [9,13]. The enhancement of solid settling is advantageous for all WRRFs, but the required expensive capital improvements make it difficult to be implemented. Thus, a technology that can be easily integrated into current CAS and SBR infrastructure and can achieve improved AS settleability is needed.

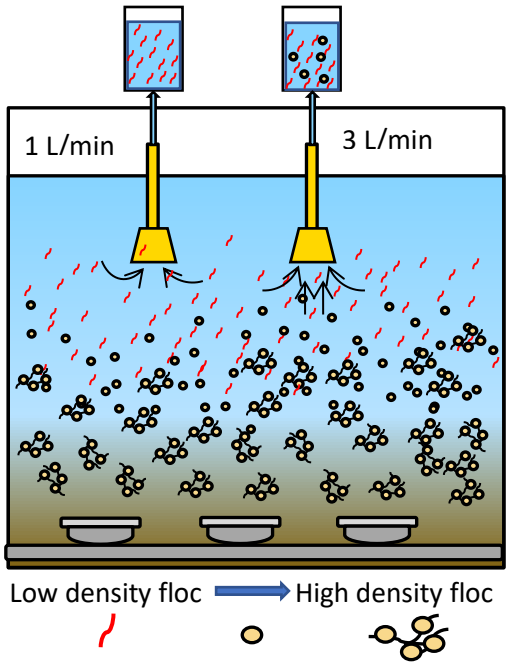

Figure 2.1 A schematic of the hydraulic selector placed in a bioreactor. At an outflow of 1 L/min the velocity gradient developed around the selector removes a higher percentage of low-density floc. At an outflow of 3 L/min the velocity gradient developed by the selector is higher and higher density floc are removed.

The selection process that occurs in AGS reactors can be reconfigured to work in any reactor, regardless of height. The selection and removal of poorly settling floc can be accomplished through the decanting of water containing the floc from the clarifier using a hydraulic selector device (Figure 2.1). The selector—a trough-like device—is placed in the bioreactor at an optimized depth below the water surface and at the level where poorly settling floc are at the highest concentration. By pumping water through the selector, a localized flow field develops that pulls poorly settling flocs from the supernatant. By changing the flowrate through the selector, the radius of influence can be increased or decreased. At lower-flow rates the lighter flocs (having slower-settling velocities) are pulled into the hydraulic selector, and heavier flocs (having faster settling velocities) are retained in the reactor. Over time, an accumulation of faster settling floc will dominate the AS. The selector developed for this study uses a uniquely designed geometry and pressure difference, optimized for the removal of poorly settling floc based on the flocs' density and diameter. This technology has the potential to be implemented in both batch and the continuous flow-through CAS process without major disruptions to the utility infrastructure.

The main objective of this study was to investigate the performance and effectiveness of the selector using a lab-scale SBR. Specifically, the study aimed at understanding how increased velocity gradients developed by the hydraulic selector affects SVI_{30}, settling velocity, and nutrient removal abilities over time. Characterization of the AS floc throughout the study included changes in the floc structure and microbial community. The results from this study can be used to refine the operation of hydraulic selectors and further understand the role that hydraulic selection can have on settling characteristics of AS.

2.3 Materials and methods

A lab-scale SBR equipped with two hydraulic selectors was constructed and operated for 112 days (July to November). The experiments were conducted with raw wastewater produced from the dormitories (Mines Park) of the Colorado School of Mines (Golden, Colorado).

2.3.1 System configuration

The lab-scale system comprised of a 250-L raw wastewater equalization tank, a 200-L primary clarifier (PC), a 110-L PC decant tank, and a 120-L bioreactor. The bioreactor had a depth-to-diameter ratio of 1.3 and was seeded with 84 L of AS from an onsite demonstration scale sequencing batch membrane bioreactor (SBMBR), described by Vuono et al. [14]. A schematic of the system is shown in Figure 2.2.

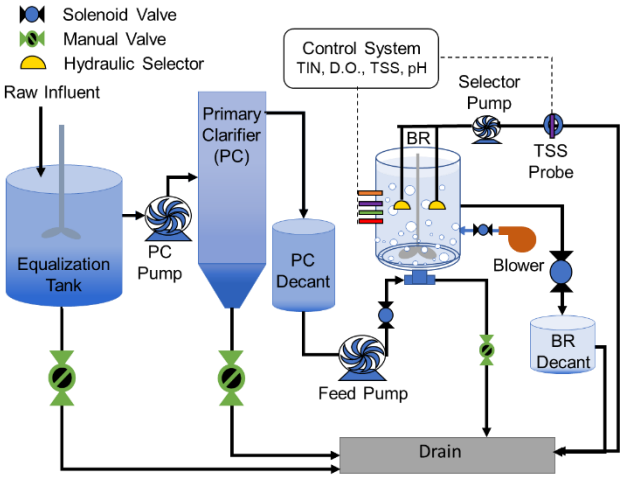

Figure 2.2 A schematic of the pilot system. Raw wastewater was diverted from an on-campus student apartment complex and activated sludge from an onsite SBMBR was used as seed sludge for the bioreactor.

The equalization tank was replenished every hour with 190 L of raw wastewater form an onsite underground storage tank. A peristaltic pump (Cole-Parmer, Vernon Hills, IL) is used to deliver raw wastewater from the equalization tank to the PC at 2 L/min. Supernatant from the PC overflows into the PC decant tank that feeds the bioreactor. The bioreactor is operated in cycles consisting of seven phases, including fill, mix, aeration, initial settling, selector discharging, final settling, and decant. During the static fill phase, a feed peristaltic pump transfers a set volume of clarified wastewater from the PC decant tank into the bottom of the bioreactor, where the sludge blanket has settled. In the mix phase, a wide blade impeller mixes the reactor content at 25 RPM. During the aeration phase, the blower (Elmo Rietschle, Milwaukee, WI) delivers 10-15 L/min of air through two aluminum oxide diffusers (Pentair, Minneapolis, MN) installed at the bottom of the bioreactor. In the settling phase mixing and aeration stop and AS can settle. In the selector discharge phase poorly settling floc are removed from the bioreactor by the hydraulic selector (selector operation is further discussed in Section 2.2). In the decant phase treated water is decanted over an adjustable weir, initiated using an automated ball valve. AS wasting from the bottom of

the bioreactor began on day 68 and was conducted manually using a graduated cylinder. The calculated solid retention time (SRT) varied between 40 and 80 days.

2.3.2 Hydraulic selector design

The hydraulic selector concept is based on the separation and removal of poorly settling floc through the development of a velocity field. Important parameters that affect the velocity field include the entrance area and flow rate through the hydraulic selector. The area of the selector used in this study was 60 cm^2 and flow through the selector varied between 1 and 4 L/min. The hydraulic selector was designed in SolidsWorks (SolidWorks 2018, Dassault Systemes, Waltham, MA) and 3D printed with polylactic acid filament (Pro2 Plus, Raised 3D, Irvine, CA). Two hydraulic selectors were placed in the single bioreactor and were separated by 20 cm, the entrance of the hydraulic selectors was 12 cm below the surface of the wastewater in the bioreactor when the SBR is full. The selectors are connected to a positive displacement rotary vane pump (Series 2, Procon, Smyrna, TN). The supernatant removed by the selector flows through an in-line total suspended solids (TSS) probe (HACH, Loveland, CO).

2.3.3 Influent wastewater characteristics

The characteristics of the wastewater varied over the study period due to fluctuations in the student housing population. These periods of different wastewater strength are separated into three stages: Stage 1, system startup characterized by low wastewater strength lasting from day 0 to day 40; Stage 2, characterized by dynamic and increasing wastewater strength lasting from day 41 to day 80; and Stage 3, characterized by stable and moderate wastewater strength lasting from day 81 to the end of the experiment. The average influent wastewater characteristics during the three stages are summarized in Table 2.1.

Table 2.1. Average influent wastewater characterisitcs and concentrations

	pH	COD (mg/L)	sCOD (mg/L)	Ammonium (mg/L)	Phosphorus (mg/L)	Conductivity (µS/cm)	Alkalinity (mg/L $CaCO_3$)
	n = 18	n = 18	n = 18	n = 18	n = 18	n = 18	n = 18
Stage 1	7.5±0.2	318±52	196±38	37±5	11±3	761±42	225±27
Stage 2	7.1±0.4	501±45	332±40	46±9	14±2	821±53	268±32
Stage 3	7.4±0.2	430±37	223±24	43±2	12±3	915±68	218±15

2.3.4 Operating conditions

The objective of the study was to enhance AS settleability while maintaining an effluent chemical oxygen demand (COD) and TSS concentration below 30 mg/L and total nitrogen concentration less than 10 mg/L. Due to the variations in influent wastewater characteristics during the experiment, the bioreactor operating phases are changed periodically to meet the effluent quality targets. The operating conditions are modified by adjusting one or several of the phases, including bioreactor fill, mixing (anoxic/anaerobic),

aeration, and settling times. The bioreactor operating phases for Stages 1, 2, and 3 of the experiment are summarized in Table 2.2.

Table 2.2. Operation phases of the bioreactor during Stage 1, 2, and 3. Each stage represents different influent wastewater characteristics and concentrations as described in Table 1.

Phase	**Stage 1**	**Stage 2**	**Stage 3**
Fill (min.)	36	24	36
Mixing (min.)	15	15	60
Aeration (min.)	168	168-330	310
Initial settling (min.)	6	6→2	1
Selector discharge (min.)	3	3	3
Final settling (min.)	10	10	10
Decant (min.)	5	5	5
Total cycle Time (min.)	243	231-389	425
Duration (days)	0-40	40-85	85-120
Exchange ratio (%)	30	20	30

The Stage 1 fill time was 36 minutes and the exchange ratio—the ratio of wastewater volume treated in a cycle to the entire reactor volume—was 30%. In Stage 2 the carbon and nitrogen concentrations exceeded their effluent limit and therefore the fill time and exchange ratio were reduced to 24 minutes and 20%, respectively; thus, reducing the carbon and nitrogen loading. In Stage 3, the fill time and exchange ratio were returned to 36 minutes and 30%, respectively, due to the decreased strength of the influent. The Stage 1 mixing time was set to 15 minutes and did not change until Stage 3. The Stage 3 mixing time increased to 60 minutes. This provided a longer anoxic/anerobic time that eliminated the high concentration of predatory nematodes that were observed in the AS during Stage 2. The Stage 1 aeration time ensured the removal of COD and ammonia to effluent target concentrations. The Stage 2 aeration time gradually increased from 168 to 330 due to the increasing influent COD and nitrogen concentrations; longer aeration times ensured that feast/famine conditions were present. Stage 3 aeration time decreased to 310 minutes due to the decrease in wastewater strength.

The Stage 1 initial settling time, prior to the hydraulic selector discharge, was set to 6 minutes, this allowed an initial separation between fast and slow settling floc. During Stage 2 the settling properties of the AS improved. To increase the selection pressure, the initial settling time was reduced from 6 to 2 minutes over a period of 45 days, allowing the selector to enhance the removal of poorly settling floc. During Stage 3 the initial settling time was 1 minute to further increase the selection pressure. The final settling time remained 10 minutes for all stages; this ensured that all biosolids were settled prior to the decant phase.

2.3.5 Data acquisition

The bioreactor DO and TSS concentrations and pH are measured continuously using online probes (HACH, Loveland, CO). Ammonia and nitrate are measured continuously using a Varion nitrogen probe (Yellow Springs Instruments, Yellow Springs, OH). The pilot system is controlled by a programmable logical controller (UE9-Pro, LabJack Corp., Lakewood, CO) and a data acquisition instrument control software (LabVIEW, National Instruments Corp., Austin, TX).

2.3.6 Analytical methods

2.3.6.1 Sludge volume index (SVI)

SVI represent how well the AS blanket compacts after a given time—lower SVI values indicate better AS compatibility. The SVI measurement is a function of settled bed volume and the mixed liquor suspended solids (MLSS) concentration, Eq 2.1. For this study AS samples were taken from the bioreactor twice a week during the aeration phase, settled bed volume was measured in a 1 L beaker at 4 (SVI_4) and 30 (SVI_{30}) minutes.

$$SVI_x\left(\frac{mL}{g}\right) = \frac{Settled\ AS\ volume\ after\ x\ mins\ (mL)}{AS\ MLSS\ \left(\frac{g}{L}\right)} * \frac{1}{Beaker\ volume\ (L)} \tag{2.1}$$

2.3.6.2 Chemical analysis

AS samples were taken from the bioreactor twice a week during the aeration phase; settling velocity and MLSS concentration were measured according to standard methods [15]. Composite samples (24-hour) from the equalization tank and bioreactor decant were collected once a week. Composite samples were measured for COD, ammonia, nitrate, pH, and alkalinity. These analyses (excluding pH) were performed using HACH TNT Plus™ (Loveland, CO) reagent vials and Hach DR 5000™ spectrophotometer.

2.3.6.3 Floc characterization

Samples of AS were drawn from the bioreactor during the aeration phase into 15-mL sample vials and stored at 5 °C. The particle size distribution of the AS floc was measured twice a week by a laser particle size analyzer (S3500, Microtrac) with an absorption coefficient of 1 and refractive index of 1.52 [16]. The Microtrac measures the light scattered by floc and correlates this to a known volume, this measurement is independent of density. Thus, the floc distribution developed are a function of displaced volume over floc diameter, known as a volume based cumulative distribution. Electrochemical properties of the AS were tracked through zeta potential; average pH of the samples was 7.3±0.2. The undiluted AS samples were analyzed three times with a Zeta-Potential Analyzer (Zetasizer Model Nano-ZS, Malvern, UK) [17,18]. AS samples were also gram stained using crystal violet, iodine, decolorizer, and safranin. AS samples were also characterized with a phase contrast microscope (Olympus CX41, Center Valley, PA) at 100X magnification; phase contrast images were processed with Infinity 2 software (Lumenera, Ontario, Canada).

2.4 Results and discussion

2.4.1 AGS development and characteristics

The performance of the SBR equipped with the selector was monitored over 112 days of continuous operation. The bioreactor MLSS concentration and mass of biosolids removed by the selector over the study period are shown in Figure 2.3A, and the changes in the SVI_4 and SVI_{30} during the study are shown in Figure 2.3B. The flow rate through the selector was increased on days 15, 28, and 48 to investigate the impact of increased hydrodynamic forces on AS settleability, floc structure, and nutrient removal. The selector flow rate was decreased from 4 to 2 L/min on day 63 to allow the MLSS concentration to increase.

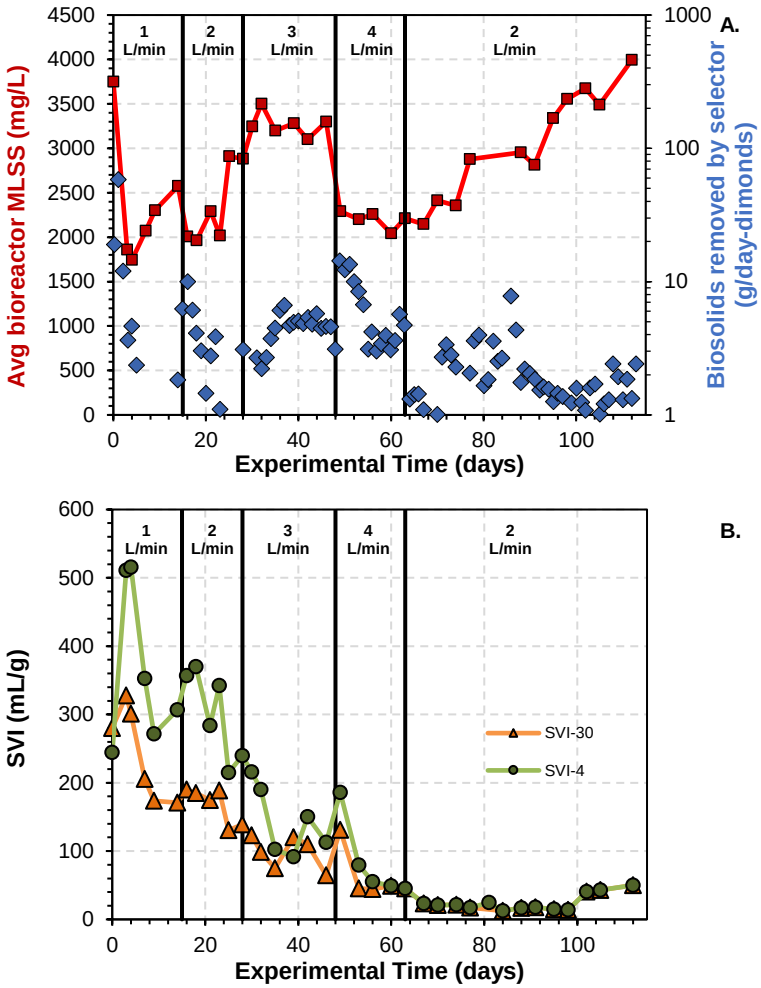

Figure 2.3 A) mixed liquor suspended solids (MLSS) and biosolids removed by the hydraulic selector and B) sludge volume index (SVI) at 4 and 30 minutes. Changes in selector operating flow rates are shown in Figure 3 as a vertical line.

The MLSS, SVI_4, and SVI_{30} of the seed AS (day 0) were 3750 mg/L, 244 mL/g, and 280 mL/g, respectively. Although the selector was operated at a low flowrate at the beginning of the experiment to limit the loss of biosolids, approximately 60 g of biomass were lost from the SBR during the first day – resulting in a 55% decrease in the MLSS concentration (Figure 2.3A). The seed AS was made up of a very

loosely formed matrix of filamentous bacteria that settled very slowly; thus, the selector was still immersed in the AS after the 6-minute settling period and large amounts of the biosolids were removed through the selector when the selector pump was in operation. This resulted in increased SVI_{30} (300 mL/g) and SVI_4 (500 mL/g) on day 1 (Figure 2.3B). Over the next several days the floc became more discrete and the selector was able to better remove slower settling floc while keeping dense floc in the bioreactor; by day 9 the MLSS concentration recovered to 2,300 and the SVI_4 and SVI_{30} decreased to 270 and 174 mL/g, respectively.

The selector outflow was increased from 1 to 2 L/min on day 15, this resulted in the MLSS concentration decreasing from 2,575 to 1,970 mg/L between day 15 and day 18. The sharp decline in MLSS concentration was a result of the selector removing more biosolids from the reactor at the higher outflow rate. Over the next 7 days (18-25), the AS settling characteristics improved, the selector steadily removed less biosolids from the reactor, and the MLSS concentration increased to almost 3,000 mg/L. The improvement in AS settleability is illustrated by the SVI_4 decreasing from 300 to 215 mL/g and the SVI_{30} decreasing from 190 to 130 mL/g during this time.

The selector outflow increased from 2 to 3 L/min on day 28 and unlike the previous increase in selector outflow the MLSS concentration remained constant. The biosolids removed by the selector at an outflow of 3 L/min was not enough to impact the MLSS concentration. After day 30 biosolids removed by the selector slowly increased until reaching a constant removal rate of approximately 4.5 g/day between day 35 and 48. The increase in biosolids removed by the selector can be explained through the presence of pin floc, small/weak flocs that lack the ability to settle. During the same period, the SVI_4 and SVI_{30} increased from 75 to 131 mL/g and 102 to 185 mL/g, respectively.

On day 48, the selector outflow was increased from 3 to 4 L/min. Over a period of one day the MLSS concentration decreased by 33%, from 4500 to 2290 mg/L. The selector initially removed 14 g/day, which led to a decline in MLSS concentration, then biosolids discharged by the selectors slowly declined to 3.5 g/day. The reduction in biosolids removed by the selectors resulted in the stabilization of the MLSS concentration. The biosolids removed by the selector and decant were dominated by pin floc; this did not have a negative impact on SVI's; both SVI_4 and SVI_{30} initially increased and then decreased to 49 mL/g by day 60. The improvements in SVI were not driven by MLSS concentration, which remained stable when the SVI's decreased—the SVI's decreased due to the enhanced settleability and compressibility of the floc in the AS. A microscopic investigation on day 60 revealed that the AS was being damaged by predatory worms and resulting in the pin floc that was observed in the supernatant (section 3.1.4). Nematodes require aerobic conditions to survive [19]; thus, to eliminated the nematode problem the anaerobic mixing time was increased on day 63 from 15 to 60 minutes.

The selectors outflow was lowered from 4 to 2 L/min on day 63 to reduce biosolids discharged by the selector. The removal of biosolids through the selectors remained below 5 g/day with the exception of day 86, allowing the concentration of MLSS to slowly increase and eventually reach a max concentration of 4,000 mg/L on day 112. The SVI_{30} and SVI_4 continued to decrease due to increased MLSS concentration

and averaged 30 mL/g from day 67 to day 112, a 90% and 88% decrease from the day 0 values, respectively. The settling characteristics of the AS at the end of the experiment began to resemble that of AGS [5,8,20,21].

The development of AGS is attributed to both a feast/famine feeding regime and physical selection process. The feast occurs during the anaerobic phase when there is high substrate uptake then famine follows during the aerobic phase when substrate concentration in the bioreactor is low and microorganisms use their internal stored substrate [22,23]. Previous experiments that have tried to develop AGS solely using a feast/famine in a reactor with a depth-to-width ratio less than 2.5 have failed [9,10,24,25]. Although the hydraulic selector provided most of the physical selection process because the experiment did not have a control, a bioreactor without a hydraulic selector, it cannot be concluded the selector was the only selection process that enable the growth of AGS. Another factor that could influenced the granulation of AS is the long SRT, which are common in batch scale AGS system. Reducing the SRT would mimic operating conditions at full-scale CAS facilities. Various publications have shown the ability to grow granules with SRT less than 30 days and one recent study managed to develop granules with a 4 – 9 SRT in a continuous flow system [26–29]. Future experiments will need to reduce experimental variables to further evaluate the hydraulic selection operation process.

2.4.1.1 Sludge settling velocity

Although SVI_{30} provides a good inidcation of the AS's settleability, it is a function of both MLSS concentration and compactability and not of how quickly the AS settles. Poor settling AS with a high MLSS concentration could still have an average SVI_{30} between 150 to 200 mL/mg. Therefore, the additional measurement of AS settling velociy is required. The settling velocity of typical AS floc ranges from 1 to 10 m/h [20,30]. Slower settling AGS have been shown to settle ~50% faster than the fastest settling AS, and fast settling AGS has settling velocities exceeding 68 m/h [10]. The settling velocity of the seed AS measured 0.2 m/h. Important factors that influence the improvement of the AS settling velocity are the selector's entrance velocity and the minimum settling velocity. The selector's entrance velocity is calculated using the outflow rate of the selector and entrance area of the selector and the minimum settling velocity, is calculated using distance between the bottom of the selector and the top of the AS level. Settling velocity of the AS, selector's entrance velocity, and minimum settling velocity was measured or calcuated throughout the duration of the experiment and results are shown in Figure 2.4.

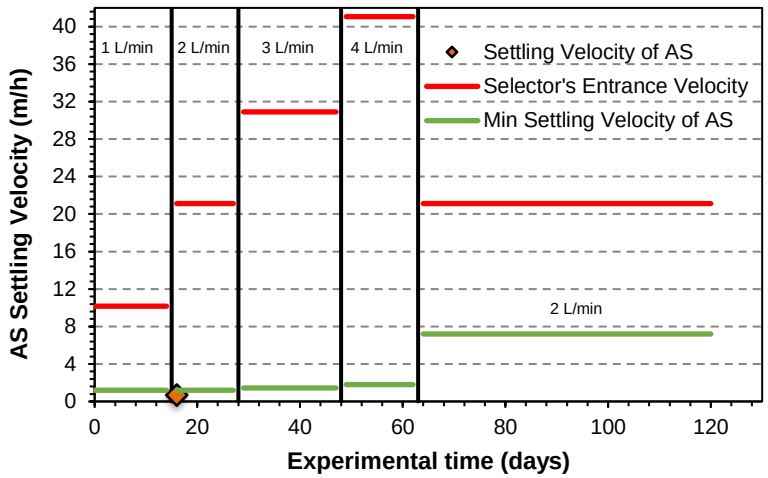

Figure 2.4 AS settling velocities (orange), selector's entrance velocity (red), and minimum settling velocity (green) was measured or calcuated over the study period. Changes in selector outflow rate are identified by vertical lines.

The settling velocity of the AS increased to 1.1 m/h by day 4 and remained relatively constant up to day 14. The selector outflow was increased from 1 to 2 L/min on day 15, resulting in AS settling velocity steadily increasing and reaching 2.7 m/h on day 23. Over the same period MLSS concentration (Figure 2.3A) increased and both SVI's (Figure 2.3B) decreased. The hydraulic selectors outflow was increased from 2 to 3 L/min on day 28 and the settling velocity continued to increase from 2.7 to 3.5 m/h between days 28 and 48. The higher settling velocities did not correspond to a substaintial change in MLSS concentration nor improvement in SVI's—the MLSS concentration remained between 3100 to 3500 mg/L and SVI_{30} decreased from 139 to 131 mL/g between day 28 and 48.

On day 48 the selectors outflow was increased to 4 L/min and the settling velocity began to rise rapidly, this improved settling was likely related to the increased removal of poor settling floc by the selector. The AS settling velocity reached 9.5 m/h by day 56, which is considered a fast settling velocity for traditional AS [20,30]. The settling velocity of the AS continued to increase reaching 19.5 m/h on day 63, in the range of AGS settling velocities [10,31,32]. While settling velocity rapidly increased (days 48 to 63), On day 63 of the experiment the ouflow of the selector was decreased from 4 to 2 L/min. Settling velocity of the AS remained between 19.4 and 20.5 for the remainder of the experiment and MLSS concentration gradually increased to 4000 mg/L and both SVI's remained below 50 mL/g, reaching 14 mL/g on day 84. This stability of the settling velocity was due to consistent removal of poorly settling floc through the hydraulic selector at 1.5 g/d, this allowed dense biosolids concentration to increase while preventing accumulation of poor settling biosolids.

In addition to the hydraulic selector the minimum settling velocity, velocity required for a floc to pass the selector during the initial settling period, provided an additional selection pressure. The minimum settling velocity increased throughout the experiment beginning at 1.2 m/h and increasing to 7.2 m/h. For the first 27 days the minimum settling velocity was set to 1.2 m/h. The settling velocity of the AS on day 4, was almost identical to the minimum settling velocity at 1.1 m/hr, while the hydraulic selector entrance velocity

was far above the AS settling velocity at 10 m/hr. The AS settling velocity cannot be directly related to the operation of the selector. After day 21 the settling velocity of the AS always exceeded the minimum settling velocity indicated that an additional hydraulic selection process was in effect. At this point the increase in AS settling velocity is most likely due to the operation of the hydraulic selector. Interestingly, after day 63 the entrance velocity of the selector is reduced to 21 m/h at that point the settling velocity of the AS also stabilized and remained at 20 m/h for the remainder of the experiment. Further investigations on how the combination of selection pressures such as the hydraulic selector and settling times, influenced the formation of AGS are needed.

2.4.1.2 Floc diameter

The diameter of a typical slow settling AS floc is between 50 and 100 µm [33,34] and the diameter of a fast settling AGS varies between 200 and 7000 µm [10]. The settling velocity of AS has been related to its diameter, with larger floc diameter resulting in faster settling AS [20]. Floc diameter measurements were periodically taken over the course of the study and results of these measurements are shown in Figure 2.5.

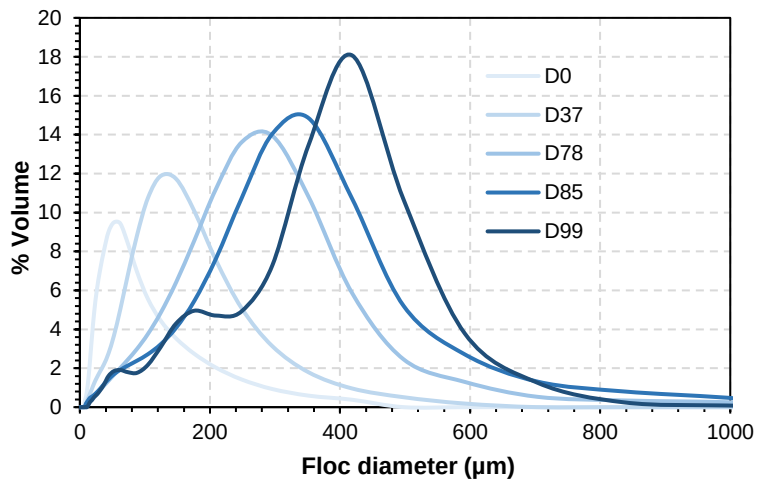

Figure 2.5 Volume based cumulative distribution of AS floc diameter over the duration of the experiment. The mean floc diameter of the seed AS (day 0) was less than 62 µm.

The mean floc diameter of the seed AS was 62 µm and 95% of the AS had a diameter less than 200 µm, mean floc diameter are not explicitly shown in the distribution but were calculated by the Microtrac software. The mean floc diameter of the seed AS was on the low end of typical floc diameters reported for CAS systems, between 50 and 200 µm [33,34]. By day 37 the mean floc diameter increased to 130 µm, the percentage of floc with a diameter larger than 200 µm increased from <5% to 15%, and the SVI_{30} improved from 280 to 120 mL/g. More than 50% of the AS had a floc diameter larger than 200 µm by day 78, and by day 99, more than 65% of the floc had a diameter larger than 200 µm—the average floc diameter was 430 µm, and the SVI_4 and SVI_{30} were below 25 mL/g. The diameter and settling characteristics of the floc after day 99 were well within the range of the values reported for AGS granules [9,10]. For the last

three floc diameter measurements, the selector outflow remained constant while floc diameter increased. This indicates that growth in floc diameter was related to bioreactor operational parameters, at the same time floc diameter at 200 µm decreases from 10.8% to 5% between days 78 to 99. The decrease of floc with a diameter of 200 µm may have been caused by the floc diameter growing or the removal of the floc through the hydraulic selector. Thus, additional studies analyzing the floc removed by the selector are needed to understand the impact on floc diameter growth and settling velocity.

2.4.1.3 Zeta potential

Poor settling floc in AS typically has a highly negative zeta potential that results in repulsive electrostatic interactions. The zeta potential of traditional AS ranges between -20 to -15 mV [17,18]. When environmental stress such as feast/famine conditions is applied to the AS, the microorganisms produce positively charged extracellular polymeric substance (EPS) that reduces the repulsive electrostatic interactions between the floc, increasing zeta potential, and allowing the floc to agglomerate into larger particles. EPS production is a mechanism that allows granulation to occur and results in a more positive zeta potential, between -14 and -9 mV [17,18]. The zeta potential of the AS was measured throughout the study to evaluate changes in floc charge and an additional indication of granule formation. Results from these measurements are shown in Figure 2.6.

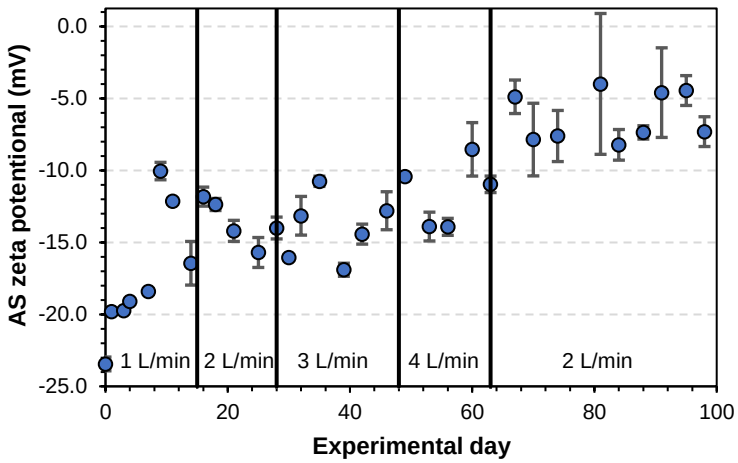

Figure 2.6 Zeta potential measurements of the AS for 98 days of the experiment. The seed AS was highly negative resulting in repulsive electrostatic integration and poor settleability. With the production of positively charged EPS the zeta potential becomes more positive and settleability is improved.

The zeta potential of the seed AS was highly negative (-23.3 mV) but quickly became more positive, reaching -18.4 mV within the first week and fluctuating between -17 to -10 mV from day 9 to day 60 of the experiment. On day 67 AGS floc were first visually detected in the bioreactor, the zeta potential measured -10 mV and reached a maximum value of -4.0 mV on day 81; the SVI's, floc diameter, and settling velocity on day 81 were 21 mL/g, 293 µm (mean value), and 20 m/h, respectively. A change in pH does have the potential to alter the zeta potential of AS, the average sample pH was 7.3±0.2, a variation of this magnitude

would not cause such changes AS zeta potential. The zeta potential likely became more positive between day 60 and day 81 because the total cycle time was increased from 283 to 419 minutes (60 anaerobic minutes and 310 aerobic minutes), which would have increased the feast/famine conditions and placed additional environmental stress on the AS. Zeta potential could not be measured and related to other observation after day 98 because the floc settled too quickly in the instrument for accurate measurements to be taken.

2.4.1.4 Phase contrast

Phase contrast images of the AS at 100x magnification were taken throughout the experiment to evaluate changes in the structure and general microbial composition of the AS floc. Gram stained and unstained-live photos of the AS are shown in Figure 2.7.

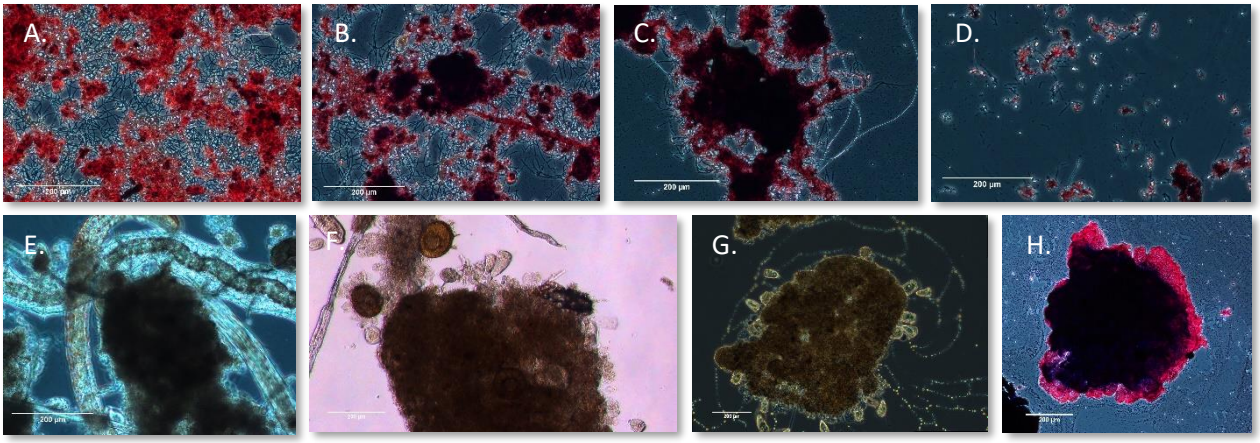

Figure 2.7 Phase contrast photos of AS, pictures A, B, C, D, and H are gram stained, E, F and G are live samples. A) Day 0 AS is dominated by filamentous bacteria. B) Day 9, concentration of filamentous bacteria begins to decrease. C) Day 32, larger floc began to develop, low concentrations of filamentous bacteria remain. D) Day 46, pin floc had developed, and high concentration of biosolids are detected in the decant. E) Day 60, high concentrations of nematodes were destroying floc. F) Day 74, anaerobic phase was increased on day 63, the majority of the nematodes were eliminated, and floc began to regrow. G) Day 82, aerobic granular sludge has developed. H) Day 101, aerobic granules dominate the AS, no filamentous bacteria are observed.

The seed AS was dominated by loose floc connected by a dense matrix of filamentous microorganisms (Figure 2.7A). Images of the floc taken on day 9 show improvements in the AS floc structure, the floc was denser with more defined edges and there was a clear reduction in filamentous bacteria (Figure 2.7B). By day 32, very few filamentous bacteria were present, and floc had increased in diameter (Figure 2.7C). Images taken on day 46 of the experiment showed the physical characteristics of the AS had changed (Figure 2.7D), the flocs began to break apart and although the AS still settled quickly the presence of pin floc was observed in the bioreactor decant. At the time it was unknown why pin floc had developed. The typical cause, deterioration of small and weak floc due to the lack of filamentous bacteria [35,36] was not considered a factor because filamentous bacteria were still present in the AS. On day 60 of the experiment

phase contrast images revealed that a high concentration of nematodes had accumulated in the bioreactor (Figure 2.7E). The nematodes were observed preying on the AS floc and breaking up the floc into smaller pin floc. Nematodes were no longer observed by day 74 and the AS floc had begun to redevelop (Figure 2.7F). The first phase contrast photos of the AGS were taken on day 82 (Figure 2.7G), these images showed the presence of stalked ciliates. Stalked ciliates are considered one of the main building blocks of AGS [37,38]. AGS dominated the AS by the 100th day of the experiment (Figure 2.7H).

2.4.2 Nutrient removal

The source of the wastewater used in this study was from a student housing complex that experiences large swings in the student population throughout the year. Previous wastewater treatment work conducted at this location has shown that the sCOD and ammonia concentrations fluctuates throughout the year with the student population [14,39]. The influent ammonia and sCOD concentration were measured regularly during the study to monitor changes in the bioreactor loading and to make process adjustments, if necessary. The measurements from the influent sCOD and ammonia analyses are presented in Figure 2.8.

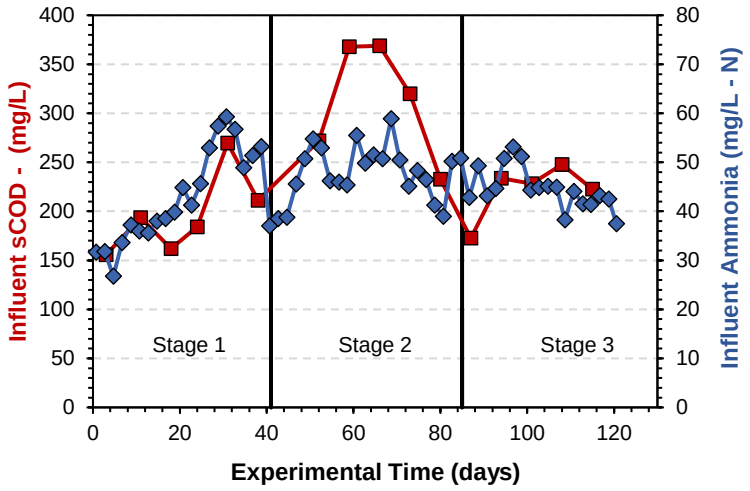

Figure 2.8 Influent sCOD and ammonia measured over the 120-day experiment. Due to the fact that the majority of the wastewater is provided by a student housing complex there are large swings in the sCOD and ammonia concentration that require a dynamic treatment cycle. Each stage provides a unique treatment cycle designed to reduce sCOD and ammonia below 30 mg/L and 10 mg/L-N, respectively.

The influent sCOD and ammonia concentrations varied during the experiment with the lowest concentrations measured on day 0, peak concentrations measured on day 66, and more moderate and consistent concentrations measured after day 85. The influent sCOD at the start of the experiment was particularly low (sCOD = 150 mg/L), which resulted in a C:N ratio of less than 5 (100:20) – lower than what is considered ideal (100:10 – 100:5) for nitrogen removal [40,41]. The sCOD and ammonia concentrations began increasing steadily over the next 40 days of the experiment and the C:N ratio improved to 100:13. Due to the increased sCOD concentration in the effluent, bioreactor operation changed on day 41. Stage 2 operations decreased the exchange ratio from 30 to 20% and increased the aeration time from 168 to 330

minutes. Following the operational changes, the influent sCOD concentration continued to increase until peaking to 369 mg/L on day 66, the C:N ratio at the peak was 100:12. After the influent sCOD concentration peaked, the sCOD concentration steadily declined and reached a low concentration of 170 mg/L on day 87. The influent ammonia concentration remained between 40 and 50 mg/L over this same period, resulting in the influent having a low C:N ratio, approximately 100:20. The exchange ratio was increased on day 85 (Stage 3) from 20 to 30% and the aeration time was reduced to 310 minutes to accommodate the lower and more stable influent sCOD. For the remainder of the experiment C:N ratio varied between 100:19 to 100:30.

2.4.2.1 sCOD removal

One of the main operating objectives in this study was to maintain an effluent sCOD of less than 30 mg/L, which is a common effluent discharge limit for many WRRFs. Because the influent sCOD concentration varied during the study, the bioreactor operation had to be changed periodically to account for the swings in loading and maintain the effluent sCOD concentration below 30 mg/L. The influent and effluent sCOD concentration and percent sCOD removal measured during the study are shown in Figure 2.9.

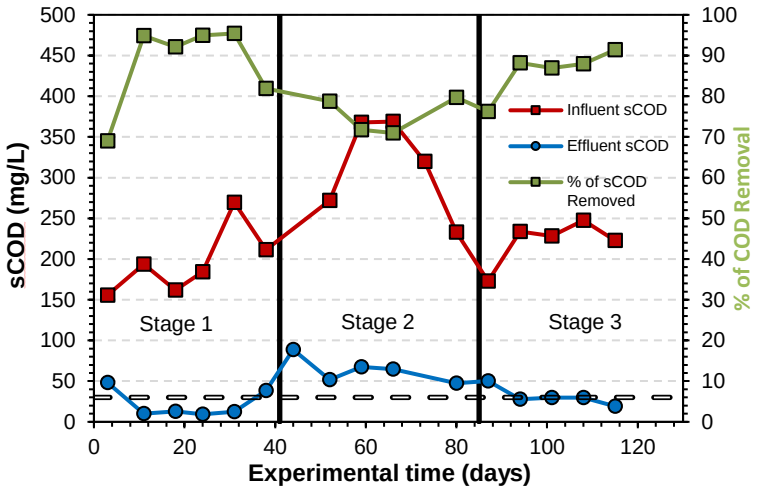

Figure 2.9 Influent and effluent sCOD and percent sCOD removal measured over the 120-day experiment. The target effluent sCOD concentration (30 mg/L) is shown as a dashed line and operational changes made on day 40 and 85 of the experiment are shown as solid vertical lines.

The sCOD removal was above 90% and the effluent sCOD concentration was below 20 mg/L over the first 20 days of the experiment, except for day 3 when the system was recovering from the initial loss of AS. The percent sCOD removal started to decline and the effluent sCOD concentration began to rise after day 31. This was likely due to the sCOD loading increasing by almost 50%, from 330 mg/(L d) to 480 mg/(L d), between day 38 and day 59. Stage 2 operational changes provide a longer oxidation period to account for the higher influent sCOD concentration and improve the sCOD removal.

During Stage 2 effluent sCOD continued to rise. The average sCOD removal was reduced to 75% and remained constant for the entire stage. On day 59 influent sCOD reached a peak concentration of 368 mg/L and soon after began to decrease. The effluent sCOD concentration steadily decreased and the percent removal was constant during Stage 2. The improvement in effluent sCOD concentration was impart due to the longer aeration period used during Stage 2 and the lower influent sCOD concentrations observed after day 80. At the same time the loading rate had declined to 179 (mg/(L*day)). To increase MLSS concentration and loading rate the exchange ratio was increased from 20 to 30% in Stage 3.

During Stage 3 the percentage of sCOD removal had increased to 88% or greater and effluent sCOD was below the target value of 30 mg/L with the exception of day 87. Influent sCOD had decreased to 178 mg/L on day 87 then averaged 230 mg/L for the remainder of the experiment. Loading rate of the reactor also increased from 179 to 267 mg/(L day) by the end of Stage 3. Constant effluent sCOD concentrations could have been maintained if higher concentrations of MLSS were present; future experiments could accomplish this task by setting a limit on AS removed by the selector per day. The increase in sCOD observed at the end of Stage 1, although negatively impacting effluent concentration, could have also encourage the develop of AGS, which typically have high COD loading rate of 600-3000 mg/(L d) [42].

2.4.2.2 Nitrogen Removal

There were two objectives related to nitrogen removal in this study. The first was to maintain nitrogen removal during startup and the second was to have an effluent concentration below 10 mg/L as total nitrogen over the full study period. The bioreactor operating conditions were changed twice during the study to try to maintain the effluent nitrogen concentration below this limit. The effluent ammonia and nitrate concentrations measured during the study are shown in Figure 2.10.

The effluent ammonia concentration was less than 0.5 mg/L and the percent of ammonia removal was greater than 98% over the first 30 days of the experiment, indicating nitrification was maintained during startup. The influent ammonia increased from 40 to 60 mg/L between day 22 and day 30, resulting in the effluent ammonia concentration spiking on day 37 to 10 mg/L-N. After day 37, the effluent ammonia concentration began to decrease, and ammonia removal improve due to lower influent ammonia concentrations between days 30 and 43. The improvement in ammonia removal was likely also due to the longer aeration time used during Stage 2 operation. A second spike in the effluent ammonia concentration was observed on day 57 of the experiment and was associated with the influent ammonia concentration increasing from 38 to 54 mg/L-N between days 43 and 51. The ammonia removal recovered by day 68 and the effluent ammonia remained low over the remainder of the experiment.

Nitrification was maintained throughout the experiment due to adequate DO levels and most importantly an SRT higher than 7 days. The brief lapses in nitrification were mostly due to the simultaneous presence of high strength wastewater and a low MLSS concentration. This problem could be resolved in future experiments by limiting the mass of floc discharged by the selector and thus maintaining a higher concentration of MLSS. The effluent nitrate concentration at the start of the experiment was 20 mg/L-N, this

occurred because of the high C:N ratio of 100:20, an ideal C:N would be less than 100:15. The C:N ratio improved after day 41 to 100:13 resulting in much lower effluent nitrate concentrations, reaching a low concentration of 6.5 mg/L-N on day 53. The influent sCOD began to decrease and the C:N ratio worsen at the end of Stage 2, which caused the effluent nitrate concentration to peak on day 90 to 30 mg/L-N.

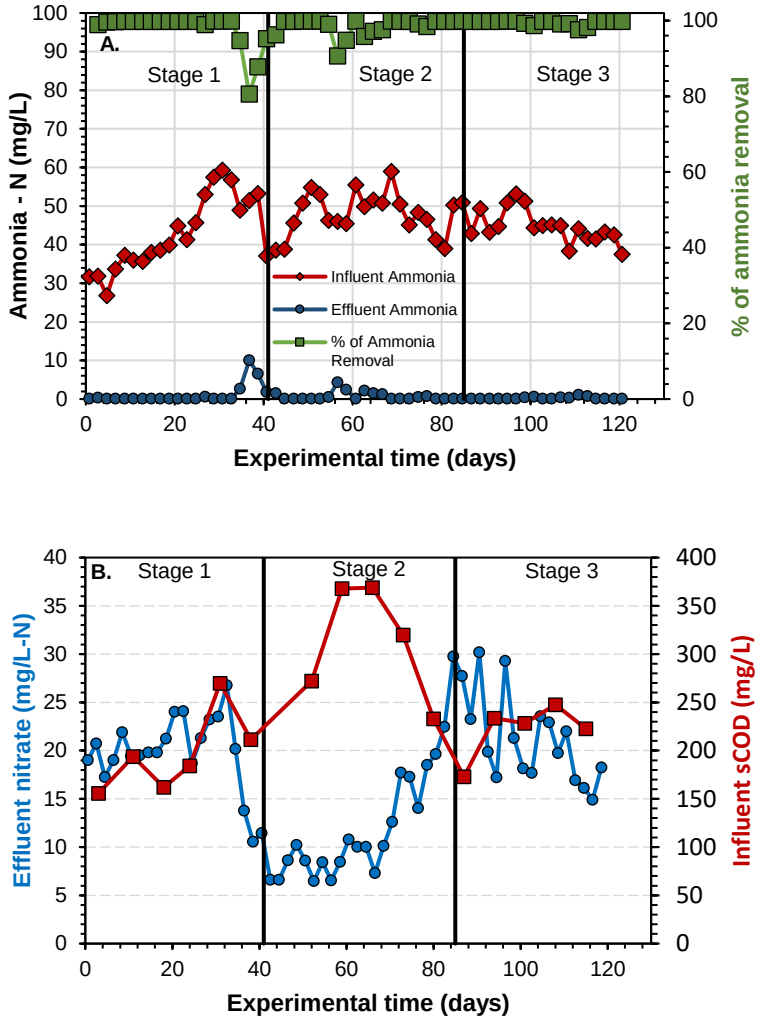

Figure 2.10 A) influent and effluent ammonia concentration and percent ammonia removal and B) influent sCOD and effluent nitrate concentration measured during the experiment. Operational changes made on day 40 and 85 of the experiment are shown as solid black vertical lines.

Although the operating conditions were ideal for nitrification, the system was not able to maintain denitrification throughout the experiment. This can be explained due to reoccurring events of low C:N ratio and the operation of the bioreactor at a DO above 2 mg/L, preventing simultaneous nitrification/denitrification. The problem of high nitrogen concentrations is common at WRRFs—supplemental carbon is typically used to shift the C:N ratio. Glycerol, a form of supplemental carbon, was dosed into the wastewater during the fill phase on days 90 and 96 to increase denitrification and reduce the effluent nitrogen concentration, and an immediate reduction of nitrate was observed. With the addition of

carbon and a second anoxic/anaerobic period it may be possible to maintain effluent nitrate concentrations below 10 mg/L-N. An example of these data for a single cycle during sufficient and limited carbon scenarios is presented in Figure 2.11.

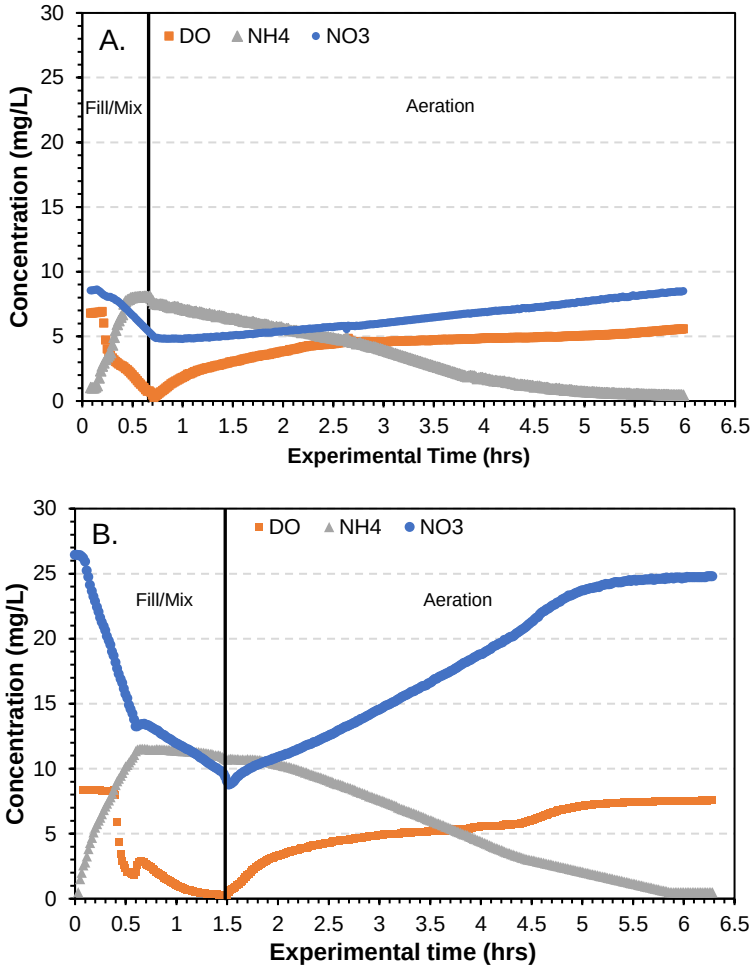

Figure 2.11 Online dissolved oxygen, ammonia, and nitrate probe data from a single fill, mix, and aeration phase cycle. Results are from A) Stage 2, sufficient carbon scenario and B) Stage 3, carbon limited scenario.

During Stage 2 (Figure 2.11A), the carbon-sufficient scenario, DO concentration remained high for the first 0.2 hours due to the sensor being exposed to the atmosphere while the tank was filling. The DO then rapidly decreased due to the mixing of the MLSS. Ammonia concentration increased steadily during the fill/mix phase. Nitrate concentration decreased rapidly during the fill/mix phase and did not stagnate, meaning that there was still sCOD present; and if the mixing time would have been extended, the nitrate concentration would have continued to decrease. During the aeration period the DO slowly rises as the microorganisms use the oxygen to oxidize the carbon to carbon dioxide and the ammonia to nitrate. The final ammonia and nitrate concentration were 0.5 and 7.5 mg/L-N, respectively, at the end of the cycle – below the target effluent inorganic nitrogen concentration of 10 mg/L-N.

During Stage 3 (Figure 11B), carbon-limited scenario, the DO remained high for the first 0.4 hours due to the sensor being exposed to the atmosphere while the tank was filling then rapidly decreased due to the mixing of the MLSS. The Stage 3 fill phase time was increased due to the higher exchange ratio. Ammonia concentration increased during the fill phase and remained stable throughout the mixing phase. Nitrate rapidly decreased during the fill phase at 0.44 mg/min; then in the mixing phase the rate of denitrification decreased due to limited soluble carbon availability, reducing the denitrification rate to 0.075 mg/L-min, reaching a low value of 9 mg/L-N. During the aeration phase DO slowly increased as ammonia was reduced from 12 mg/L-N to less than 0.5 mg/L-N. Nitrate concentration increased reaching a maximum of 24.5 mg/L-N, effluent total nitrogen concentration was 25.0 mg/L-N. With the addition of supplemental carbon, the faster dentification rate could have been sustained and effluent nitrogen concentration maintained below 10 mg/L-N.

Another possibility that resulted in high effluent nitrate is the bioreactor DO concentration constantly being above 2 mg/L, high DO levels prevent the simultaneous nitrification/denitrification to occur. Therefore, It cannot be conclusive that the C:N was the sole reason for high effluent nitrate. Additional experiments investigating C:N, lower DO levels for simultaneous nitrification/denitrification and hydraulic selection will be required.

2.4.2.3 Decant biosolids

In addition to the sCOD and nitrogen effluent quality objectives, an objective was set to keep the effluent TSS concentration below 30 mg/L, which is a typical WRRF effluent discharge limit. The effluent TSS was measured using a TSS probe installed on the bioreactor decant line. The TSS of the decant measured over the study is shown in Figure 2.12.

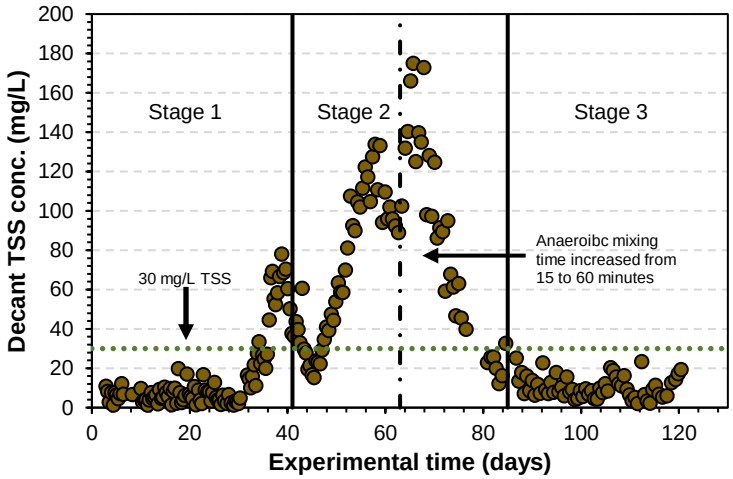

Figure 2.12 Bioreactor effluent (decant) TSS measured over the 120-day the experiment. Operational changes made on day 40 and 80 of the experiment are shown as solid black vertical lines. An increase in the anaerobic mixing time made on day 63 is shown as a vertical broken line.

The highest decant TSS concentration (800 mg/L, not shown in the Figure 12) was measured during the first bioreactor cycle on the first day of the experiment. The decant TSS concentration was so high because the seed AS did not settle well and the top of the sludge blanket was above the decant port when the effluent was drawn out of the reactor. Enough biosolids were wasted through the selector on the first cycle that the sludge blanket dropped below the decant point during the second cycle, resulting in an immediate decrease in the decant TSS concentration below 30 mg/L. The decant TSS remained low until day 30, after which the decant biosolids began to fluctuate. The decant TSS concentration peaked to 78 mg/L on day 38 and peaked again to 175 mg/L on day 65. As described in Section 3.1.4, visual inspection of the decant revealed that the effluent was full of pin floc that appeared to be contributing to the high TSS concentration. On day 60, the AS was inundated with nematodes that were observed physically breaking the floc apart. After the nematodes were eliminated the decant TSS concentration began to steadily decrease by the end of Stage 2, the decant TSS was less than 30 mg/L and remained below 30 mg/L for the remainder of the study.

2.5 Conclusion

The results from this study demonstrate that the implementation of the hydraulic selector in a batch reactor is effective in improving the settling properties of the AS. Through the removal of poor settling floc, SVI_{30} and SVI_4 decreased below 50 mL/g and settling velocity reached 20 m/hr by day 63 of the experiment. The floc diameter of the AS also increased throughout the experiment and contributed to the increased settling velocities and lower SVI values. Zeta potential measurements showed that the AS became more positive, indicating that feast/famine conditions were present in the bioreactor that most likely contributed to granulation of the AS. While previous researchers have tried to grow AGS in bench scale bioreactors with a D:W less than 2.5, they proved to be unsuccessful [9,10,24,25]. Even though the D:W ratio is an artifact of lab-scale reactors full scale AGS reactors still require a height of 5.5 m that is not typical of older AS basin or clarifier design.

Applying the hydraulic selector along with feast/famine conditions in continuous flow systems could have the ability to improve AS settleability. Stages 1 and 3 were successful in maintaining the effluent sCOD below 30 mg/L. Stage 2 was not able to obtain the same effluent quality, but the reduced exchange ratio and increased aeration time did allow the stage to maintain constant percentage of sCOD removal when influent sCOD increased. Nitrification was nearly maintained for the entire experiment with the exception of a few days due to a sudden change in influent wastewater strength, and denitrification was only maintained for a limited period during the experiment due to an unfavorable carbon to nitrogen ratio. In future experiments effluent water quality parameters can be obtained by further adjusting exchange ratios, anaerobic time, aeration time, and carbon to nitrogen ratios. This manuscript illustrates the potential of an alternative hydraulic selective technology and its ability to improve AS settling properties with potentially minimal changes to wastewater treatment infrastructure.

Acknowledgments

The authors would like to thank the National Science Foundation-funded Engineering Research Center for Reinventing the Nation's Urban Water Infrastructure (ReNUWIt) (NSF EEC-1028968), and a grant from the Colorado Higher Education Competitive Research Authority (CHECRA). The author would also like to thank Dr. James Ranville, Dr. Geoff Brennecka, Mr. Tyler LeClear, Ms. Brooke Marten, Ms. Megan Frytag, Ms. Moira Laughlin, Mr. Mike Veres and Mr. Tani Cath for their technical and scientific support.

2.6 References

[1] United States Environmental Protection Agency. Basic Information about Water Security, (n.d.). https://web.archive.org/web/20150906005124/http://water.epa.gov/infrastructure/watersecurity/basicinformation.cfm (accessed December 1, 2017).

[2] T. Sato, M. Qadir, S. Yamamoto, Global , regional , and country level need for data on wastewater generation , treatment , and use, Agric. Water Manag. 130 (2013) 1–13. doi:10.1016/j.agwat.2013.08.007.

[3] ASCE's 2017 Infrastructure Report Card, Conditions & Capacity, (2017). www.infrastructurereportcard.org/wastewater/conditions-capacity/.

[4] G. Tchobanoglous, Wastewater Engineering Treatment and Resource Recovery, 5th ed., McGraw-Hill Education, United Kingdom, 2014.

[5] B. Ni, W. Xie, S. Liu, H. Yu, Y. Wang, G. Wang, X. Dai, Granulation of activated sludge in a pilot-scale sequencing batch reactor for the treatment of low-strength municipal wastewater, Water Res. 43 (2009) 751–761. doi:10.1016/j.watres.2008.11.009.

[6] J.H. Tay, S.F. Yang, Y. Liu, Hydraulic selection pressure-induced nitrifying granulation in sequencing batch reactors, Appl. Microbiol. Biotechnol. 59 (2002) 332–337. doi:10.1007/s00253-002-0996-6.

[7] H. Horn, C. Klarmann, K. Sørensen, T. Rocktäschel, P. Boisson, J. Ochoa, Influence of the granulation grade on the concentration of suspended solids in the effluent of a pilot scale sequencing batch reactor operated with aerobic granular sludge, Sep. Purif. Technol. 142 (2015) 234–241. doi:10.1016/j.seppur.2015.01.013.

[8] M. Pronk, M.K. De Kreuk, B. De Bruin, P. Kamminga, R. Kleerebezem, M.C.M. Van Loosdrecht, Full scale performance of the aerobic granular sludge process for sewage treatment, Water Res. 84 (2015) 207–217. doi:10.1016/j.watres.2015.07.011.

[9] R.D.G. Franca, H.M. Pinheiro, M.C.M. Van Loosdrecht, N.D. Lourenço, Stability of aerobic granules during long-term bioreactor operation, 36 (2018) 228–246. doi:10.1016/j.biotechadv.2017.11.005.

[10] Y. V Nancharaiah, G.K. Kumar, Bioresource Technology Aerobic granular sludge technology : Mechanisms of granulation and biotechnological applications, 247 (2018) 1128–1143. doi:10.1016/j.biortech.2017.09.131.

[11] M.K.D.K. Ã, M. Pronk, M.C.M. Van Loosdrecht, Formation of aerobic granules and conversion processes in an aerobic granular sludge reactor at moderate and low temperatures, 39 (2005) 4476–4484. doi:10.1016/j.watres.2005.08.031.

[12] M.K. De Kreuk, C. Uijterlinde, Aerobic granular sludge technology : an alternative to activated sludge ?, (2001) 1–7.

[13] T. Rocktäschel, C. Klarmann, B. Helmreich, J. Ochoa, P. Boisson, K.H. Sørensen, H. Horn, Comparison of two different anaerobic feeding strategies to establish a stable aerobic granulated sludge bed, Water Res. 47 (2013) 6423–6431. doi:10.1016/j.watres.2013.08.014.

[14] D. Vuono, J. Henkel, J. Benecke, T.Y. Cath, T. Reid, L. Johnson, J.E. Drewes, Flexible hybrid membrane treatment systems for tailored nutrient management: A new paradigm in urban wastewater treatment, J. Memb. Sci. 446 (2013) 34–41. doi:10.1016/j.memsci.2013.06.021.

[15] American Public Health Association (APHA), Standard Methods for the Examination of Water & Wastewater 21st Edition, Am. Public Heal. Assoc. Am. Water Work. Association, Water Environ. Fed. (1999) 541. http://www.mwa.co.th/download/file_upload/SMWW_1000-3000.pdf.

[16] A. Sochan, C. Polakowski, G. Łagód, Impact of optical indices on particle size distribution of activated sludge measured by laser diffraction method, Ecol. Chem. Eng. S. 21 (2014) 137–145. doi:10.2478/eces-2014-0012.

[17] B. Su, Z. Qu, Y. Song, L. Jia, J. Zhu, Journal of Environmental Chemical Engineering Investigation of measurement methods and characterization of zeta potential for aerobic granular sludge, Elsevier. 2 (2014) 1142–1147. doi:10.1016/j.jece.2014.03.006.

[18] Z. Li, P. Lu, D. Zhang, G. Chen, S. Zeng, Q. He, Population balance modeling of activated sludge flocculation : Investigating the influence of Extracellular Polymeric Substances (EPS) content and zeta potential on flocculation dynamics, Sep. Purif. Technol. 162 (2016) 91–100. doi:10.1016/j.seppur.2016.02.011.

[19] M. Woombs, J. Laybourn-Parry, Seasonal species composition, density and role of nematodes in activated-sludge effluent treatment works, Water Res. 21 (1987) 459–467. doi:10.1016/0043-1354(87)90194-1.

[20] Z.W. Wang, Y. Liu, J.H. Tay, The role of SBR mixed liquor volume exchange ratio in aerobic granulation, Chemosphere. 62 (2006) 767–771. doi:10.1016/j.chemosphere.2005.04.081.

[21] D. Gao, L. Liu, H. Liang, W.M. Wu, Aerobic granular sludge: Characterization, mechanism of granulation and application to wastewater treatment, Crit. Rev. Biotechnol. 31 (2011) 137–152. doi:10.3109/07388551.2010.497961.

[22] B.S. McSwain, R.L. Irvine, P.A. Wilderer, The effect of intermittent feeding on aerobic granule

structure, Water Sci. Technol. 49 (2004) 19–25. doi:10.2166/wst.2004.0794.

[23] M.K. de Kreuk, M.C.M. van Loosdrecht, Selection of slow growing organisms as a means for improving aerobic granular sludge stability, Water Sci. Technol. 49 (2004) 9–17. doi:10.2166/wst.2004.0792.

[24] Y. Kong, Y.Q. Liu, J.H. Tay, F.S. Wong, J. Zhu, Aerobic granulation in sequencing batch reactors with different reactor height/diameter ratios, Enzyme Microb. Technol. 45 (2009) 379–383. doi:10.1016/j.enzmictec.2009.06.014.

[25] C. Wu, Y. Peng, R. Wang, Y. Zhou, Chemosphere Understanding the granulation process of activated sludge in a biological phosphorus removal sequencing batch reactor, Chemosphere. 86 (2012) 767–773. doi:10.1016/j.chemosphere.2011.11.002.

[26] M.K.H. Winkler, R. Kleerebezem, W.O. Khunjar, B. de Bruin, M.C.M. van Loosdrecht, Evaluating the solid retention time of bacteria in flocculent and granular sludge, Water Res. 46 (2012) 4973–4980. doi:10.1016/j.watres.2012.06.027.

[27] D. Wu, Z. Zhang, Z. Yu, L. Zhu, Optimization of F/M ratio for stability of aerobic granular process via quantitative sludge discharge, Bioresour. Technol. 252 (2018) 150–156. doi:10.1016/j.biortech.2017.12.094.

[28] J.P. Bassin, M.K.H. Winkler, R. Kleerebezem, M. Dezotti, M.C.M. van Loosdrecht, Improved phosphate removal by selective sludge discharge in aerobic granular sludge reactors, Biotechnol. Bioeng. 109 (2012) 1919–1928. doi:10.1002/bit.24457.

[29] Y. Sun, B. Angelotti, Z.W. Wang, Continuous-flow aerobic granulation in plug-flow bioreactors fed with real domestic wastewater, Sci. Total Environ. 688 (2019) 762–770. doi:10.1016/j.scitotenv.2019.06.291.

[30] K. Sears, J.E. Alleman, J.L. Barnard, J.A. Oleszkiewicz, Density and Activity Characterization of Activated Sludge Flocs, J. Environ. Eng. 132 (2006) 1235–1242. doi:10.1061/(asce)0733-9372(2006)132:10(1235).

[31] Y. Liu, J.H. Tay, State of the art of biogranulation technology for wastewater treatment, Biotechnol. Adv. 22 (2004) 533–563. doi:10.1016/j.biotechadv.2004.05.001.

[32] A.M. Maszenan, Y. Liu, W.J. Ng, Bioremediation of wastewaters with recalcitrant organic compounds and metals by aerobic granules, Biotechnol. Adv. 29 (2011) 111–123. doi:10.1016/j.biotechadv.2010.09.004.

[33] F. Jorand, F. Thomas, J.C. Block, I.J.Y. Bottero, G. Villemin, V. Urbain, J. Manem, X. Santr-environnement, S. Pharmaceutiques, N. Cedex, E. Minrralurgie, E.N.S. De, Chemical and Structural (2D) linkage between bacteria within activated sludge flocs, Water Res. 29 (1995) 1639–1647.

[34] D. hong Li, J. Ganczarczyk, Flow through activated sludge flocs, Water Res. 22 (1988) 789–792. doi:10.1016/0043-1354(88)90192-3.

[35] D. Parker, D.S, Kaufman, W.J, Jenkins, Floc breakup in turbulent flocculation processes, J.

Sanit. Eng. (1972) 79–99.

[36] D. Jenkins, M.G. Richard, G.T. Daigger, Manual on the causes and control of activated sludge bulking, foaming, and other solids separation problems, 2004.

[37] S.S. Adav, D.-J. Lee, J.-Y. Lai, Potential cause of aerobic granular sludge breakdown at high organic loading rates, Appl. Microbiol. Biotechnol. 85 (2010) 1601–1610. doi:10.1007/s00253-009-2317-9.

[38] S.D. Weber, W. Ludwig, K.H. Schleifer, J. Fried, Microbial composition and structure of aerobic granular sewage biofilms, Appl. Environ. Microbiol. 73 (2007) 6233–6240. doi:10.1128/AEM.01002-07.

[39] D.C. Vuono, J. Benecke, J. Henkel, W.C. Navidi, T.Y. Cath, J. Munakata-Marr, J.R. Spear, J.E. Drewes, Disturbance and temporal partitioning of the activated sludge metacommunity., ISME J. (2014) 1–11. doi:10.1038/ismej.2014.139.

[40] C. Choi, J. Lee, K. Lee, M. Kim, The effects on operation conditions of sludge retention time and carbon/nitrogen ratio in an intermittently aerated membrane bioreactor (IAMBR), Bioresour. Technol. 99 (2008) 5397–5401. doi:10.1016/j.biortech.2007.11.016.

[41] Z. Fu, F. Yang, F. Zhou, Y. Xue, Control of COD/N ratio for nutrient removal in a modified membrane bioreactor (MBR) treating high strength wastewater, Bioresour. Technol. 100 (2009) 136–141. doi:10.1016/j.biortech.2008.06.006.

[42] B.A. Figdore, Nitrification bioaugmentation in mainstream flocculent activated sludge systems using sidestream aerobic granular sludge, (2017).

CHAPTER 3

REDUCING SOLID RETENTION TIME THROUGH HYDRAULIC SELECTION FOR THE DEVELOPMENT OF AEROBIC GRANULAR SLUDGE

A manuscript under review in Separation and Purification Technology

Rudy A. Maltos[1], Aurora Waclawski[1], Brooke Marten, Tyler LeClear, Faylyn Bruecken[1], Sadie Jonson[1], Tani J. Cath[1], Ryan W. Holloway[2], Ganesh Rajagopalan[2], Jean Debroux[2], Tzahi Y. Cath[1*]

3.1 Abstract

The hydraulic selector (HS) provides an alternative selection process for the removal of poor settling floc in activated sludge (AS), and when combined with appropriate feast/famine conditions, traditional AS can be transformed into aerobic granular sludge (AGS). Unlike traditional AGS reactors or hydrocyclones, the HS has no minimum reactor height and does not induce high shear forces that results in floc destruction. The HS, a uniquely designed vacuum system, generates a fluid velocity field around the selector that targets and removes poorly settling floc. Previous HS studies were successful in enhancing the AS settling characteristic; however, only HS was used for the biomass wasting, and resulted in a solid retention time (SRT) >20 d. The objective of this study was to improve the AS settling characteristics, such as sludge volume index and settling velocity, while reducing the biomass wasted through the HS and maintaining an SRT below 15 d by utilizing traditional AS sludge wasting (wasting from the bottom of the reactor after the settling phase). For the duration of the study the food to microorganism ratio was maintained between 0.1 and 0.2. The 238-d study results highlight the benefits of operating HS in a reduced capacity, resulting in an increase in AS settling velocity (from <1 to 18 m/h) and an increase in mean floc diameter (from 60 to 540 µm). Thus, when operated at a limited capacity the HS induces enough selection to improve the AS settling characteristic and develop AGS.

3.2 Introduction

More than 70% of the water resource reclamation facilities (WRRFs) in the United States are conventional activated sludge (CAS) plants that use biological processes to remove nitrogen (N), phosphorus (P), carbon, and other pollutants from wastewater [1]. Many of these CAS plants were built in the 1970s and ‘80s as a response to the Clean Water Act, but the aging infrastructure now requires upgrades to meet the higher demand placed on the facilities by growing populations and more stringent discharge regulations [2,3]. To meet these demands, WRRFs are forced to undergo expensive and intrusive capital improvement projects; thus, there is an obvious need to find easily implementable and low-cost solutions to increase WRRF capacity and efficiency.

The secondary clarifier is considered a bottleneck for WRRFs—long settling times in secondary clarifiers result in an increased hydraulic retention time, higher pumping costs, and often higher concentrations of solids escaping the clarifier. Slow settling floc is a common and perpetuating problem at

WRRFs due to the design of the clarifiers, which continuously recycle slow settling floc that are <100 µm in size or are predominantly filamentous bacteria.

Aerobic granular sludge (AGS) has been recognized as a next generation activated sludge (AS) treatment because it simultaneously nitrifies and denitrifies (SND), thereby allowing for 1) the development of phosphorus-accumulating organisms (PAO), 2) resistance to spikes in nutrient loading, and 3) improved settleability properties [4–6]. Under appropriate oxic conditions, AGS can also remove ammonium via the nitrite pathway; this process requires approximately 25% less oxygen compared to CAS, and approximately 40% less electron donor for denitrification compared to nitrogen removal via nitrate [7]. Denitrifying PAOs, a desirable class of microorganisms present in AGS systems, use nitrite or nitrate as an electron acceptor to remove phosphorus, which utilizes carbon in the most effective manner and reduces the aeration requirement [5,8,9]. Lastly, the settling velocity of AGS ranges between 15 and 60 m/h, far faster than traditional CAS AS, which ranges from 1 to 10 m/h.

Although there are benefits to AGS, the development of granules has not been easily achieved. In the pursuit of the perfect operating conditions for AGS development and maintenance, numerous operation variables have been tested by many researchers at bench, pilot, and full-scale. Variables that have been tested over the last three decades include influent wastewater strength (chemical oxygen demand (COD), N, and P concentrations), aerobic to anoxic/anerobic ratio, bioreactor (BR) fill process/conditions, solid retention times (SRT), hydraulic retention times, and required water temperature, to list a few [7,10–13]. However, the physical selection pressure required to develop AGS has not been tested as rigorously, relying on minimum settling velocity and, more recently, hydrocyclones for the separation of fast and poor settling floc [14].

For a traditional AGS reactor, hydraulic selection may be achieved through a minimum settling velocity, which is dependent on the distance that a floc must settle prior to the beginning of the decant phase. During this settling phase the reactor height is crucial—it allows floc to overcome turbulent conditions and stratify according to their terminal velocities. Flocs with a terminal velocity less than the minimum settling velocity are then removed during the decant. Over time, this method decreases the settling time, leading to in an increase in minimum settling velocity and resulting in an accumulation of fast settling dense sludge. At full-scale, a typical AGS system requires a minimum bioreactor height of 5.5 m (18 ft) [5], a depth not commonly found at WRRFs. Additionally, the startup of a traditional AGS system results in a large loss of biomass due to the zone and compression settling that is common in activated sludge systems. Once the AS begins to transform, the flocs begin to behave like discrete particles and unintentional wasting of solids declines.

A hydrocyclone develops floc selection through pressure and density requirements. AS entering the hydrocyclone experiences a centrifugal force—the denser flocs will be close to the inside wall of the hydrocyclone and will drain out through the underflow, and flocs that are not dense enough to escape via the underflow are pulled into a vortex and overflow with the effluent. Few studies have been successful in separating slow from fast settling floc with hydrocyclones and have observed improvements in sludge volume index (SVI) [14,15]. Other studies have used hydrocyclones to deliver additional shear force on AS,

resulting in an increased production of extracellular polymeric substance (EPS) and release of soluble COD (sCOD) [15–17]. Currently, hydrocyclones lack the ability to control and obtain a specific floc diameter distribution of AS, which is important for long term operation because flocs <300 µm result in limited SND ability and flocs >1000 µm have carbon diffusion limitations. Thus, ideal conditions would be able to regulate size distribution through hydraulic selection operation.

Nevertheless, improved solid-liquid separation can still be achieved by targeting and eliminating floc with poor settling characteristics within the BRs. Recently, a pilot scale study conducted at the Colorado School of Mines (Mines) demonstrated that a new selection technology, the hydraulic selector (HS), along with feast/famine conditions could develop AGS [18]. The system produced AGS with a diameter of 250-1000 µm and an AS settling velocity of 20 m/h while operating with a BR depth of 0.9 m and depth to width ratio of 1.3. The HS technology was the only mechanism used for the AS wasting and resulted in solid retention time longer than 20 d. The HS is a uniquely designed vacuum system that generates a fluid velocity field around the selector to remove poor settling floc. At low flow discharge rates, low density floc or slower-settling floc are pulled into the selector and withdrawn from the AS while denser solids are retained in the BR.

While the previous HS study was successful, there were two aspects of the research that require further investigation. Specifically, we need to understand how the duration and operating conditions of the HS impact AS settling velocity and if the HS could be combined with traditional AS wasting to reduce SRT below 15 d. In our prior research, only one sudden increase in AS settling velocity was observed, and by that time, four unique HS operating conditions had been tested, which made it difficult to explore how each of the conditions influenced the changing settling velocity of the AS. Another aspect of the HS operation that required additional insight is an understanding of the minimum amount of biomass that must be wasted through the HS to achieve granulation. In our previous study wasting occurred solely through the HS; however, this new wasting paradigm may pose a challenge to facilities with limited dewatering capacity. Wasting solely through the selectors removes a higher percentage of poor settling floc compared to wasting from the bottom of a BR, but the HS effluent has a low total suspended solids (TSS) concentration. Thus, the total volume discharged to the dewatering process will increase if the same SRT is maintained and will pose a problem to those facilities that cannot easily increase their dewatering throughput. If the dewatering volumes are maintained constant, as in our previous study, SRT will increase and will pose a new challenge. SRT values above 15 d increase the mixed liquor suspended solids (MLSS) beyond a necessary concentration. Then, the food to microorganism ratio (F/M) values begin to decline (assuming a facility has a relatively consistent influent sCOD), thereby resulting in granule instability and prevention of new granulation [19]. The kinetics of AS with a high SRT are also less favorable (a decreased observed yield and increase in oxygen demand) [19]. Also, longer SRTs allow eukaryotic life to thrive, species such as nematode destroy AGS and traditional floc, resulting in poor settling and high concentration of pin floc in the effluent [20–22]. Thus, there is a need to determine if the HS can provide enough selection pressure to induce the development of AGS while operating at a reduced capacity.

The main objectives of this study were to further evaluate the HS's impact on AGS development using a lab-scale SBR. Specifically, we investigated the impact of long-term HS operating conditions on AS settling characteristics and AGS development. We also evaluated the impact of a 10-15 d SRT on AS settling characteristics using a combination of HS and traditional wasting to achieve a target SRT. The results from this study can further increase our understanding on how selection pressure influences aerobic granulation and can assist in the transfer of this technology from batch reactor systems to a continuous flow CAS process.

3.3 Material and methods

Three identical lab-scale SBRs were constructed and operated for 238 days (May to December). The biomass wasted for each bioreactor was dependent on MLSS concentration and desired SRT. The control bioreactor, bioreactor 1 (BR1), operated without hydraulic selection and wasted sludge from the bottom of the BR at the end of the settling phase. Bioreactor 2 (BR2), operated with a combined wasting method, the HS wasted 25-50% of the biomass and the remaining biomass was wasted from the bottom of the reactor after the settling phase. Bioreactor 3 (BR3), operated solely with HS wasting. Flow diagrams of the BR wasting configurations are illustrated in Fig. 3.1. The BRs were each seeded with 84 L of AS from an aeration basins of the Denver Metro Wastewater Facility and BRs were operated with raw wastewater produced from the dormitories (Mines Park) of the Colorado School of Mines (Golden, Colorado), described by Vuono et al. [23].

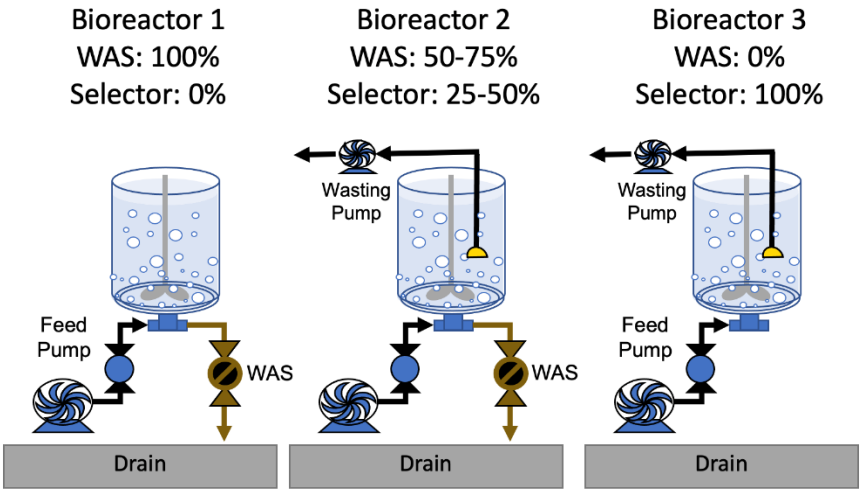

Figure 3.1 AS wasting conditions for SRT control. BR1 operated as the control, with wasting AS from the bottom of the reactor only. BR2 combined wasting from the hydraulic selector and from the bottom of the reactor. And BR3 wasted AS only through the hydraulic selectors.

3.3.1 Pilot system configuration and operation

The lab-scale system comprised of a 250-L raw wastewater equalization tank, a 200-L primary clarifier (PC), a 130-L PC decant tank, and three identical 120-L BRs with a depth to width ratio of 1.3. Every hour

a grinder pump submersed in an onsite 45,000 L septic tank (receiving wastewater from Mines Park) delivered 250 L of raw sewage to the equalization tank. A peristaltic pump then continuously delivered raw wastewater from the equalization tank to the PC at rate of 1 L/min. The clarified wastewater from the PC then overflowed into the PC decant tank and mixed with a carbon additive (glycerin) to increase sCOD concentration. The PC decant served as the feed tank for the three BRs; this ensured that all BRs were fed with identical wastewater. A flow diagram of the experimental system is shown in Fig. 3.2.

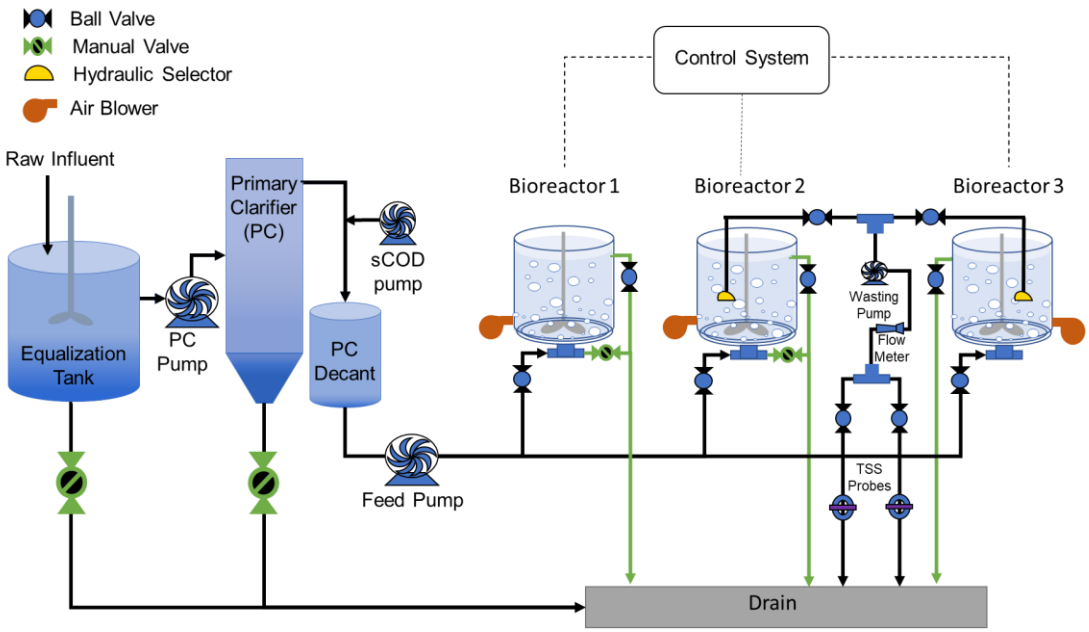

Figure 3.2 A flow diagram of the experimental system. Raw wastewater was diverted from a sewer line into an equalization tank. Glycerin was used to increase influent sCOD concentration and activated sludge from the Denver Metro Wastewater Facility was used to seed the bioreactors.

BR1 was operated in a cycle consisting of five phases, including fill, mix, aeration, settling, and decant. BR2 and BR3 operated in cycles consisting of seven phases, including fill, mix, aeration, pre-selector settling, selector wasting, post selector settling, and decant. The pH of the BRs was adjusted as needed with calcium hydroxide to maintain a pH of 6.6-7.5. All BRs operated with a 30% exchange ratio—at the end of each cycle 30% of the reactor volume (36 L) was discharged and 36 L batch of clarified wastewater was added during the fill-phase. All BRs had a 60-min static fill phase where clarified wastewater from the PC decant tank entered the bottom of the BR directly into the anaerobic/anoxic sludge blanket. The mix phase was also 60-min long—the mixer rotated at 50-60 RPM and all BRs used a 10-inch-wide impeller. The aeration phase was 180 min long, mixers operated continuously at 50-60 RPM, and the blowers delivered 15 L/min of air through two aluminum oxide diffusers. The air blowers operated automatically and remained on until the high dissolve oxygen (DO) concentration limit of 6 mg/L was reached. The blower then remained off until the low DO concentration limit of 4 mg/L was reached. Although the measured DO values are higher than what is typically observed at full-scale WRRFs, the calculated required oxygen and

assumed oxygen transfer efficiency (4%) required an air flow of 12-16 L/min, and resulted in a DO concentration higher than the traditional 2 mg/L. Previous experiments with this system were conducted with lower air flows and resulted in limited nitrification; once the air flow was elevated to 15 L/min, complete nitrification was regained. The fill, mix, and aeration phase times were intentionally exaggerated to ensure that feast/famine conditions were present and thus maximize EPS concentration. This research focused on maintaining constant feast/famine conditions to ensure that the variation of HS wasting and impact on AGS development could be evaluated.

After the aeration phase, all BRs transitioned into a settling phase, where both aeration and mixing were turned off and AS was allowed to settle. BR2 and BR3 preselector settling time was only a fraction of the BR1 settling phase. During the selector wasting phase for BR2 and BR3 a programable logical controller (PLC, LabJack DAQ and LabVIEW software) was used to regulate the biomass wasted through the selector. This was accomplished by using an inline magnetic flow meter (OMEGA, Norwalk, CT), which monitored HS discharge rate (L/min) and TSS (mg/L) probe (HACH, Loveland, CO). The PLC could then monitor and calculate the mass of biosolids wasted in real-time. When the target biomass to be removed was reached, the HS discharge pump was turned off.

Following the HS wasting phase, BR2 and BR3 proceeded to the post-settling phase, where any remaining suspended AS was allowed to settle for 5-10 min. The sum of the preselector settling, selector wasting, and post selector wasting times were set to be equal to the BR1 settling phase of 20 min. For example, if the total preselector settling and selector wasting times were 15 min, then the post selector settling time was set to 5 min. Traditional wasting for BR1 and BR2 was conducted manually 3-4 times a week and was conducted 5 min prior to the beginning of the decant phase. The volume of AS wasted for each BR was dependent on AS concentration and desired SRT. The duration of the decant was 5 min and was the same for all BRs; water was decanted through an adjustable weir, initiated using an automated ball valve and sent to a decant tank for composite sample analysis.

3.3.2 Influent wastewater characteristic

A critical aspect of the BR operation was maintaining a suitable F/M ratio (sCOD concentrations to mix liquor volatile suspended solids (MLVSS) concentration). Numerous successful AGS studies have operated with a high F/M ratio of 0.6 to 1.4, compared to a traditional CAS value of 0.05 to 0.5 [3,24,25] . It was initially believed that carbon limited facilities with low F/M ratio would not be able to granulate due to the absence of the feast phase [25,26]. However, studies operating with traditional CAS F/M ratios were successful in granulation due to a slow static fill phase, which promoted feast conditions by maximizing the sCOD concentration in the AS blanket [8,11,27]. Due to the limited population at Mines Park, influent sCOD was <100 mg/L at the start of the study, below the normal 200 mg/L for average influent wastewater [3]. To resolve this problem, a carbon dosing system was integrated into the headworks and dosing volume was adjusted to ensure that the BRs operated with an F/M ratio of 0.1-0.2. A range of F/M values were calculated based on variable influent sCOD and MLVSS concentrations (Table 3.1). To monitor the impact of carbon

dosing on influent wastewater parameters, samples were collected and analyzed before carbon dosing (mixing tank) and after carbon dosing (PC Decant) (Table 3.2).

Table 3.1. The calculated F/M values of the BRs based on influent sCOD and BR MLVSS. Green highlighted cells represent F/M within the 0.1-0.2 range and red cell represent F/M values above or below the specified range

	Cycle (hrs)	5.4	Vol (L)	120
	Exchange Ratio %		Exchange Vol (L)	
	30		36	
	MLVSS (g/L)			
Influent sCOD (mg/L)	2.0	3.0	4.0	5.0
	F/M (g COD/ g VSS)			
100	0.07	0.04	0.03	0.03
200	0.13	0.09	0.07	0.05
250	0.17	0.11	0.08	0.07
300	0.20	0.13	0.10	0.08
350	0.23	0.16	0.12	0.09
400	0.27	0.18	0.13	0.11
450	0.30	0.20	0.15	0.12
500	0.33	0.22	0.17	0.13

The seed sludge MLSS concentration was ~4250 mg/L and influent sCOD was 97 mg/L; at these concentrations the F/M ratio was below 0.1 and carbon dosing was required. It was assumed that the MLVSS concentration would vary between 3000 and 5000 mg/L throughout the study, and would require an sCOD concentration between 250 and 500 mg/L. The average influent total COD (tCOD) was 265±80; and after carbon dosing the tCOD in the PC decant increased to 479±166. The average sCOD was 127±33, and it increased to 376±144 after carbon dosing. On average, the synthetic carbon dosing increased sCOD by 249 mg/L. The tCOD increased due to the soluble fraction of COD but decreased in particulate COD by 35 mg/L. Total nitrogen concentration in the PC decant tank stayed relatively constant, orthophosphate concentration slightly decreased, and ammonia concentration remained constant. Conductivity, pH, and alkalinity slightly decreased in the decant tank.

Table 3.2. Average influent wastewater parameters from the mixing tank (before carbon dosing) and PC decant (after carbon dosing)

Influent Parameter	**Mixing Tank (n=27)**	**PC Decant (n=27)**
tCOD (mg/L)	265±80	479±166
sCOD (mg/L)	127±33	376±144
Total Nitrogen (mg/L-N)	35±9	34±10
Orthophosphate (mg/L)	12±3	10±2
Ammonia (mg/L-N)	28±8	28±8
Conductivity (µS/cm)	776±92	737±68
pH	7.2±0.3	6.8±0.2
Alkalinity (mg/L as $CaCO_3$)	167±38	138±38

3.3.3 Hydraulic selector design

The geometry of the HS was designed to maximize the separation of poor settling floc, minimize accumulation of solids on the selector, and deliver uniform flow distribution across the entrance of the selector (Fig. 3.3). The HS was designed in Solidworks (SolidWorks 2020, Dassault Systemes, Waltham, MA), and 3D printed using polylactic acid filament (Pro2 Plus, Raised 3D, Irvine, CA). The entrance to the selector had a length of 16 cm and width of 4.3 cm. A single selector was placed in each BR, with the entrance of the selector 20 cm below the surface of AS when the BR is full. BR 2 and 3 shared one selector pump (Series 2, Procon, Smyran, TN) and one flow meter, as illustrated in Fig. 3.2. The BRs were operated as sequencing batch reactors (SBRs) to ensure that only one BR would require the selector pump at a time. Additionally, two pairs of ball valves were used to control and direct discharge from the HS. The HS operated with a range of flows of 0.5-3 L/min, and was limited to discharge up to 8 L per cycle.

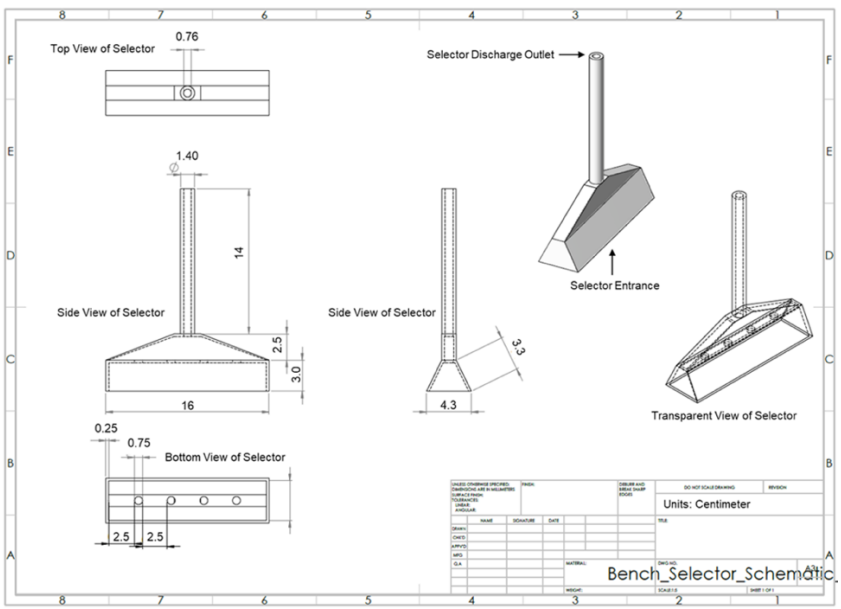

Figure 3.3 A schematic of the hydraulic selector, all units are in centimeters.

3.3.4 Data acquisition

The lab-scale system was controlled by a programmable logical controller (UE9-Pro, LabJack Corp., Lakewood, CO) and a data acquisition instrument control software (LabVIEW, National Instruments Corp., Austin, TX). The BR TSS and DO concentrations and pH were measured continuously using online probes (HACH, Loveland, CO). Ammonia and nitrate were measured using a Varion nitrogen probe (Yellow Springs Instruments, Yellow Springs, OH)

3.3.5 Analytical methods

The AS settling velocity, MLSS, SVI5, and SVI30 were measured using grab samples collected during the aeration and mixing phases to ensure homogeneity. Measurements were conducted 2-3 times a week and followed standard methods procedures [28]. The settling velocity of the AS was measured in a 2 L graduated cylinder and was calculated from the settling time of the AS blanket over a 24 cm distance. Both SVI30 and 5 were measured in a 1 L beaker, with the sludge volume measurements taken at 30 and 5 minutes, respectively. Traditionally, SVI30 values have been monitored by WRRFs and would normally range between 100 and 250 mL/g. However, with rapid settling AS, the SVI5 measurement has been adopted by researchers and is used as an indication of granulation when both SVI30 and 5 are equal and <100 mL/g. Composite samples (24-hours) from the equalization tank, PC decant tank, and decant from all BRs were collected once a week and were measured for tCOD, sCOD, ammonia, nitrate, orthophosphate, pH, and alkalinity. These analyses (excluding pH) were performed using HACH TNT PlusTM (Loveland, CO) reagent vials and a Hach DR 5000^{tm} spectrophotometer.

3.3.6 Floc characterization

3.3.6.1 Biomass-based floc diameter distribution

The biomass-based floc diameter distribution was measured three times during the study, on days 0, 105, and 179. To measure the floc diameter distribution, a 1 L sample of AS was collected from the BR during the mixing and aeration phase, the sample was then poured through a 1.4 mm sieve. An additional 5 L of DI water were then used to wash the biomass through the sieve. The biomass retained on the sieve was removed by pouring 1 L of DI water in the reverse direction on the sieve. This process was repeated for the 1 mm, 0.5 mm, and 0.25 mm sieves. The TSS for each floc diameter category was then measured according to standard methods [28].

3.3.6.2 Volume based floc diameter distribution

Samples for the volume-based floc diameter distribution measurements were collected from the BR and HS discharge once every 1-3 weeks. A 50 mL sample of AS was collected during the mixing and aeration phase and a 100 mL sample of the HS discharge was collected from a sampling port located after the inline TSS probe. To sample the HS, the BR would have to be switched from an auto to HS optimization mode. Then, the entire selector discharge system would be drained to remove any stagnant sludge in the lines. Next, the desired operating conditions for the HS were set. The BR would then go into mixing and aeration mode for 1 min, then the preselector settling time, followed by selector wasting. This process was repeated 2-3 times to ensure that a consistent and reliable sample was collected. Samples were stored at 5 °C until the measurements were conducted (1-4 hours after collection).

Samples were analyzed with a laser particle size analyzer (S3500, Microtrac) with an absorption coefficient of 1 and refractive index of 1.52 [29]. The data produced by the Microtrac is a distribution of volume displaced by the various floc diameters in the AS or HS discharge, known as a volume-based

cumulative distribution. This is calculated when floc passes through a laser chamber, light is scattered by the floc and an associated volume is calculated. The Microtrac algorithm also considers the absorption and refractive properties of the floc that is not related to particle size. The Microtrac relies on an ensemble technique, which requires a cloud of particle (the instrument does not count individual particles); and because individual particles are not available directly, the distribution is forced to add to 100%.

3.3.6.3 Microscopy

AS samples were also characterized with a phase contrast microscope (Olympus CX41, Center Valley, PA) at 100X and 40x magnification. Phase contrast images were processed with Infinity 2 software (Lumenera, Ontario, Canada) and open-source ImageJ software.

3.4 Results and discussion

3.4.1 Activated sludge MLSS and SRT

The performance of the lab-scale BRs was monitored over a 238-day period. The seed sludge MLSS concentration was 4250 mg/L and the target SRT was between 10 and 15 days. HS operation was modified multiple times throughout the study via reduction of preselector settling time or increased selector outflow. These modifications have been broken down into five unique HS operating stages. Modifications to the HS operation were conducted when the biomass removed by the selectors was not sufficient to reach the target SRT or when settling velocity of the AS reached steady state. MLSS concentration and SRT as a function of time in BRs 1-3 are shown in Fig. 3.4.

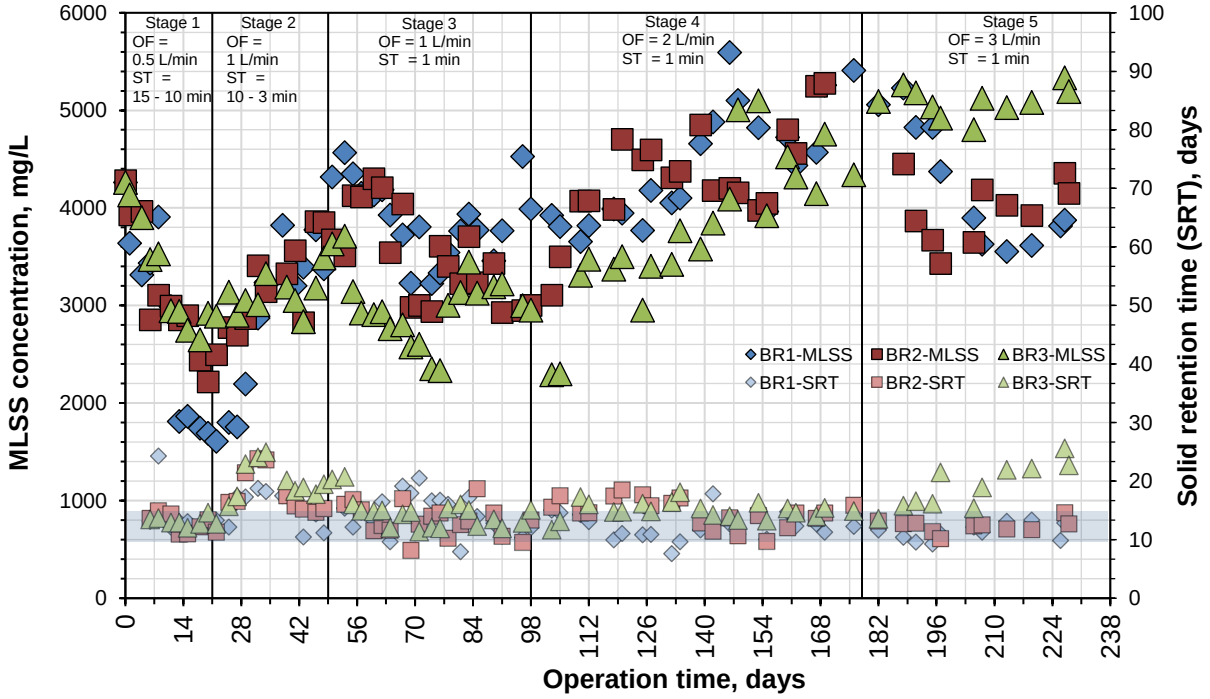

Figure 3.4 MLSS and SRT in the BRs as a function of time. The black vertical lines represent a change in hydraulic selector operation, in preselector settling time (ST) or hydraulic selector outflow (OF).

In Stage 1, all BRs experienced a slow decrease in MLSS concentration. This period of limited growth may have been induced by a reduced maximum specific growth rate of MLSS caused by transportation and new feast/famine conditions. During this stage, the SRT target was easily achieved due to consistently slow AS settling.

In Stage 2, the MLSS concentration of all BRs began to recover, nearly reaching the initial MLSS concentration of the seed sludge, and at the same time the SRT of all BRs increased. BR1 reached a maximum SRT of 19 d on day 32; thus, wasting from BR1 was increased and SRT declined to 11 d by the end of the stage. For BR2 and BR3, the HS discharge was increased from 0.5 to 1 L/min, and the preselector settling time remained at 10 min. However, soon after the stage began, the MLSS in both BR2 and BR3 increased rapidly, and by day 28 the SRT reached 15 d. To reduce SRT, the preselector settling time was decreased to 5 min to increase biomass removal through the HS. On day 35 the MLSS continued to climb and SRT increased to 25 d; therefore, the preselector settling time was again decreased, this time to 3 min. This change in HS operation reduced SRT in both BR2 and BR3, reaching 15 and 18 d, respectively. Still, these changes in selector operation were not sufficient to drop the SRT below 15 days, mainly due to increasing AS settling velocity. By the end of stage 2 AGS began to appear in both BR2 and BR3.

In Stage 3, all BRs experience a decrease in MLSS concentration between days 49 and 74. SRT for BR1 was maintained between 10 and 15 d, with an exception occurring on day 81 due to an accidental wasting event. In BR2 and BR3 the new HS operating conditions reduced their respective SRT below the 15 d target for nearly the entire stage.

In Stage 4, BR1 MLSS concentration increased and reached a maximum concentration of 5400 mg/L on day 176. The SRT in BR1 remained between the desired 10-15 d, with the exception occurring on day 132, caused by excessive wasting. During Stage 4, BR2 MLSS concentration had various fluctuations while increasing from 3000 to 5200 mg/L by the end of the stage. BR3 MLSS concentration initially decreased over the first week of Stage 4, reaching 2300 mg/L, then it increased for the remaindered of the stage, reaching 4300 by day 176. The SRT in BR2 and BR3 remained near the upper limit of 15 d. At the same time, the settling velocity of the AS continued to rise, and the HS in BR 3 struggled to remove enough biomass at the maximum allowable discharge volume of 8 L. At this point (day 133) the majority of the MLSS in BR2 and BR3 was composed of AGS. Normally, the HS operating condition would have been changed; however, to achieve operation length of three SRTs under the same operating condition, the maximum HS discharge volume limit was increased to 12 L. After day 133 the SRT for both BRs 2 and 3 remained below 15 d.

In Stage 5, BR1 MLSS concentration decreased between days 178 and 213, from 5400 to 3500 mg/L, then increased to 3800 mg/L by day 228. BR2 MLSS concentration also decreased, from 5300 to 3400 mg/L between days 178 to 197, and then increased to 4200 mg/L by day 228. At the start of Stage 5 the waste activated sludge (WAS) volume from BR1 and BR2 were increased to reduce the high MLSS concentration, this resulted in an SRT below 10 d. Once the MLSS decreased, the WAS volume was

reduced, increasing the SRT to 12.5 d, and MLSS for BR1 and BR2 stabilized. Unlike BR1 and BR2, BR3 MLSS stabilized at 5000 mg/L for the remainder of the stage. By day 189 the BR3 HS was not able to remove enough biomass, and SRT was maintained just below 15 d, and by day 197 the SRT target was exceeded. With increasing AS settling velocity and the HS removing the maximum allowable discharge volume, the SRT for BR3 continued to increase, reaching 23 d by the end of the study.

BR 1 and 2 maintained nearly identical MLSS concentrations throughout the entire study while BR3 always maintained a slightly lower MLSS concentration, until the final stage. BR3, operating only with HS, removed a higher concentration of faster growing AS, thereby accumulating slower growing AS, which resulted in a lower MLSS concentration when compared to BR1 and BR2. Traditional wasting allowed BR1 and BR2 to have much more control over the SRT, providing the ability to quickly adjust and maintain the average SRT below the desired 15-d target. At the start of the study, BR3 also was able to maintain the desired SRT; however, the increasing AS settling velocity and the selector's inability to quickly adjust operating condition restricted biomass removal and control. Future operation of the HS could address this problem by adjusting the selector's operating conditions in real-time such as adjusting the depth of the selector to increase the mass of biosolids discharged by the HS.

3.4.2 Activated sludge settling velocity and hydraulic selector operation

Previous HS research demonstrated the selector's ability to increase the settling velocity of AS; however, the results were not clear on how the combination of selector's entrance velocity and minimum settling velocity influenced the AS settling velocity. Typically, the minimum settling velocities represent the velocity required for a floc to pass the effluent port before the start of the decant phase; however, in this study, the minimum settling velocity is dependent on the preselector settling time and 20 cm, the distance between the top of the BR when it is full and the entrance of the HS. This minimum settling velocity does not take into account the turbulent conditions that may still be present during the preselector settling time, nor does it consider the required velocity a floc must have to escape the suction of the HS. The current study focuses on various operating conditions of the HS to determined how minimum settling velocity and outflow through the HS impact AS settling velocity.

AS settling velocity as a function of time under different preselector settling times and HS outflow rates are shown in Fig. 3.5. The settling velocity of the seed sludge was slow, <1 m/h. For this reason, a long preselector settling time of 15 min was initially chosen, which resulted in a minimum settling velocity of 0.8 m/h and allowed for an initial separation of faster settling biosolids. During this stage the HS outflow was set to 0.5 L/min, which resulted in a HS entrance velocity of 4.4 m/h. Details of floc characteristic discharged by HS are presented and discussed in Section 3.3. This initial setup did not improve the AS settling velocity in BR2 and BR3 so the pre-selector settling time was reduced on day 14 to 10 min, which increased the minimum settling velocity to 1.2 m/h. However, the AS settling velocity of all BRs remained below 1 m/h for the remainder of the stage. While the AS settling velocity was stagnate, the MLSS concentration for all BRs decreased (Fig. 3.4), indicating that the slow settling was caused by floc characteristic such as floc diameter

and zeta potential.

During Stage 2, the preselector settling time was maintained at 10 min and the HS outflow was increased to 1 L/min, resulting in a selector entrance velocity of 8.5 m/h. On day 39 the settling velocities in all BRs increased to approximately 1.8 m/h, including BR1 without HS. Thus, it is unlikely that these improvements in settling velocity were only influenced by the HS or the minimum settling velocity, but most likely caused by the feast/famine conditions present in all BRs. During feast/famine conditions, increased EPS production allows for the agglomeration of floc and a subsequent increase AS settling velocity [18,30]. However, on day 43 the differences between BR settling velocities became noticeable; for the rest of Stage 2, BR1 maintained a settling velocity of ~1.8 m/h while the settling velocities in BR2 and BR3 continued to increase, reaching 4 and 4.6 m/h, respectively, on day 49. These settling velocities were similar to that of the minimum settling velocity to escape the HS of 4.15 m/h.

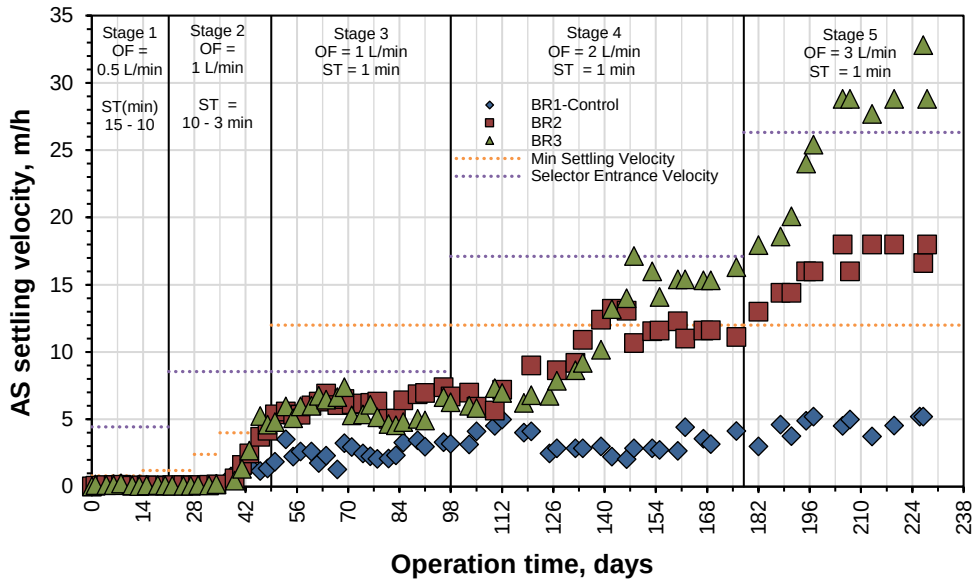

Figure 3.5 AS settling velocities for BR1 (no hydraulic selector), BR2 (traditional wasting and hydraulic selector), and BR3 (only hydraulic selector) over the study period. The orange dashed line is the minimum settling velocity required to escape the HS before selector operation begins. The purple dashed line represents the selector's entrance velocity. Changes in hydraulic selector operation are identified by the solid black vertical lines.

During Stage 3, the preselector settling time was further decreased to 1 min, resulting in a minimum settling velocity of 12 m/h, and the HS outflow was maintained at 1 L/min (equivalent to an entrance velocity of 8.5 m/h). These conditions allowed for consideration of how a higher minimum settling velocity (compared to the HS entrance velocity) impacts AS settleability. BR1 settling velocity continued to increase without the presence of HS, going from 1.8 to 3.3 m/h by day 98. The settling velocity for BR2 and BR3 increased from 5.4 to 7.4 and 4.6 to 6.6, respectively. Although AS settling velocity for both BR 2 and 3 improved, it did not

reach or surpass the minimum settling velocity of 12 m/h. This stage of the study was 49 days long; and with an average SRT of 14.2 d, the system operated 3.5 SRT cycles. Operating for this duration under constant conditions ensured that the biological system was stable before proceeding to the next stage.

During Stage 4, the preselector settling time remained at 1 min, resulting in a minimum settling velocity of 12 m/h, and the HS outflow was increased to 2 L/min, resulting in an entrance velocity of 17 m/h. During this stage of the study the HS induced a higher selection pressure. The AS settling velocity in BR1 was highly variable—reaching 5 m/h on day 112, decreasing to 2.5 m/h by day 127, the then slowly increasing to 4 m/h by the end of the stage. At the start of Stage 4, the AS settling velocity of both BR2 and BR3 decreased, reaching a low of 5.7 m/h on day 110. Shortly after, the settling velocity in both BRs began to increase, with BR2 reaching a maximum of 13 m/h on day 142 and BR3 reaching a maximum of 17 m/h on day 148, and subsequently the settling velocity decreased, reaching 11 and 15.5 m/h in BR2 and BR3, respectively. During this stage it was clear that the selection pressure induced by the HS had a substantial impact on AS settling velocity—both BRs surpassed the traditional AS settling velocity limit of 10 m/h and BR3 surpassed the minimum AGS settling velocity of 15 m/h. The benefits of operating solely with HS were also apparent, the AS settling velocity in BR3 was 33% higher compared to BR2. The entire duration of Stage 4 was 78 d (approximately 5.5 SRTs). The decision to change the selector operating condition was due to the stagnating AS settling velocities.

During Stage 5, the preselector settling time remained at 1 min, resulting in a minimum settling velocity of 12 m/h, and the HS outflow was increased to 3 L/min, resulting in an HS entrance velocity of 26.3 m/h. During this stage of the study the HS once again induced a higher selection pressure than the minimum settling velocity. The BR1 AS settling velocity increased slightly to 5 m/h over the first 3 weeks of the stage and was stable for the remainder of the study. BR2 AS settling velocity experienced a similar trend, reaching a peak value of 18 m/h on day 205, surpassing the 15 m/h minimum settling velocity of AGS. The AS settling velocity in BR2 was again less than BR3, but this time higher than the minimum settling velocity threshold, indicating that the HS operating at a reduced capacity can successfully induce enough selection pressure to increase the AS settleability. BR3 AS settling velocity also continued to increase, reaching 28 m/h by 205. As in Stage 4, the AS settling velocity in BR3 is similar to the HS entrance velocity and demonstrates ability of the HS to influence and control AS settling velocity. The duration of Stage 5 was 62 days (4.4 SRTs), ensuring that the biological system was stable.

Another important AS characteristic that WRRFs monitor is SVI, which is typically measured after a 30-min settling time. SVI of poor settling AS is often higher than 250 mL/g while SVI of fast settling AS is lower than 100 mL/g. With improved AS settleability, many researchers have incorporated SVI measurements based on a 5-min settling time. When SVI5 becomes close to SVI30, the SVI5/SVI30 ratio approaches 1, which indicates that AGS is being developed. However, this rule only applies when SVI30 is <100 mL/g, because SVI30 and SVI5 values can also be similar when AS has extremely slow settling. Both SVI30 and SVI5 were measured throughout the study in all BRs. SVI5 and SVI30 as a function of time throughout the study are shown in Fig. 3.6.

During Stage 1, the seed sludge of the BRs began with SVI30 and SVI5 of 168 and 222 mL/g, respectively. Both SVI30 and SVI5 in all the BRs increased for nearly the entire duration of the stage and after 21 days BR1 had the highest SVI30 and SVI5 values of 426 and 488 mL/g, respectively. The high SVI was a result of rapid loss of AS, as indicated in Fig. 3.4, combined with slow settling and slow development of new floc.

During Stage 2, SVI30 and SVI5 in all BRs rapidly decreased—after day 39 all SVI30 values were below 100 mL/g, an important achievement desired by all WRRFs. For the remainder of Stage 2 BR 1 SVI30 remained just below 100 mL/g while values for BR2 and BR3 continued to decrease, reaching 38 and 29 mL/g, respectively, by the end of the stage. At the same time, SVI5 for BR1, BR2, and BR3 all decreased; their SVI5/SVI30 ratio was 1.8, 1.1, and 1.0, respectively. The SVI5/SVI30 ratios in BR2 and BR3 indicate the presence of AGS, although the settling velocity in the BRs at the time was well below the standard AGS settling velocity of 15 m/h.

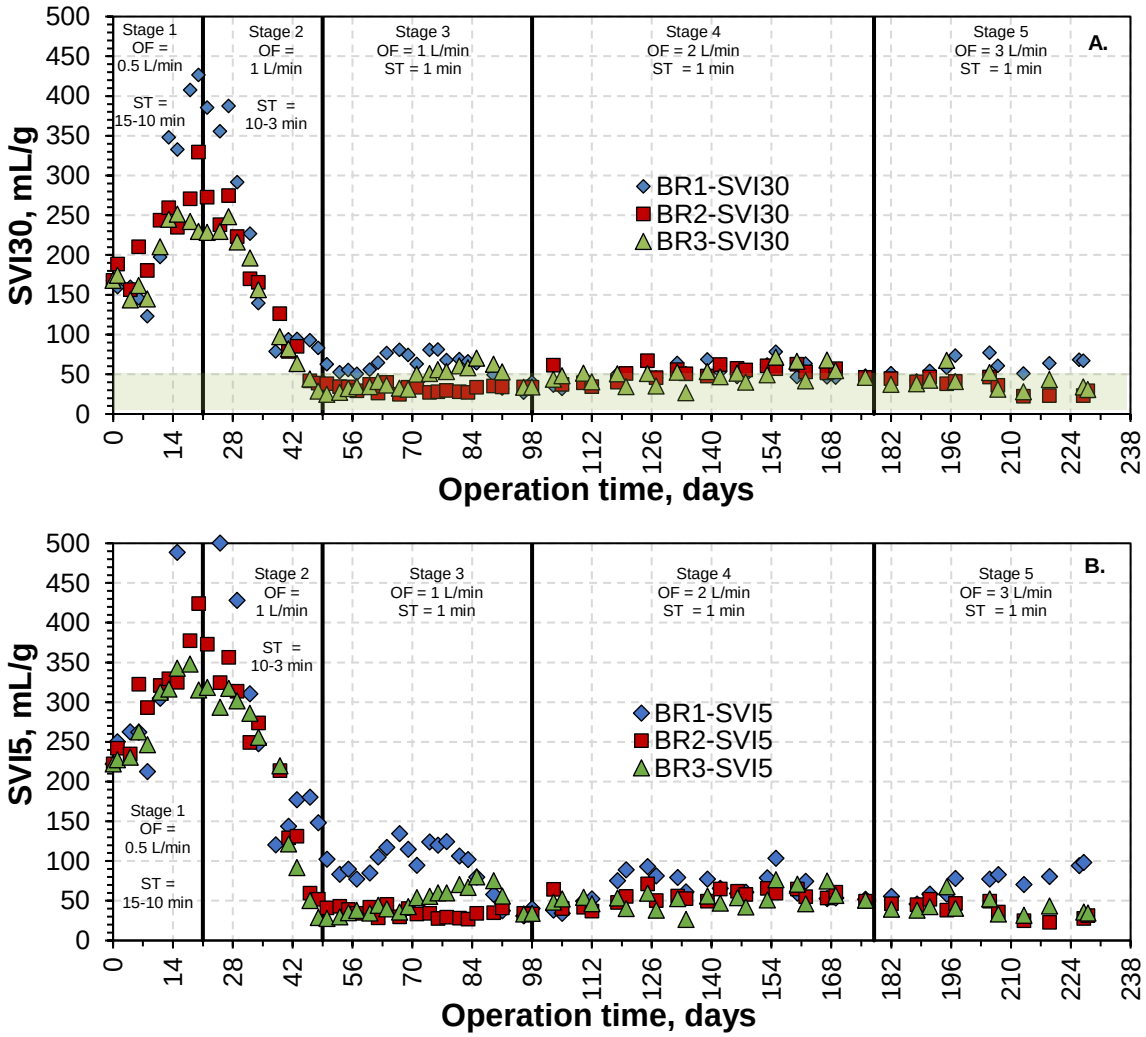

Figure 3.6 A) Sludge volume index 30 and B) sludge volume index 5 for BR1 (blue diamonds), BR2 (red squares), and BR3 (green triangles) as a function of time over the duration of the study.

During Stage 3, SVI30 and SVI5 in BR1 continued to decrease, reaching low values of 53 and 77 mL/g by day 57. SVIs for BR1 then began to fluctuate, increasing to 81 and 125 mL/g, at the same time the mean floc diameter (MFD) of BR1 AS declined below 100 µm (further discussed in Section 3.4). The instability of the MFD may have been caused by the increased SRT, resulting in an accumulation of predatory eukaryotic life that destroys AS floc. By the end stage the MFD had increased and both SVIs decreased below 50 mL/g. In BR2, SVI30 and SVI5 remained below 50 mL/g for the entire duration of the stage, with an SVI5/SVI30 ratio of 1 between days 71 and 98. In BR3, SVI30 and SVI5 remained below 50 mL/g until day 70, then both SVIs suddenly increased; this sudden change correlated with a decrease in the AS MFD, which may have been caused by a rapid decrease in F/M ratio (see Supplementary data).

During Stage 4, SVI30 in all BRs were nearly identical for the entire stage, ranging from 37 to 75 mL/g. The BR1 SVI5/SVI30 varied between 1.2 and 1.9. BR2 SVI5/SVI30 varied between 1 and 1.1 and BR3 SVI5/SVI30 varied between 1 and 1.2, indicating that BR2 and BR3 was dominated by AGS. During Stage 5, SVI30 and SVI5 in BR1 remained below 50 mL/g until day 195, both SVIs began to increase, reaching 68 and 98 mL/g, respectively, by the end of Stage 5. This increase in BR1 SVIs may have been caused by increased WAS volume, which was intended to reduce the MLSS concentration but also removed a high concentration of fast settling and dense sludge. Both BR2 and BR3 began Stage 5 with SVI30 and SVI5 below 50 mL/g, and by the end of the stage, both SVI30 and SVI5 in BR2 decreased to 31 mL/g and BR3 SVI30 and SVI5 decreased to 31 and 36 mL/g, respectively.

3.4.3 Hydraulic selector optimization

Under ideal operating conditions, the HS removes the highest concentration of poor settling biomass. However, with time, AS settling characteristics improve, resulting in a transformation of floc diameter distribution. A readjustment of the HS operation is necessary to continue removing the highest concentration of poor settling floc. To determine ideal HS operating conditions, a variety of preselector settling times between 0.5 and 15 min, combined with various HS outflows of 0.5-3 L/min were tested. For each HS operation combination, a 100 mL sample was collected from the discharge for floc analysis. The floc diameter distribution and MLSS concentration of each sample was measured to quantify the volume of poor settling floc removed from the BR. Samples were also compared to AS (collected during the mixing and aeration phase) of the BR to determine the effectiveness of the HS operating condition. The selector must also remove enough biomass within the maximum discharge volume of 8 L to maintain the target SRT. An example of HS optimization for BR3 on days 7 and 42 are shown in Fig. 3.7.

On day 7 of the study, the AS had extremely poor settling characteristics and nearly all operating conditions tested on the HS showed a similar distribution to the AS sample. The preselector settling time of 1 min and HS outflow of 1 L/min had an identical distribution as the AS sample, indicating that no selection occurred. Maintaining the same preselector settling time and reducing the selector outflow to 0.5 L/min resulted in a slight shift of floc diameter distribution (yellow line in Fig. 7a). By increasing the preselector settling time to 15 min, the AS had begun to settle and selection of poor settling floc slightly improved (green

and black lines). At an outflow rates of 0.5 and 1 L/min the removal of floc with a diameter of 100-250 µm decreased (green and black lines). Also, the outflow rate of 0.5 L/min did not remove floc >400 µm and removed a higher percentage of floc with a diameter of 52 µm. On day 7, the MLSS concentration of the HS discharge varied between 2 and 2.8 g/L. To achieve the desired SRT of 12.5 d, the HS would need to discharge 5.4 g/cycle. Due to the high MLSS concentration of the HS discharge, any of the operating conditions would remove enough biomass within the maximum discharge volume of 8 L/cycle. Therefore, a preselector settling time of 15 min and selector outflow of 0.5 L/min were chosen for the HS operating conditions on day 7.

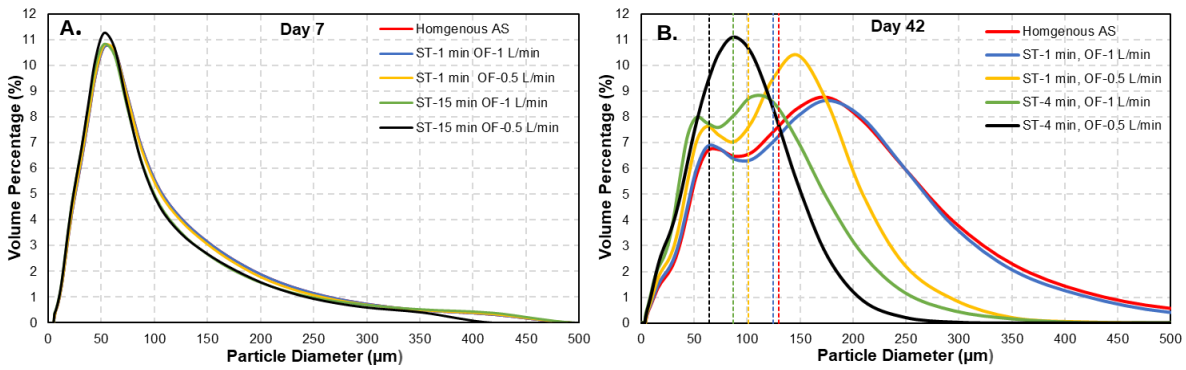

Figure 3.7 Optimizing HS operation for the removal of poor settling floc for BR3 on day 7 and day 43 by comparing the volume percentage floc diameter distribution of various HS operating conditions. The HS operation was modified by changing the preselector settling time (ST) or the selector outflow (OF). The AS represents the control. The dotted vertical lines on day 42 represent the average floc diameter of the corresponding color.

As the study progressed, the AS settling characteristic improved, and on day 42 the HS operation was reevaluated. Due to the multiple variables in the HS operation, Table 3.3 was created to assist with the optimization of HS operating conditions for day 42.

Table 3.3. List of the four HS optimization scenarios tested on BR3 for day 42.

Scenario	Operating Condition	HS Outflow MLSS (mg/L)	Required biomass removal for SRT (g/cycle)	Volume Discharge (L/cycle)	Mean Floc Diameter Removed (µm)
1	Settling time: 1 min Outflow: 1 L/min	1963	5.8	3.0	125
2	Settling time: 1 min Outflow: 0.5 L/min	1328	5.8	4.4	101
3	Settling time: 4 min Outflow: 1 L/min	784	5.8	7.4	87
4	Settling time: 4 min Outflow: 0.5 L/min	412	5.8	14.1	64

On day 42, the MFD of the AS was 130 µm. Scenarios 1 and 2, described in Table 3.3, are identical to the operating conditions used on day 7. Scenario 1 resulted in a nearly identical floc diameter distribution as the AS (MFD decreased to 125 µm, blue dashed line in Fig. 3.7b). In scenario 2, the outflow rate was reduced to 0.5 L/min, the floc diameter distribution of the HS discharge improved, and the MFD of the HS discharge decreased to 101 µm (yellow dashed line in Fig. 3.7b). Additionally, all floc >350 µm were retained in the BR. The selection of poor settling floc is further enhanced in scenario 3, when the preselector settling time is increased to 4 min. At an outflow of 1 L/min, the MFD is reduced to 87 µm (green dashed line in Fig. 3.7b). And for scenario 4, HS outflow decreased to 0.5 L/min and the MFD once again decreased to 64 µm (black dashed line in Fig. 3.7b), and all biomass >250 µm was retained in the BR.

Although scenario 4 had the floc diameter distribution with the lowest MFD, it also had the lowest discharge MLSS concentration of 412 mg/L. Again, to achieve the target SRT of 12.5 days, the selector would need to remove 5.8 g/cycle, or 14.1 L, surpassing the maximum volume of 8 L discharge per cycle. Scenario 2, met the required criteria—enough biomass was removed within 4.4 L, and the MFD was 19% smaller than the AS. However, scenario 3 was chosen because it removed the required biomass within 7.4 L and the MFD was 33% smaller than the AS. The process described for HS optimization on Day 7 and 42 was repeated every time the HS operation conditions were changed for BR 2 and 3. This ensured a 10-15 d SRT and the maximum removal of poor settling solids.

3.4.4 Floc characteristic of activated sludge and hydraulic selector discharge

The effects of constant feast/famine conditions and HS operation are evident in the diameter of the AS floc. The average AS floc diameter can range between 80 and 200 µm [31,32]. The average diameter of the seed floc from the Denver Metro Facility was 60 µm, measured after the transportation of the floc to Mines Park. Measurements of each BR's AS floc diameter were taken periodically over the course of the study and each measurement generated a volume-based floc diameter distribution, the MFD of each distribution are presented in Fig. 3.8. During Stage 1, the AS MFD for all BRs increased, with BR 1, 2, and 3 reaching 81, 105, 98 µm, respectively, by the end of the stage. Although the MFD of all BRs had increased, there was no substantial improvement for AS settling velocity, SVI30 or SVI5.

During Stage 2, BR1 maintained an MFD of 83 µm for the entire stage, the settling velocity of the AS had increased to 1.8 m/h and SVI30 had improved, nearly reaching <100 mL/g. The MFD for BR2 and BR3 also increased, reaching 118 and 124 µm, respectively, on average 31% larger in diameter than BR1. The MFD increase for BR2 and BR3 also resulted in improved AS settling velocity, reaching 4 and 4.6 m/h, respectively, and SVIs <40 mL/g. Throughout this stage there were only minor MFD increases; however, the AS settling characteristic of all the BRs improved substantially during this time, indicating that the EPS production may have been responsible for these improvements.

During Stage 3, BR1 MFD experienced several fluctuations as did the BR1 AS settling velocity and SVIs and by the end of the stage MFD had increased to 230 µm, which had a positive impact on AS settling velocity and SVIs. A potential explanation for this variability was a low F/M ratio (<0.1) followed by a rapid

increase in BR1 F/M, reaching 0.24. BR2 MFD increased linearly throughout the stage, going from 167 to 250 µm. Subsequently, the settling velocity increased by 2 m/h and SVIs for BR2 remained below 50 mL/g. BR3 also experienced linear MFD increase between days 49 and 84, increasing from 142 to 223 µm. The last two MFD measurements on days 90 and 96 decreased to 172 and 198, respectively; this decrease was related to rapid F/M ratio decline but did not have a negative impact on AS settling velocity or SVI values.

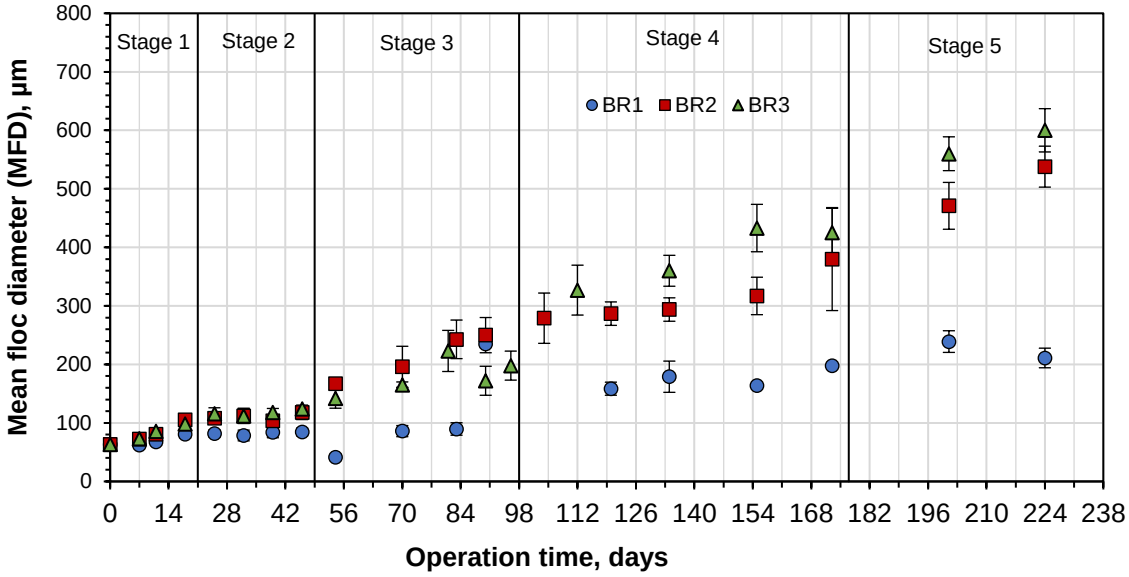

Figure 3.8 Mean floc diameter of AS from BRs 1-3 as a function of time, measured via volume-based floc diameter distribution. Each sample was measured 3-5 times. Error bars represent standard deviation between measurements.

During Stage 4, the BR1 MFD decreased to 160 µm, this occurred when F/M decreased below 0.2 and for the remainder of the study the F/M ratio which was maintained between 0.1 and 0.2. By the end of Stage 4 BR1 MFD had increased to 200 µm without the assistance of HS. For BR2 and BR3, the floc diameter growth stagnated for the first half of Stage 4, maintaining an MFD of 290 µm, at the same time the MLSS concentration and SRT in both reactors were increasing. For the second half of the stage, HS discharge volume was increased from 8 to 12 L, which allowed the MFD to further develop. BR2 MFD increased from 290 to 380 µm, SVIs remain below 50 mL/g and the settling velocity increased by 66%. For BR3, the MFD increased to a point where it surpassed the BR2 MFD and for the remainder of the stage was consistently higher, increasing from 198 to 425 µm, a 115% increase over 79 days. During this stage SVIs remained below 50 mL/g and settling velocity increased by 156%, reaching 15.4 m/hr. By the end of Stage 4 both BR2 and BR3 MFD surpassed 200 µm, achieving what many researchers consider the minimum diameter for AGS classification [7,11]. However, in this study AGS settling characteristics did not become dominant until the AS MFD reached 275 µm. Another important observation that occurred during this stage was the higher variability between MFD measurements for BR2 and BR3. It is believed that this variability was

caused by floc >2 mm (the maximum particle diameter limit of the S3500, Microtrac) being destroyed in the instrument and altering the MFD value.

During Stage 5, BR1 MFD stabilized at 230 µm for the remainder of the study. Both BR1 SVIs increased during the final stage and settling velocity rate was maintained at 5 m/h. For BR2 the MFD continued to increase, reaching a final value of 538 µm by day 224. During this time the SVIs decreased further, averaging 35 mL/g, and the settling velocity reached a maximum of 18 m/h. For BR3, the MFD also continued to increase, reaching a final mean value of 600 µm on day 224. BR3 SVIs continued to improve and AS settling velocity reached a maximum of 28.8 m/h.

BR1 required 90 days to develop a MFD >100 µm while BR2 and BR3 only required 25 days. BR1 experience a substantial MFD improvement over the entire study; however, this was not enough to improve the AS settling velocity beyond typical CAS settling velocities. A final important observation regarding MFD, once BR2 developed an MFD >275 µm, the AS settling velocity exceeded the maximum traditional value of 10 m/h, indicating that a minimal amount of HS in BR1 may have resulted in significant improvements in AS settling velocity.

The MFD of the AS was important for tracking the development of AGS, it also influenced the operation of the HS as did the HS discharge MLSS concentration and MFD. The HS removed floc based on the velocity gradients developed at the entrance of the selector. The objectives of the HS operation were to remove the highest percentage of poor settling floc, avoid removing the largest floc, and remove enough biomass to maintain the desired SRT. BR2 operated with a combined AS wasting method while BR3 solely relied on the selector for biomass wasting. The MFD of the HS discharge for BR2 and BR3 are presented in Fig. 3.9.

In Stage 1, the AS in both BR2 and BR3 had extremely slow settling, resulting in little to no stratification during the preselector settling phase. However, even with these extremely poor settling characteristics, the MFD of the HS discharge was 8% lower than that of the seed sludge MFD. By the 11th day of the study, the difference between AS MFD and selector discharge MFD in BR2 had increased to 20% while BR3 remained at an 8% difference. On day 18, the difference between BR2 AS and selector discharge MFD decreased to 15% and for BR3, the difference between the two streams increased to 19%. During this stage, multiple HS operating conditions were implemented in a short period of time, making it is difficult to draw a direct relationship between the HS operation and discharge MFD.

In the first half of Stage 2, the AS and HS discharge of BR2 and BR3 had a consistent MFD of 112 and 99 µm, respectively. In the second half of Stage 2, the MLSS and SRT of the BRs decreased, at the same time AS settling velocity of both BRs rapidly increased, and the HS discharge MFD for BR2 and BR3 decreased, reaching 54 µm, a 45% decrease when compared to the AS MFD. During this stage there was not a substantial increase in BR2 and BR3 MFD, the decrease in MLSS concentration may have reduced flocculation and hindered settling zones, resulting in increased AS settling velocity. With the improved AS settling velocity, the HS could have continued to remove floc in the 50 µm range. However, if the HS would

have operated under the same conditions, BR 3, relying solely on HS wasting, would have exceed the maximum total discharge volume of 8 L.

During Stage 3, the new HS operating conditions resulted in an increased MFD for BR2 and BR3 HS discharge, measuring 127 and 117 µm, respectively. Unlike in all other stages, an increase in AS MFD did not result in an improved AS settling velocity. This was also the only stage where the minimum settling velocity of 12 m/h was higher than the HS entrance velocity of 8.5 m/h. Ultimately, the HS operating conditions dictated AS wasting and as a result, were the limiting factor that influenced the AS settling velocity. By the end of the stage the MFD of the HS discharge for BR2 and BR3 was 32 and 24% less than the AS MFD, compared to the 45% difference that occurred in Stage 2. This difference in MFD removal is also directly related to the minimum settling velocity; with a higher minimum settling velocity, the HS was not as effective in floc removal. This is evident in BR3 and resulted in an increasing MFD for the HS discharge.

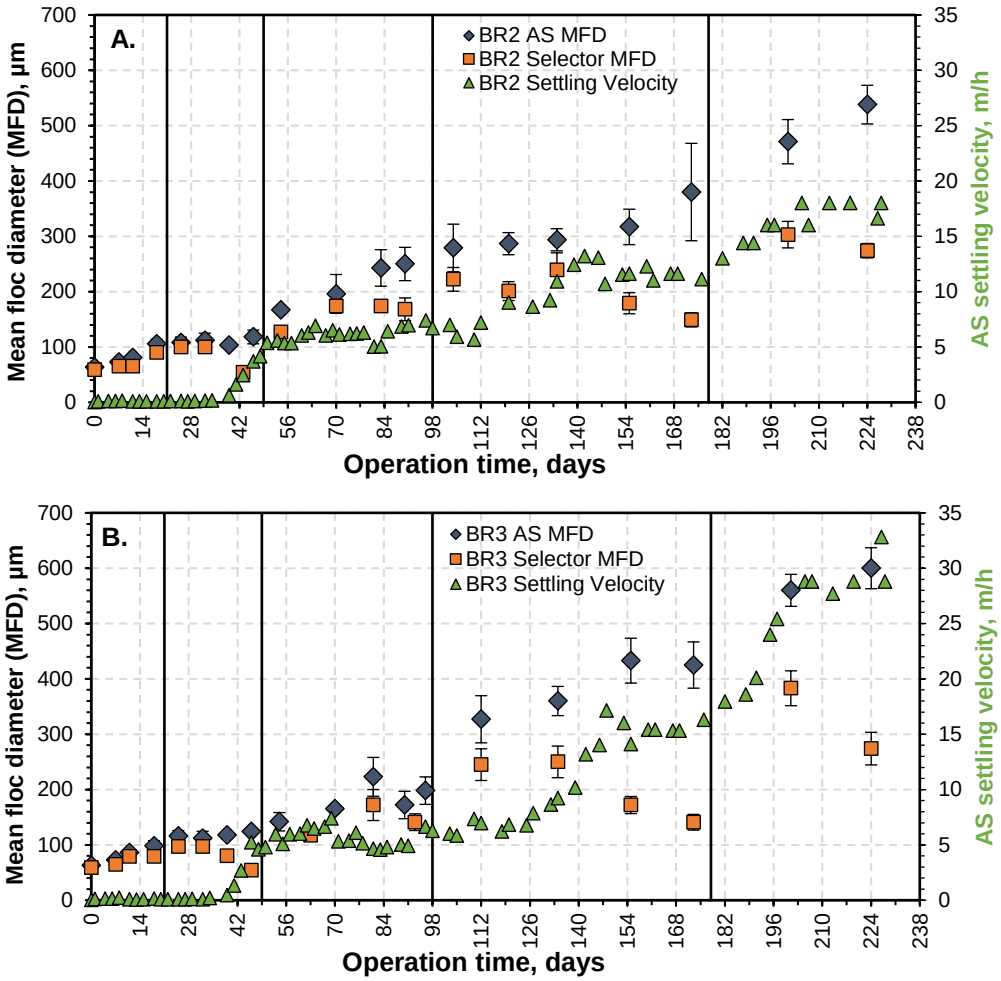

Figure 3.9 A) BR2 and B) BR3, AS MFD (blue diamonds), hydraulic selector discharge MFD (orange squares) and activated sludge settling velocity (green triangles) as a function of time over the duration of the study.

During Stage 4, the MFD of the HS discharge for BR2 and BR3 increased by 32 and 74%, respectively and remained between 222 and 250 µm from day 104 to 134. By day 155 the AS MFD in both BR2 and BR3 had increased, which correlated with an increase in settling velocity and lead to a decrease in HS discharge MFD. Because the HS induced the higher selection velocity, in the following weeks, BR2 and BR3 MFD of the HS discharge decreased, reaching 149 and 141 µm, a 61 and 67% difference when compared to the AS MFD. During this time both the MFDs and settling velocities of the AS stabilized, the HS operation required readjustment to further develop the diameter of the AGS.

During Stage 5, the MFD of the HS discharge for BR2 and BR3 once again increased due to the new HS operating conditions, measuring 303 and 383 µm, respectively. By day 224, as observed before, a larger AS MFD lead to an increased AS settling velocity, and as a result the MFD of HS discharge began to decrease. By the end of the stage BR2 and BR3 MFD of the HS discharge was 50 and 54%, respectively, less than the AS MFD. When the HS discharge had an MFD 10-40% less than the AS MFD, the remaining AS in the BR developed and increased in floc diameter. Once the MFD of the HS discharge decreased beyond 50% (when compared to the AS MFD) the AS MFD and settling velocity stabilized.

The transformation of the AS was also captured through phase contrast imaging. Images of the AS were taken periodically throughout the study both at 40 and 100X magnification and are presented in Fig 3.10.

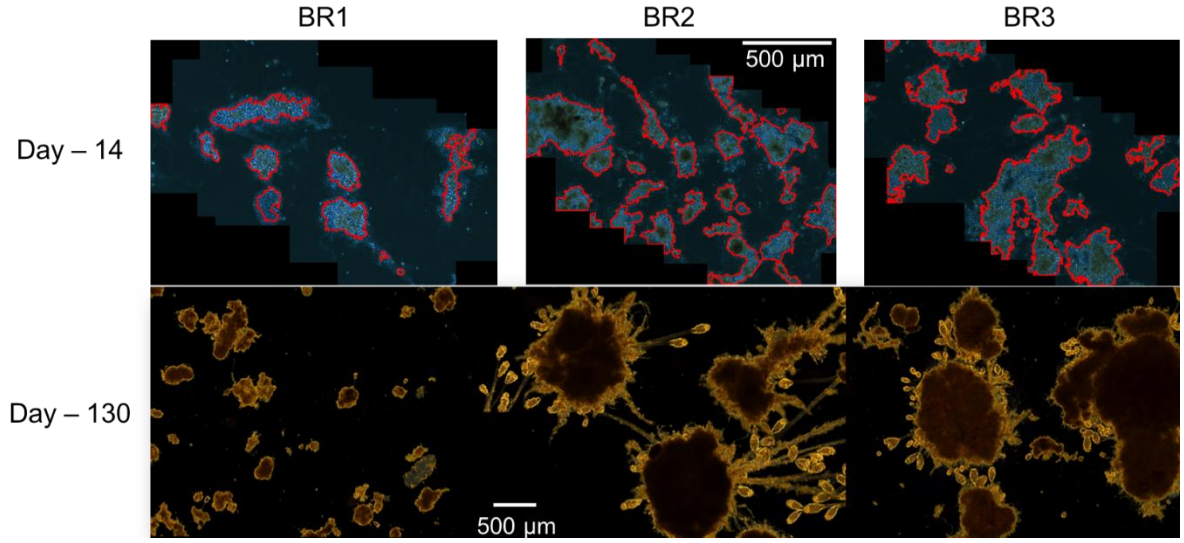

Figure 3.10 Phase contrast images of the AS from BRs 1-3 on days 14 and 130. Images take on day 14 used a 100x magnification and floc were outlined in red through ImageJ software. Images taken on day 130 used 40X magnification.

On the 14th day, the AS from all BRs ranged between 60 and 200 µm. All BR AS floc had a similar appearance, a small and compact core surrounded by filamentous bacteria. By the 130th day the AS had transformed immensely. BR1 floc diameter increased, no filamentous bacteria were present, and the core of the floc appeared dense. The BR2 and BR3 floc diameter had increased substantially, for these particular

images, increasing beyond 500 µm. On the outside of the AGS, the presence of stalked ciliates was apparent, a protozoa that is common in the development of AGS and often indicates a healthy AS system.

3.5 Conclusion

The effects of operating the HS in combination with traditional wasting on the AS settling characteristics were investigated for 283 days. The results from this study showed that when the F/M ratio was maintained between 0.1 and 0.2, a limited HS operation induces enough selection pressure to improve the settling characteristics of the AS and allowed AGS to dominate the biomass. By the end of the study settling velocity of BR2 had increased to 18 m/h and the MFD had reached 538 µm. The AS settling improvements are further magnified in BR3, which only relied on the HS technology. BR1, which operated without HS and only relied on feast/famine conditions, also saw improvements in AS settling characteristics with an SVI30 remaining below 100 mL/g during stages 3-5; however, the final settling velocity of the BR1 AS remained in the traditional CAS range, never exceeding 5 m/h. Thus, maintaining the specified F/M along with feast/famine was key in reducing the negative charge of AS, as demonstrated in Chapter 3, and improves flocculation. However, without the HS technology the development of AGS was hindered in BR1. F/M management may also be achieved at full-scale facilities—a full-scale batch reactor system could adjust the exchange ratio according to the influent sCOD and MLVSS concentration to obtain the desired F/M ratio, or a plug flow reactor could adjust the percentage of activated sludge returned to the headworks so that the desired F/M is achieved.

This study also analyzed the effects of the HS entrance velocity and minimum settling velocity on the AS settling velocity. During Stage 3 the minimum settling velocity induced a higher selection pressure than the HS, but this did not translate into improved AS settling velocities. During Stages 4 and 5 the HS induced the higher selection pressure and the AS settling velocity for both BR2 and BR3 increased beyond the minimum settling velocity. Also, maintaining the HS discharge MFD 10-40% less than the AS MFD ensured a high removal of poor settling floc while maximizing biomass removal. Thus, the HS is a promising technology for the development of AGS and the increase in AS settling velocity.

Acknowledgements

The authors would like to thank the National Science Foundation Engineering Research Center (ERC) for Reinventing the Nation's Urban Water Infrastructure (ReNUWIt) (NSF EEC-1028968) and the Colorado Higher Education Competitive Research Authority (CHECRA) for the funding this research. The author would also like to thank Dr. John Spear, Dr. Geoff Brennecka, Ms. Megan Frytag, Ms. Moira Laughlin, Mr. Mike Veres, and the Denver Metro Wastewater Reclamation District for their technical and scientific support.

3.6 References

[1] T. Sato, M. Qadir, S. Yamamoto, Global , regional , and country level need for data on wastewater generation , treatment , and use, Agric. Water Manag. 130 (2013) 1–13. https://doi.org/10.1016/j.agwat.2013.08.007.

[2] D. Keiser, J. Shapiro, Consequences of the clean water act and the demand for water quality, Quarterly J. Econ. (2018) 1–48. https://doi.org/10.1093/qje/qjy019.Advance.

[3] G. Tchobanoglous, Wastewater Engineering Treatment and Resource Recovery, 5th ed., McGraw-Hill Education, United Kingdom, 2014.

[4] M. Winkler, C. Meunier, O. Henriet, J. Mahillon, M. Suarez-Ojeda, G. Del Moro, M. De Sanctis, C. Di Iaconi, D. Weissbrodt, An integrative review of granular sludge for the biological removal of nutrients and recalcitrant organic matter from wastewater, Chem. Eng. J. 336 (n.d.) 489–502. https://doi.org/10.1016/j.cej.2017.12.026.

[5] M. Pronk, M.K. De Kreuk, B. De Bruin, P. Kamminga, R. Kleerebezem, M.C.M. Van Loosdrecht, Full scale performance of the aerobic granular sludge process for sewage treatment, Water Res. 84 (2015) 207–217. https://doi.org/10.1016/j.watres.2015.07.011.

[6] M.K. De Kreuk, J.J. Heijnen, M.C.M. Van Loosdrecht, Simultaneous COD, nitrogen, and phosphate removal by aerobic granular sludge, Biotechnol. Bioeng. 90 (2005) 761–769. https://doi.org/10.1002/bit.20470.

[7] Y. V Nancharaiah, G.K. Kumar, Bioresource Technology Aerobic granular sludge technology : Mechanisms of granulation and biotechnological applications, 247 (2018) 1128–1143. https://doi.org/10.1016/j.biortech.2017.09.131.

[8] R. Pishgar, J.A. Dominic, Z. Sheng, J.H. Tay, Influence of operation mode and wastewater strength on aerobic granulation at pilot scale: Startup period, granular sludge characteristics, and effluent quality, Water Res. 160 (2019) 81–96. https://doi.org/10.1016/j.watres.2019.05.026.

[9] M. Pronk, M.C.M. Van Loosdrecht, Formation of aerobic granules and conversion processes in an aerobic granular sludge reactor at moderate and low temperatures, 39 (2005) 4476–4484. https://doi.org/10.1016/j.watres.2005.08.031.

[10] S.S. Adav, D. Lee, K. Show, J. Tay, Aerobic granular sludge : Recent advances, i (2008) 411–423. https://doi.org/10.1016/j.biotechadv.2008.05.002.

[11] R.D.G. Franca, H.M. Pinheiro, M.C.M. Van Loosdrecht, N.D. Lourenço, Stability of aerobic granules during long-term bioreactor operation, 36 (2018) 228–246. https://doi.org/10.1016/j.biotechadv.2017.11.005.

[12] B.S. McSwain, R.L. Irvine, P.A. Wilderer, The effect of intermittent feeding on aerobic granule structure, Water Sci. Technol. 49 (2004) 19–25. https://doi.org/10.2166/wst.2004.0794.

[13] M.K.H. Winkler, R. Kleerebezem, W.O. Khunjar, B. de Bruin, M.C.M. van Loosdrecht,

Evaluating the solid retention time of bacteria in flocculent and granular sludge, Water Res. 46 (2012) 4973–4980. https://doi.org/10.1016/j.watres.2012.06.027.

[14] I. Avila, D. Freedman, J. Johnston, B. Wisdom, J. McQuarrie, Inducing granulation within a full-scale activated sludge system to improve settling, Water Sci. Technol. (2021) 1–12. https://doi.org/10.2166/wst.2021.006.

[15] Y. Xu, H. Wang, Z. Wang, Y. Fang, Y. Liu, T. Zeng, Z. Liu, M. Liu, Hydrocyclone breakage of activated sludge to exploit internal carbon sources and simultaneously enhance microbial activity, Process Saf. Environ. Prot. 117 (2018) 651–659. https://doi.org/10.1016/j.psep.2018.06.002.

[16] Y. Liu, H. lin Wang, Y. xiang Xu, Y. yuan Fang, X. rong Chen, Sludge disintegration using a hydrocyclone to improve biological nutrient removal and reduce excess sludge, Sep. Purif. Technol. 177 (2017) 192–199. https://doi.org/10.1016/j.seppur.2016.11.001.

[17] J. Xu, Y. Sun, Y. Liu, W. Yuan, L. Dai, W. Xu, H. Wang, In-situ sludge settleability improvement and carbon reuse in SBR process coupled with hydrocyclone, Sci. Total Environ. 695 (2019). https://doi.org/10.1016/j.scitotenv.2019.133825.

[18] R.A. Maltos, R.W. Holloway, T.Y. Cath, Enhancement of activated sludge wastewater treatment with hydraulic selection, Sep. Purif. Technol. 250 (2020) 117214. https://doi.org/10.1016/j.seppur.2020.117214.

[19] C.P. Leslie Grady, Jr., Glen T. Daigger, Nancy G. Love, Biological Wastewater Treatment, 3rd ed., London Uk, IWA Publishing, 2011.

[20] P. Oliveira, M. Alliet, C. Coufort-Saudejaud, C. Frances, R. Nawaz, L.Y. Tan, H. Nisar, M.B. Khan, J. Zhang, G. Chen, Z. Jia, M.B. Khan, H. Nisar, C.A. Ng, K.H. Yeap, K.C. Lai, J.C. Costa, D.P. Mesquita, A.L. Amaral, M.B. Khan, H. Nisar, N.C. Aun, P.K. Lo, D. Eikelboom, Process Control of Activated Sludge Plants by Microscopic Investigation, Water Sci. Technol. 77 (2000) 2415–2425. https://www.iwapublishing.com/sites/default/files/ebooks/9781900222297.pdf.

[21] J.J. Bisogni, Relationships between biological solids retention time and settling characteristics of activated sludge, Water Res. 9 (1971) 753–763.

[22] E. Amanatidou, G. Samiotis, E. Trikoilidou, G. Pekridis, N. Taousanidis, Evaluating sedimentation problems in activated sludge treatment plants operating at complete sludge retention time, Water Res. 69 (2015) 20–29. https://doi.org/10.1016/j.watres.2014.10.061.

[23] D. Vuono, J. Henkel, J. Benecke, T.Y. Cath, T. Reid, L. Johnson, J.E. Drewes, Flexible hybrid membrane treatment systems for tailored nutrient management: A new paradigm in urban wastewater treatment, J. Memb. Sci. 446 (2013) 34–41. https://doi.org/10.1016/j.memsci.2013.06.021.

[24] A.J. Li, X.Y. Li, H.Q. Yu, Effect of the food-to-microorganism (F/M) ratio on the formation and size of aerobic sludge granules, Process Biochem. 46 (2011) 2269–2276.

https://doi.org/10.1016/j.procbio.2011.09.007.

[25] R.A. Hamza, Z. Sheng, O.T. Iorhemen, M.S. Zaghloul, J.H. Tay, Impact of food-to-microorganisms ratio on the stability of aerobic granular sludge treating high-strength organic wastewater, Water Res. 147 (2018) 287–298. https://doi.org/10.1016/j.watres.2018.09.061.

[26] A. Jafari Kang, Q. Yuan, Long-term stability and nutrient removal efficiency of aerobic granules at low organic loads, Bioresour. Technol. 234 (2017) 336–342. https://doi.org/10.1016/j.biortech.2017.03.057.

[27] B.S.M.S. Sturm, R.L. Irvine, Dissolved oxygen as a key parameter to aerobic granule formation, Water Sci. Technol. 58 (2008) 781–787. https://doi.org/10.2166/wst.2008.393.

[28] American Public Health Association (APHA), Standard Methods for the Examination of Water & Wastewater 21st Edition, Am. Public Heal. Assoc. Am. Water Work. Association, Water Environ. Fed. (1999) 541. http://www.mwa.co.th/download/file_upload/SMWW_1000-3000.pdf.

[29] A. Sochan, C. Polakowski, G. Łagód, Impact of optical indices on particle size distribution of activated sludge measured by laser diffraction method, Ecol. Chem. Eng. S. 21 (2014) 137–145. https://doi.org/10.2478/eces-2014-0012.

[30] Z. Li, P. Lu, D. Zhang, G. Chen, S. Zeng, Q. He, Population balance modeling of activated sludge flocculation : Investigating the influence of Extracellular Polymeric Substances (EPS) content and zeta potential on flocculation dynamics, Sep. Purif. Technol. 162 (2016) 91–100. https://doi.org/10.1016/j.seppur.2016.02.011.

[31] M. Spe, C. Cabassud, A. Masse, Comparison of sludge characteristics and performance of a submerged membrane bioreactor and an activated sludge process at high solids retention time, 40 (2006) 2405–2415. https://doi.org/10.1016/j.watres.2006.04.015.

[32] K. Barbusilqski, H. Koscielniak, Influence of substrate loading intensity on floc size in activated sludge process, Water Research, 29 (1995) 1703–1710.

CHAPTER 4

SHIFTS IN ACTIVATED SLUDGE MICROBIOLOGY DUE TO FEAST/FAMINE CONDITIONS AND THE OPERATION OF A HYDRAULIC SELECTOR

In preparation for submission to Bioresource Technology

Rudy A. Maltos, Gary F. Vanzin, Tzahi Y. Cath

4.1 Abstract

The settling velocity of aerobic granular sludge (AGS) is often considered the most important characteristic of the technology. AGS settling velocity ranges between 15 and 60 m/h compared to conventional activated sludge (CAS) which varies between 2 and 10 m/h. Fast settling biomass reduces the hydraulic retention time of secondary clarifier and may potentially increase the capacity of a wastewater facility. While multiple studies have focused on improving AGS settling velocities, few have focused on the microbial communities of the various floc diameters that are developed and their potential impact on nutrient removal. Thus, there is a need to understand how feast/famine and hydraulic selection independently impact the AS microbiology so that each component may be tailored to produced fast settling AGS with a high abundance of nutrient-removing bacteria. For 238 days three bench scale bioreactors (BRs) were operated continuously—all BRs operated with feast/famine conditions, and each had a unique biomass wasting method. BR1 wasted sludge solely from the bottom of the reactor (traditional wasting), BR2 combined hydraulic selection and traditional wasting, and BR3 operated solely with hydraulic selection. The operating conditions of BR1 did promote the growth of AGS, but their accumulation was limited and resulted in a modest settling velocity of 5 m/h, while BR2 and BR3 reached settling velocities of 18 and 29 m/h, respectively. Throughout the study, 16S and 18S rRNA sequencing was used to quantify filamentous bacteria, phosphorus-accumulating organisms (PAO), ammonia-oxidizing bacteria (AOB), and nitrite-oxidizing bacteria (NOB) abundance. The hydraulic selector discharge for BR2 and BR3 contained a higher relative abundance of filamentous bacteria throughout the study compared to the BR abundance and AGS between the 250-500 µm contained highest abundance of PAO, AOBs, and NOBs. Thus, by combining AS wasting method, BR2 provided fast settling AGS, excellent nutrient removal, and prevented accumulation of Diplogasterida, an order of nematodes that resulted in the destruction of AGS in BR3.

4.2 Introduction

Current wastewater treatment facilities have been configured and engineered to removed nutrients and suspended solids through the accumulation of various helpful bacteria such as ammonia oxidizers (AOB), denitrifiers, and phosphorus-accumulating organisms (PAOs). This combined microbial community is known as activated sludge (AS). Operational parameters that control the concentration of nutrient removing bacteria include solid retention time (SRT), organic loading rates (ORL), dissolved oxygen (DO) concentration, and anaerobic/anoxic phases [1]. In addition to nutrient removal, wastewater treatment facilities are also responsible for complying with stringent effluent solids regulations. This results in facilities

attempting to maximize their solids capture in the secondary clarifier. The secondary clarifier is a gravity driven process engineered to retain AS and preventing its escape to the disinfection process and receiving environments. The AS captured in the secondary clarified is then either returned to beginning of the aeration basins or dewatered and wasted. Minimizing solids leaving the clarifier decreases effluent pathogen concentration and thus reduces required disinfection. However, the current operation mode of secondary clarifiers also leads to accumulation of slow settling floc, and ultimately reducing clarifier capacity or surface overflow rate. Due to the inherent design of clarifiers, flocs that can settle quickly are removed from the treatment train at a higher rate than the slow settling flocs; thus, propagating the attributes of the slow settling floc.

Poor settling floc has traditionally been labeled as sludge bulking, characterized by sludge that settles slowly and compacts poorly. Bulking sludge occurs when floc is dominated by filamentous bacteria, which become abundantly present when the food to microorganism ratio (mass of influent substrate per day over the total reactor biomass as volatile suspended solids) drops below 0.08 [2,3]. At this low carbon concentration, the majority of heterotrophic bacteria are outcompeted by filamentous bacteria, which also have favorable cold temperature kinetics that allows them to thrive during the winter season. Additionally, during the winter season, high concentrations of AS are retained in bioreactors to compensate for the slower microbial kinetics, this further reduces the F:M and prevents the development of dense fast settling AS [4]. These problems with filamentous bacteria are well understood, and strategies such as feast/famine conditioning prevent the exponential growth of filaments [5,6]. A feast occurs during the anaerobic phase, when there is high substrate uptake; then famine follows during the aerobic phase when there is a low substrate concentration in the bioreactor and microorganisms use their internal stored substrate.

Another potential cause of poor settling is related to the floc structure; specifically, the floc density, diameter, morphology, and bulk zeta potential. Feast/famine leads to the production of extracellular polymeric substance (EPS)—this electropositive polymer increases the highly negative zeta potential of the bulk AS, which then allows floc to aggregate and increase in diameter and density [7–9]. Yet, even if feast/famine conditions are implemented, a new selection process would be required to retain faster settling sludge at a higher rate than the traditional AS wasting method.

During the 1980's and 90's, surface wasting of AS basins was practiced to remove foaming and bulking sludge [4,10]. Thus, unintentionally, surface wasting was providing a selection process of slow settling floc, the first of its kind. However, surface wasting removed a large volume of water that contained a low biomass concentration, and spraying chlorinated water on the AS surface was more effective in mitigating the bulking problem. The development of aerobic granular sludge (AGS) also began in the 90's and it continued to develop over the next 30 years. AGS systems effectively combine the required feast/famine conditions with a selection process that reliably produced granules. AGS is highly desirable due to its higher density and circular morphology that results in improved sludge settleability. AGS also contains aerobic and anaerobic zones that allow simultaneous nitrification and denitrification, and have an increased abundance of phosphorus-accumulating organism, stalked ciliates, and ammonia-oxidizing archaea—resulting in

improved nutrient removal capacity [11–13]. However, this granulation system only applies to batch reactors, which represents a small fraction of the wastewater facilities in operation. Also, this system require an uncommon minimum reactor height of 5.5 m.

Recently, alternative technologies like the hydrocyclone and the hydraulic selector (HS) have been able to successfully demonstrate floc selection process through the use of low-pressure separation that could easily be integrated into current continuously flow infrastructure without the need of any specific reactor dimensions [14,15]. Combining feast/famine conditions with an alternative selection process allows conventional facilities to take advantage of AGS's fast settleability while increasing the AS MLSS concentration, which allows for higher organic and nutrient loading rates. However, only few studies have investigated the impacts on the microbial community when floc is transformed to AGS when using a common F:M ratio of 0.1-0.2 [15–18]. There is a need to understand how feast/famine and hydraulic selection independently impact and transform the AS microbiology so that each component may be tailored to produced AGS with fast settling and a high abundance of nutrient removing bacteria. Using only a hydraulic selection technology for AS wasting may also pose difficulties as described in our previous publication [14]. Even when enough biomass is removed through the selection process, accumulation of AS with a higher SRT than desired occurs. Thus, a combination of traditional wasting methods along with hydraulic selection is required to maintain a desired SRT [14]. Combining wasting approach would also provide greater SRT control over and potentially prevent the accumulation of predatory eukaryotic species such as nematodes. Also, by investigating the abundance of AOBs, nitrite-oxidizing bacteria (NOB), and PAOs in various AGS diameter ranges, an ideal granule diameter for carbon and nutrient removal can be identified. This new metric, along with settling velocity, can then be used to determine the optimal mean AGS diameter for a BR.

Floc selected and removed from AS basins has often been overlooked and rarely discussed in detailed. At a full-scale facility, the volume discharge through the selection process may range between 4-400 m^3/day. Thus, understanding the microbial composition of what is selected and how it changes over time is an important parameter for AGS's success, and would allow for the waste stream to be properly managed. Studying the microbial communities of the AS discharged and comparing it to the communities that remain in the reactor also allows for the development of a microbiology mass balance. This would help determine if the hydraulic selection process provides an additional environmental selection pressure that shifts the microbial community or if the community shifts are purely driven by operation conditions, and the selection process is simply based on settling velocity principles.

In this study, an in-depth investigation via 16S and 18S-RNA gene analysis was conducted to determine how feast/famine and hydraulic selection independently influence the microbial shifts in the AGS community. We also evaluate the shifts in AS microbiology caused by the operation of the hydraulic selector combined with traditional AS wasting to control floc diameter and SRT. Lastly, in our previous publications [14,19] we demonstrated the hydraulic selector's ability to develop an AGS with a specific mean floc diameter; however, many researchers have simply focused on developing the larger granules due to their

higher density and faster settling. Few studies have investigated how the microbiome of the AGS changes as its diameter increases and the potential effects on carbon and nutrient removal. Thus, this study also evaluated floc in various diameter ranges through 18S-RNA gene sequencing to develop an understanding of the microbial community in each floc category and how they change over time when being fed municipal strength wastewater.

4.3 Material and methods

4.3.1 Experimental setup and operation

Three lab-scale bioreactors (BRs) were used in this study [19]. All BRs were seeded with 84 L of AS from the Denver Metro Wastewater Reclamation District aeration basins. The control bioreactor, bioreactor 1 (BR1), operated without hydraulic selection and wasted sludge from the bottom of the BR at the end of each settling phase. Bioreactor 2 (BR2), operated with a combined wasting method in which 25-50% of the biomass was wasted from the hydraulic selector and the remaining biomass was wasted from the bottom of the reactor after the settling phase. Bioreactor 3 (BR3), operated solely with hydraulic selector wasting. Through these wasting mechanisms the SRT was maintained between 10 and 15 days. The influent wastewater was carbon limited and thus required additional carbon; glycerin was dosed as needed to maintain a F:M between 0.1 and 0.2. The operation of the hydraulic selector was dependent on the settling velocity of the AS; selector operating conditions are described in Table 4.1. The purpose of the hydraulic selector was to increase the AS settling velocity, and when settling velocities became stagnant, the operation of the hydraulic selector was changed to increase the removal of poor settling floc.

Table 4.1. The study was conducted over five stages for a total of 238 days. Each stage had a unique HS operating condition, described by the settling time (prior to the hydraulic selection process) and hydraulic selector outflow.

	Stage 1	Stage 2	Stage 3	Stage 4	Stage 5
Days of operation	21	21-49	49-98	98-178	178-238
Settling time (min)	15-10	10-3	1	1	1
Outflow (L/min)	0.5	1	1	2	3

The operation of all BRs had identical fill, mixing, and aeration phases, as summarized in Table 4.2. The times of these phases were intentionally exaggerated to ensure the presence of feast/famine conditions. BR2 and BR3 operated with a hydraulic selector; therefore, there was an initial settling period before the hydraulic selector operation and a final settling time after the selection process. The final settling for BR1 was 20 minutes and for BR2 and BR3 the sum of the initial settling selector discharge time, selector discharge time, and final settling time was always equal to a total of 20 minutes.

Table 4.2. The operation of the three BRs was composed of 5 or 7 phases. Total cycle time was approximately 325 min and all BRs operated with a 30% exchange ratio.

Phase	BR1	BR2	BR3
Fill (min.)	60	60	60
Mixing (min.)	60	60	60
Aeration (min.)	180	180	180
Initial settling (min.)	NA	15 – 1	15 – 1
Selector discharge (min.)	NA	0.5 – 3	0.5 – 3
Final settling (min.)	20	5 - 18	5 – 18
Decant (min.)	5	5	5
Total cycle time (min.)	≈325	≈325	≈325
Exchange ratio (%)	30	30	30

4.3.2 Sample collection and physicochemical processing

Three different methods were used to collect biological samples, this allowed for a comprehensive analysis of the microbial communities and their shifts over time. The sampling procedures are shown in Fig. 4.1

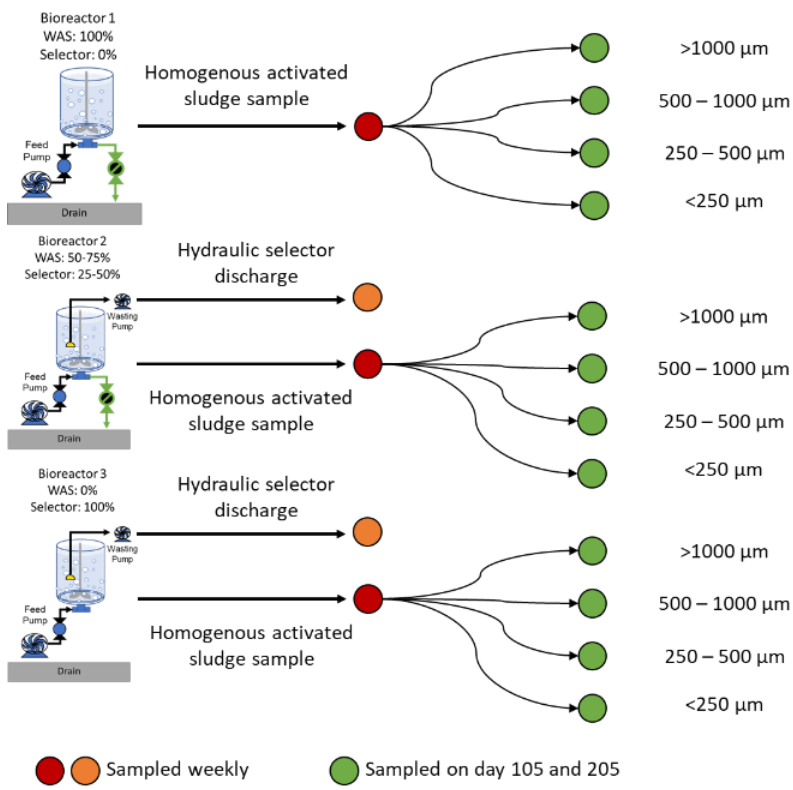

Figure 4.1 Biological sampling protocol for the three BRs. Activated sludge samples were collected once every week (red dots) and on days 150 and 205. Activated sludge was sieved into 4 floc diameter categories (green dots). Hydraulic selector discharge from BR2 and B3 was also collected once a week (orange dots).

Method 1 – AS samples: each week, approximately 250 mL of AS from each bioreactor was collected during the mixing and aeration phases. Method 2 – sieve sampling: samples were collected to analyze the development of floc across various diameters through biomass floc diameter distribution and 16S/18S rRNA sequencing. A 1 L sample of AS was collected from the BR during the mixing and aeration phases, the sample was then filtered through a 1.4 mm sieve. An additional 5 L of DI water were then used to wash the biomass through the sieve. The biomass retained on the sieve was removed by pouring 1 L of DI water in the reverse direction. This process was repeated with 1 mm, 0.5 mm, and 0.25 mm sieves. The TSS for each floc diameter category was then calculated according to standard methods [20]. Method 3 – hydraulic selector discharge samples: discharge of the selector, which normally flows directly to the drain, were collected in a 20 L container. Before biological samples of the hydraulic selector were collected, the entire selector piping system was drained, to ensure that fresh samples were collected. Composite samples (24-hours) were collected once a week from the equalization tank, primary clarifier (PC) decant tank, and decant, and were measured for total COD (tCOD), soluble COD (sCOD), ammonia, nitrate, orthophosphate, pH, and alkalinity. These analyses (excluding pH) were performed using HACH TNT PlusTM (Loveland, CO) reagent vials and a Hach DR 5000^{tm} spectrophotometer.

4.3.3 DNA extraction, PCR and 16S/18S rRNA sequencing

Triplicate biological samples were centrifuged for 10 minutes at 5,000 rpm, the supernatant was discarded, and the pellet was weighted and stored at -20 °*C* until further analysis. DNA was isolated using the DNeasy PowerSoil HTP 96 Kit *(Qiagen, Inc., Germantown, MD, USA)* following the manufacturer's protocol and employing two rounds of mechanical disruption using a Biospec Mini-Beadbeater-96 for two minutes per disruption cycle. DNA amplification and barcoding was based on methods in Gohl et al. using the small subunit rRNA universal primers 515F and 926R from Parada et. al. [21,22]. The forward primer contains a 5' extension corresponding to the Illumina Nextera Read1 sequence while the reverse primer contains a 5' extension corresponding to the Illumina Nextera Read2 sequence. Taken together, the primary pcr primers correspond to 515F-NexteraRead1 and 926R-NexteraRead2. PCR was performed in 25 microliter reactions using 3 ng of DNA per sample and the KAPA HiFi Hot Start PCR kit (Kapa Biosystems, Inc.) as described in Table 4.3.

Table 4.3. PCR thermocycling conditions, a total of 22 cycles were required

Phase	**Temperature (°C)**	**Time**
Initial Denaturation	95 °C	3 minutes
	Single Cycle	
Denature	98 °C	30 seconds
Anneal	55 °C	30 seconds
Extend	72 °C	60 seconds
Final Extension	72 °C	5 minutes

Primary PCR products were purified by solid phase reversible immobilization using KAPA Pure Beads (Kapa Biosystems, Inc.) following the manufacturer's protocol at 0.8X bead concentration (e.g., 20 microliters KAPA Pure Beads mixed with 25 microliter PCR reaction). Ten nanograms of the primary PCR products were indexed using unique pairs of either Illumina Nextera XT or Illumina TruSeq indexing primers. PCR conditions were identical to conditions described in Table 3, except only eight cycles were run. Indexed PCR products were purified using KAPA Pure Beads as noted above, quantified using the Qubit broad range DNA quantification kit (Thermofisher,Inc.) and pooled at equimolar ratios. The final library was sequenced using an Illumina 2X300 kit at University of Colorado Anschutz Medical Campus Genomics and Microarrary Core.

rRNA sequences (henceforth called 'amplicon sequence variants', or ASVs) [23,24] were initially processed using DADA2 [23] and Phyloseq [25] in R version 3.4.2. Key processing steps include sequence trimming to Q>30, error rate estimation using seed=100, dereplication, paired-end read merging, and chimera removal. Samples were processed separately for eukaryotic 18S rRNA gene characterization, where only forward sequence was used. This was necessary due to the variable length of the 18S amplicon that exceed the 600 nucleotide read length. Taxonomy for 16S rRNA genes were assigned using Silva database version 138 while Silva 132 was used for the 18S rRNA gene taxonomy. Using two databases was required because the official DADA2-formatted Silva version 138 reference sequences are optimized for classification of bacteria and archaea and are not suitable for classifying eukaryotes.

4.3.4 Abundance analysis

Prior to abundance analysis, data from biological replicates were merged and single sequences were removed. Data were converted to relative abundance prior to heatmap and bar chart development and are presented at the genus level. Genera identified from 16S rRNA gene sequencing were cross referenced against the MiDAS (Microbial Database for Activated Sludge) field guide, which contains curated physiology data for wastewater related microorganisms. Specific functions queried were AOB, NOB, PAO, FIL.

4.3.5 Microscopy

Live wet mounted phase contrast images of all bioreactors were taken approximately every two weeks, for the first 41 days, images were taken at 100X magnification, due to the increasing floc size 40X magnification was then used for the remainder of the experiment. Images were captured using Infinity 2 software (Lumenera, Ontario, Cananda). Beginning on day 200, AGS images were also taken using a Sony Alpha a6000, with 16-50 mm zoom lens and 16 mm tube extender. ImageJ, an open source software, was used to stitch photos together, detect and calculate floc area, and scale images appropriately [28,29].

4.4 Results and discussion

4.4.1 The development of AGS, AS settling velocity and hydraulic selector operating conditions

The three BRs were operated continuously for 238 days. The seed sludge taken from the Denver Metro Wastewater Reclamation District had a settling velocity of less than 1 m/h. The settling time prior to the HS selector operation was long, 15-10 minutes and the outflow was set to 0.5 L/m, equal to an hydraulic selector entrance velocity of 4.4 m/h. As the settling velocity of the AS improved, the outflow of the hydraulic selector was increased, resulting in a higher selector entrance velocity. The higher the entrance velocity the more biomass is discharged and the mean floc diameter increases. The BRs settling velocity, the minimum settling velocity, described in Chapter 3, and selector entrance velocity are shown in Fig. 4.2.

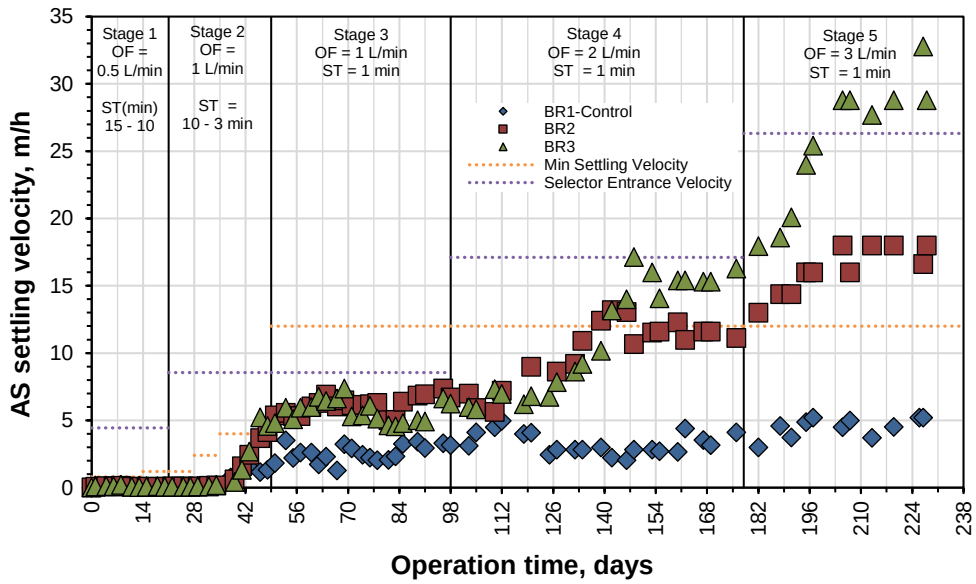

Figure 4.2 AS settling velocity of the three BRs, as indicated by the blue diamonds, red squares, or green triangles, respectively. The dashed orange line is the minimum settling velocity and the purple dashed line is the selector entrance velocity as described in Chapter 3.

4.4.2 Activated sludge floc diameter and biomass distribution

In Chapter 3 floc diameter was measured through a laser particle size analyzer, but for this chapter, a size distribution based on sieved biomass was developed. The laser particle size analyzer was not used because it relies on a volume-based floc diameter distribution, and if the AS across all floc sizes have the same density, it would be possible to convert the distribution into biomass. However, multiple studies have shown that the density of floc varies with size and AGS is known to have the highest densities [30,31]. At three different time points of the study, a sample of AS from each BR was sieved into five separate floc categories. The biomass retained on the sieve was then collected and weighed, as described in section 4.2.2. The five floc categories are <250 µm, 250–500 µm, 500–1000 µm, 1000–1400 µm and >1400 µm, results are shown in Fig. 4.3.

The seed sludge contained 86% of its biomass in the smaller than 250 µm floc diameter category. This was expected based on its poor settling characteristics. On day 105, BR1 had a substantial biomass increase in 250-500 µm category, at the same time the AS settling velocity had improved to 3.5 m/h. BR2 had similar biomass percentage in the 250-500 µm category as BR1; however, the BR2 settling velocity had increased to 5.8 m/h. This higher settling velocity may have caused a lower biomass percentage in the smaller than 250 µm category or a higher biomass percentage in the 500-1000 µm category or a combination of both. BR2 and BR3 had nearly the same settling velocities but their biomass distributions differed. BR3 had the highest biomass percentage in the 1000-1400 µm category. This difference of biomass is most likely due to the effects of solely operating with the hydraulic selector, which lead to the accumulation of larger floc diameter.

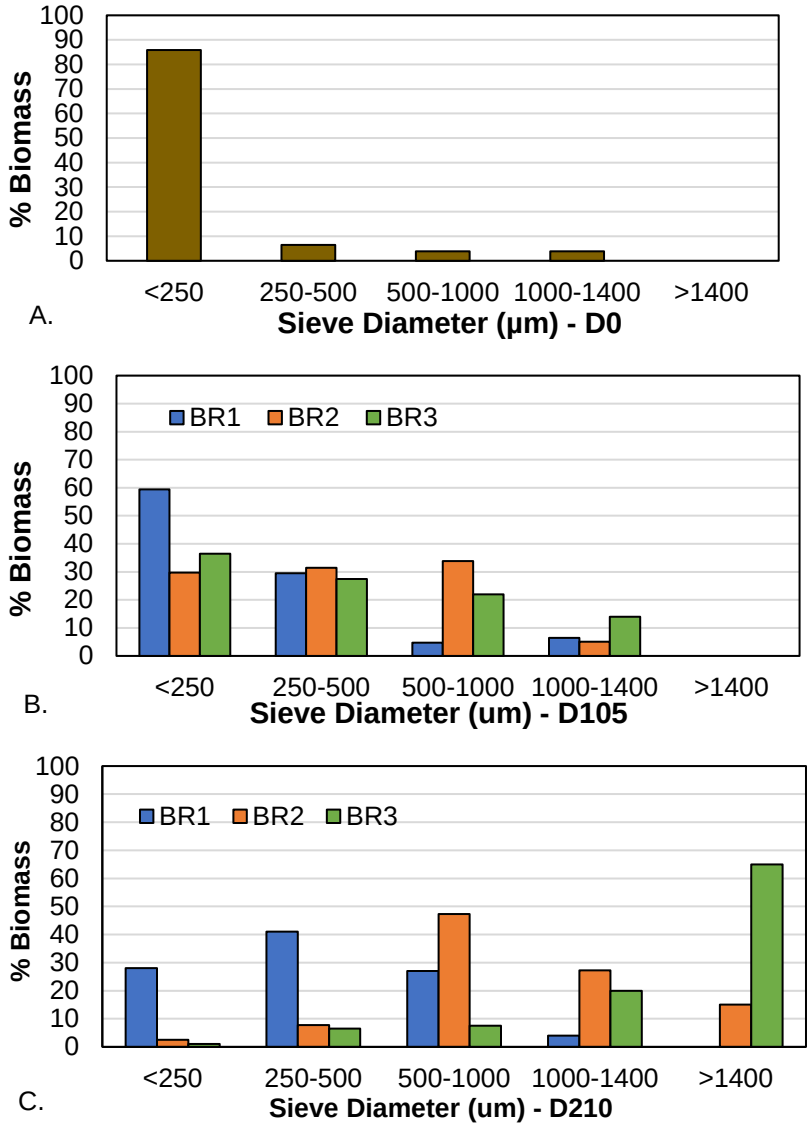

Figure 4.3 Activated sludge floc diameter biomass distribution, separated into five floc diameter categories (A) Seed sludge from Denver Metro, (B) BRs 1-3 on day 105, and (C) BRs 1-3 on day 210.

By day 205, the effects of wasting with and without the hydraulic selector were apparent. Without hydraulic selection, and only relying on feast/famine conditions, BR1 was able to slowly transform the sludge, and by the end of the study the majority of the biomass resided in the 250-500 µm category. Although the floc diameter distribution improved, the settling velocity only increased by 17%, reaching 4.1 m/h. When BR2 and BR3 had a similar distribution their approximate settling velocity was 6 m/h, indicating that the density of the BR2 and BR3 floc may have been higher. Also, BR1 did not accumulate any biomass larger than 1400 µm, indicating that the selection pressures required for the development of larger floc were not present or that the continuous wasting from the reactor bottom prevented their accumulation. BR2 used the combined wasting approach, this resulted in a normal distribution among the five biomass categories with the 500-1000 µm category as the mean. With this wasting approach, the selector provided enough poor settling floc removal while allowing the accumulation of larger floc to occur. This resulted in an AS settling velocity of 18 m/h, three times faster than BR1. On the other end of the wasting spectrum BR3 only used hydraulic selection. The high minimum settling velocity required to be retained in the reactor resulted in accumulation of biomass only larger than 1000 µm. While this developed the highest settling velocity (28 m/h), granules of this diameter fed municipal strength wastewater experience limited substrate diffusion into the granule core. This occurs due to consumption of carbon by new biomass on the outer layers of the granule. This prevents carbon from reaching denitrifies and PAO in the core of the granule and often leads to the deterioration of the AGS.

4.4.3 Activated sludge imaging and physical transformation over time

The seed floc taken from Denver Metro wastewater facility had little to no filamentous bacteria; still, the floc had very poor settling characteristic, slower than 1 m/h, due to the abundance of small floc, with an average diameter 60 µm, phase contrast images are presented in Fig. 4.4. The AS from Denver Metro also had an SRT of less than 10 days, which reduces the microbial diversity of the AS. Specifically, it limits the development and accumulation of protozoa and metazoa organisms. This is beneficial because it reduces the population of nematodes and worms that destroy and consume floc; but this also prevents the development of protozoa such as ciliates that are required for the growth of AGS.

Two weeks into the experiment and the AS floc did not have any drastic changes to morphology or increase in floc diameter, and filamentous abundance continued to remain low. During these two weeks, the AS for all BRs had similar settling velocities of less than 1 m/h and SVI_{30} higher than 200 mL/g. On day 35 the first visual improvements were observed, ciliates where first observed BR1 floc and floc in BR2 and BR3 had increased in dimeter, all BRs had an improved SVI_{30} of less than 150 mL/g, while the settling velocity of all BRs still remained 1 m/h. On day 41 ciliates were first observed in BR2 (free swimming) and BR3 (stalked), but floc diameter in BRs 1-3 remained relatively the same size. However, SVI_{30} continued to improve with all BRs lower than 150 mL/g. As the floc were increasing in diameter, it was clear that a larger image area of each sample would be required to accurately capture images that represent the AS;

therefore, magnification was decreased to 40X. Phase contrast images captured with 40x magnification between days 59 and 195 of BRs 1-3 are shown in Fig. 4.5.

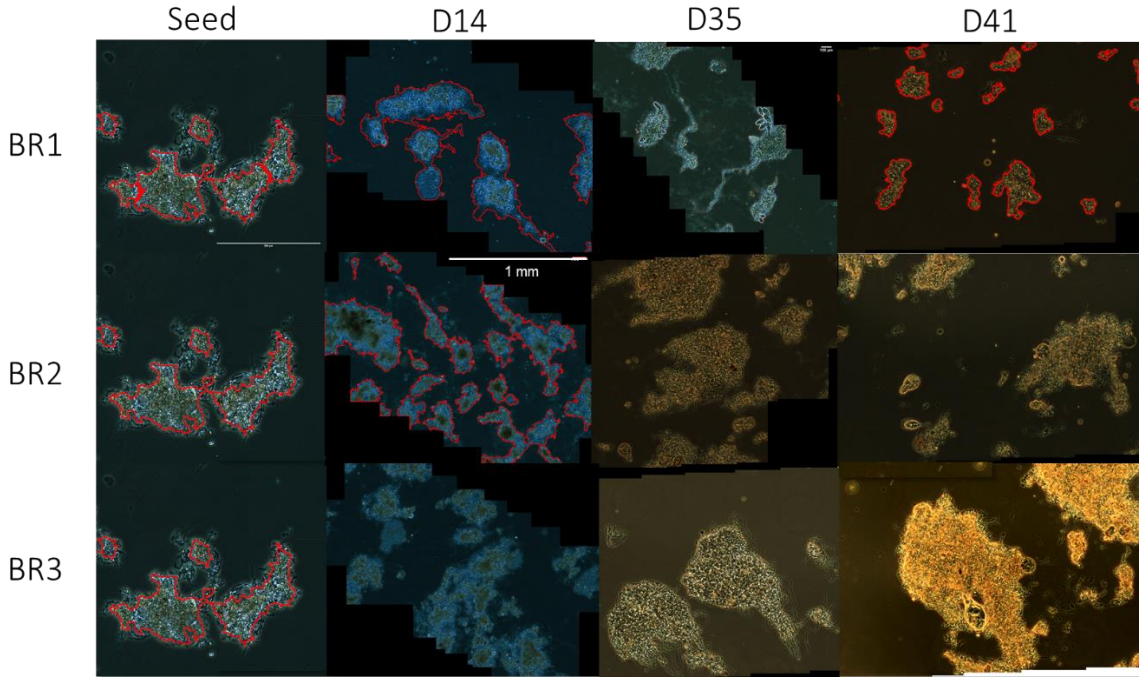

Figure 4.4 Phase contrast images at 100x magnification of the Denver Metro Wastewater seed floc and activated sludge of BR 1-3 from day 14 to 41. The redlines outline floc detected by the ImageJ software.

On day 59 BR1 AS was still dominated by dispersed floc, with a diameter smaller than 100 µm while floc in BR2 and BR3 began to compact and became spherical. By day 99, BR1 floc also began to compact, floc diameter was still smaller than 200 µm; however, the presence of stalked ciliates indicated the floc would continue to develop. Flocs in BR2 and BR3 also increased in diameter, reaching on average a 300 µm. Interestingly, BR3 also had multiple floc smaller than 100 µm, these small flocs most likely caused the increase in BR3 decant TSS. By day 124 the settling velocities of BR 1, 2, and 3 were 2.6, 8.5 and 7.2 m/h, respectively. BR1 had multiple, dense floc approximately 150 µm in diameter while BR2 and BR3 had floc diameters closer to 400 µm. Granules in BR 3 had a large presence of stalked ciliates, which are common during AGS development and serve as a structure or mesh for AGS expansion in replacement of filamentous bacteria. Once a granule is formed, stalked ciliates may also grow on the outside of the granule. As the stalk increases in length, bacteria develop on the stalk and fill the gap between the end of the ciliate and core of the granule, this allows the granule to increase in diameter. While ciliates are beneficial, once a ciliate extends far beyond the core of the granule, the granule may become irregular in shape and increase drag during settling. A potential explanation of the high presence of stalked ciliates is a lack of shear force that would prevent their growth and lead to smooth granules [32,33]. On day 159 the floc in BR1 looked relatively the same and did not increase in diameter, with many flocs defined by irregular shapes. BR2 and BR3 continued to increase in diameter with BR2 containing various stalked ciliates nearly 1 mm in length.

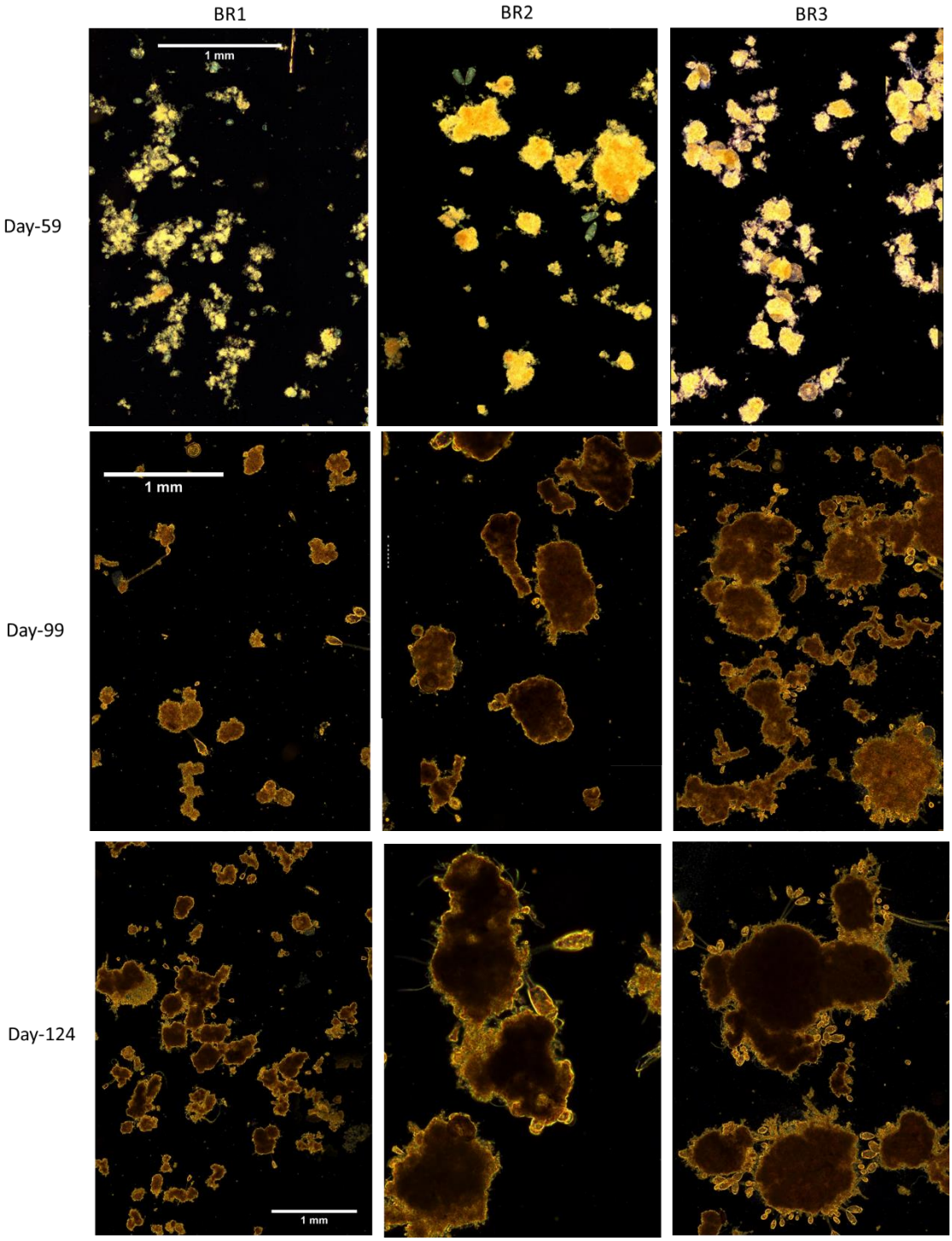
BR1
BR2
BR3
Day-59
Day-99
Day-124
1 mm
1 mm
1 mm

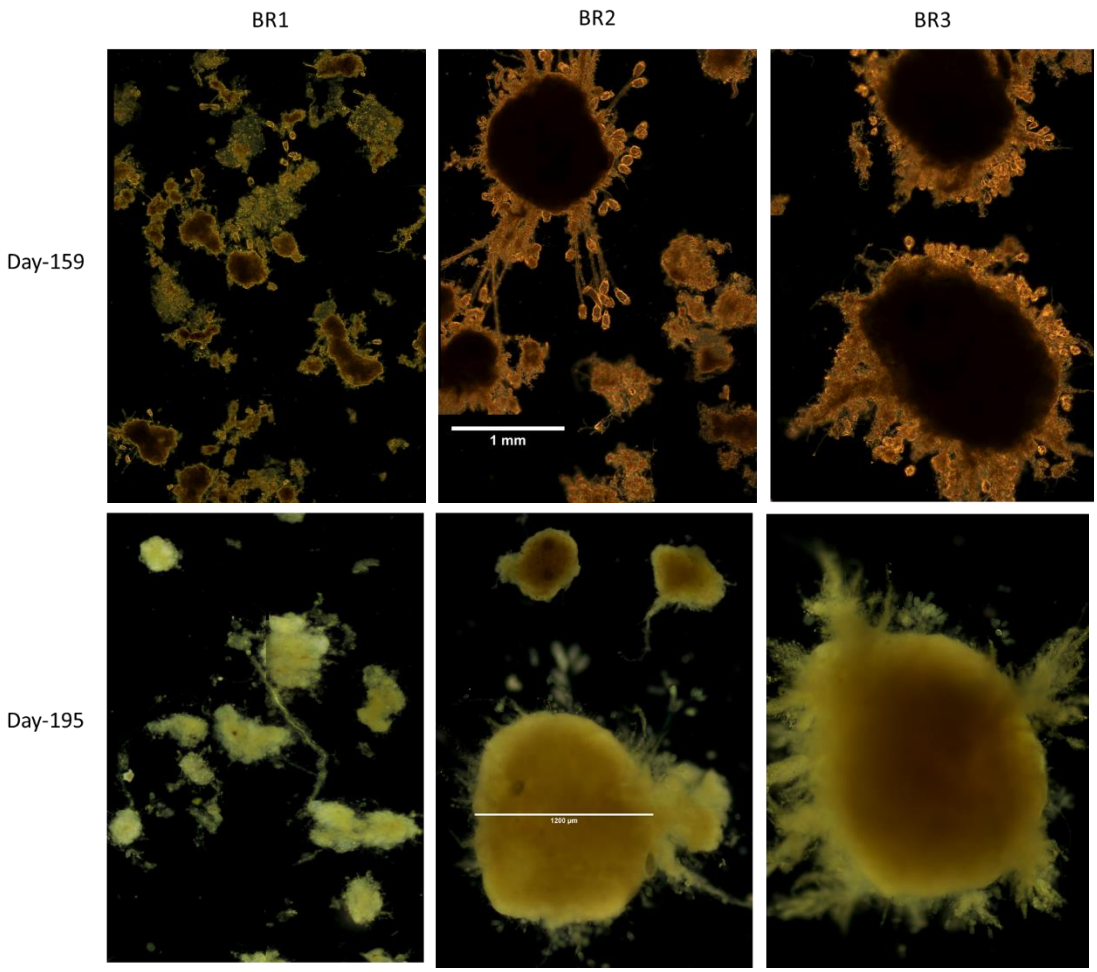

Figure 4.5 Phase contrast images of BR 1-3 at 40X magnification on days 59, 99, 124, 159, and 195. Floc in all BRs increase in diameter but BR2 and BR3 are always substantially larger than BR1.

The final phase-contrast photos were taken on day 195. Due to the large volume of the AGS in BR2 and BR3, the normally used cover slip was flattening the AGS. For this reason, a coverslip was not used, images are not entirely in focus due to the three-dimensional nature of the granules. Floc in BR1 exceeded 200 µm; yet, the floc still maintained an irregular shape and appeared less dense compared to BR2 and BR3. Flocs in BR2 and BR3 continued to increase in diameter, BR2 contained a variety of floc diameters while BR3 was dominated by floc >1000 µm. Floc in BR3 was dominated by outgrown stalked ciliates, indicating unstable growth and potentially causing sudden increases in effluent decant TSS. On day 224 AS larger than 250 µm for BR2 and BR3 was suspended in DI water, images of the AGS are shown in Fig. 4.6. Both BRs are dominated by floc larger than 500 µm, BR2 contains mostly spherical granules while the granules in BR3 have become irregular caused by the outgrowth of stalked ciliates and are dominated by nematodes. The high abundance of nematodes in BR3 may eventually lead to the destruction of the AGS and washout of biomass. This high abundance was most likely caused by only wasting through the hydraulic selector.

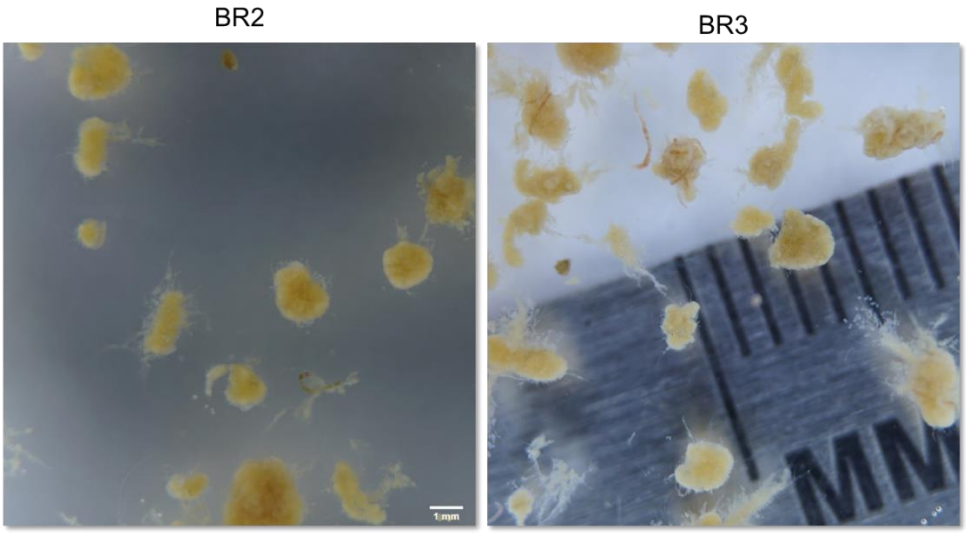

Figure 4.6 On day 224 floc >250 µm for BR2 and BR3 was suspended in DI water. Photos were taken using a Sony Alpha 6000, with a 16-50 mm zoom lens and 16 mm tube extender.

4.4.4 Nutrient removal

The carbon and nutrient removal performance of the lab-scale BRs was monitored over a 238-day period. Composite influent sCOD and COD as well as effluent sCOD were measured weekly and are shown as a function of time in Fig. 4.7. Average influent COD and sCOD concentrations were 479±166 mg/L and 376±144, respectively. Organic carbon in the form of glycerin was added at the headworks to increase sCOD and maintain F:M between 0.1 and 0.2, as described in section 4.2.1. The difference between the COD and sCOD concentrations represents the particulate COD (pCOD) fraction. Minimizing the pCOD is highly desirable because high concentrations of pCOD in the BRs prevent feast/famine conditions. Higher concentrations of pCOD results in the hydrolysis of the particles during the aeration/famine phase, and this turns biologically unavailable carbon into sCOD and disrupts the famine phase and allows filamentous bacteria to develop. The primary clarifier was consistent in removing pCOD, and removed approximately 30% of the influent pCOD. This was an important factor for maintaining feast/famine conditions throughout the study. Future research may focus on refining the pCOD removal in the headworks, which may reduce the time required to develop AGS and increase the longevity of granules.

All BRs maintained an sCOD of less than 30 mg/L throughout the majority of the study. However, on day 81, influent COD suddenly spiked, potentially induced by students moving into the dormitories and reached 2000 mg/L. COD then decreased to 1580 mg/L on day 84, and by day 104 the influent COD was within its normal range. During this time, the MLSS concentration of all the BRs were relatively similar; yet, BR1 had two days with effluent sCOD higher than 30 mg/L. BR2 and BR3 did not experience the same problems as BR1, mostly due to the development of AGS, which has the ability to handle sudden changes in influent loading rates, as described in various studies [16,34,35]. For the remainder to the experiment, all BRs had nearly similar effluent sCOD.

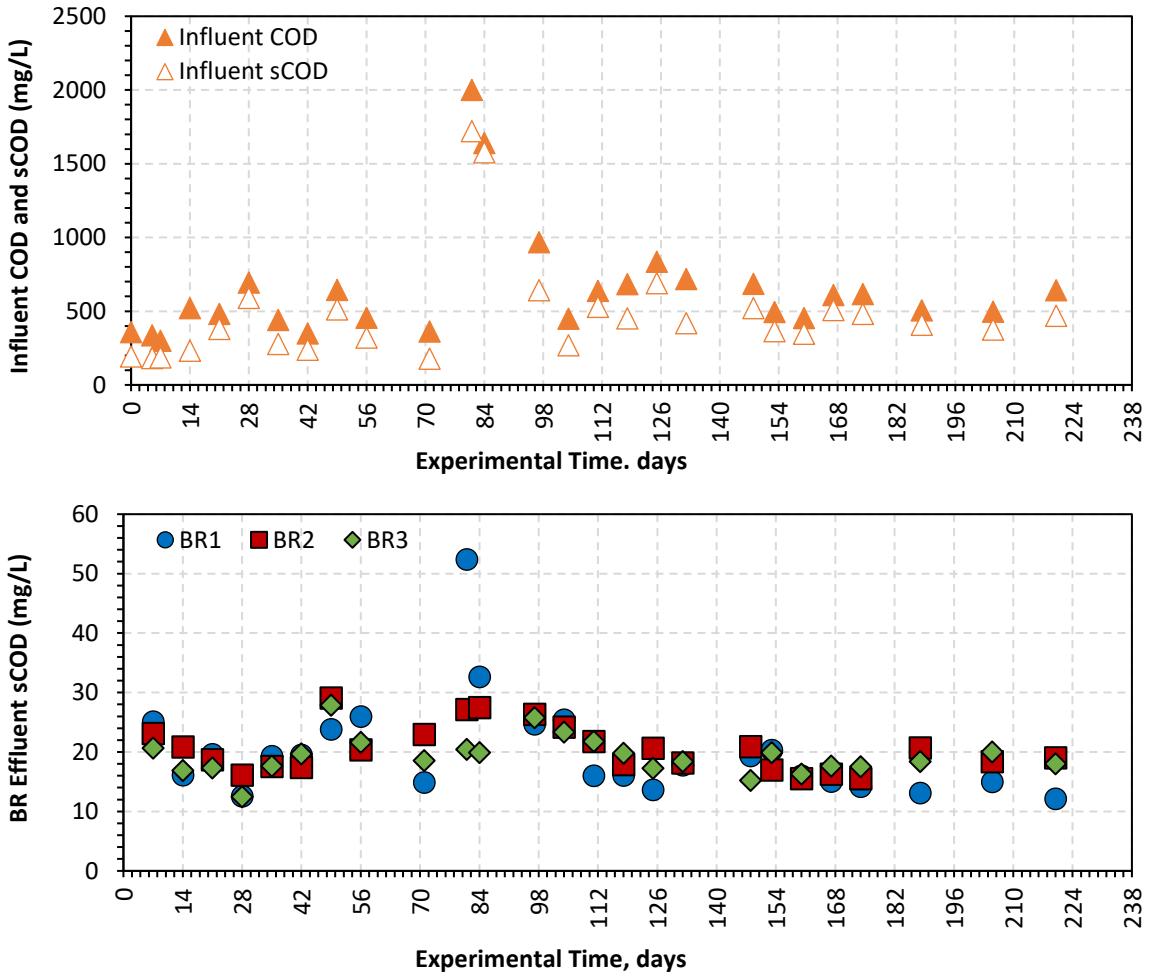

Figure 4.7 A) influent sCOD and COD concentration (mg/L) as a function of time and B) effluent sCOD concentrations (mg/L) as a function of time. The average influent COD was 479±166 mg/L and all BRs with the exception of BR1 on days 81 and 84 maintained effluent sCOD lower than 30 mg/L.

The influent and effluent ammonia and nitrate concentrations were measured periodically over the duration of the study and are shown in Fig. 4.8. Unlike carbon, nitrogen was not supplemented, thus the wastewater feeding the BRs contained a lower than average ammonia concentration over the first 42 days of the study. Influent ammonia increased when students moved into the dormitories and reached a maximum of 40 mg/L-N on day 104. Soon after, influent ammonia concentration decreased and stabilized at an average of 30 mg/L.

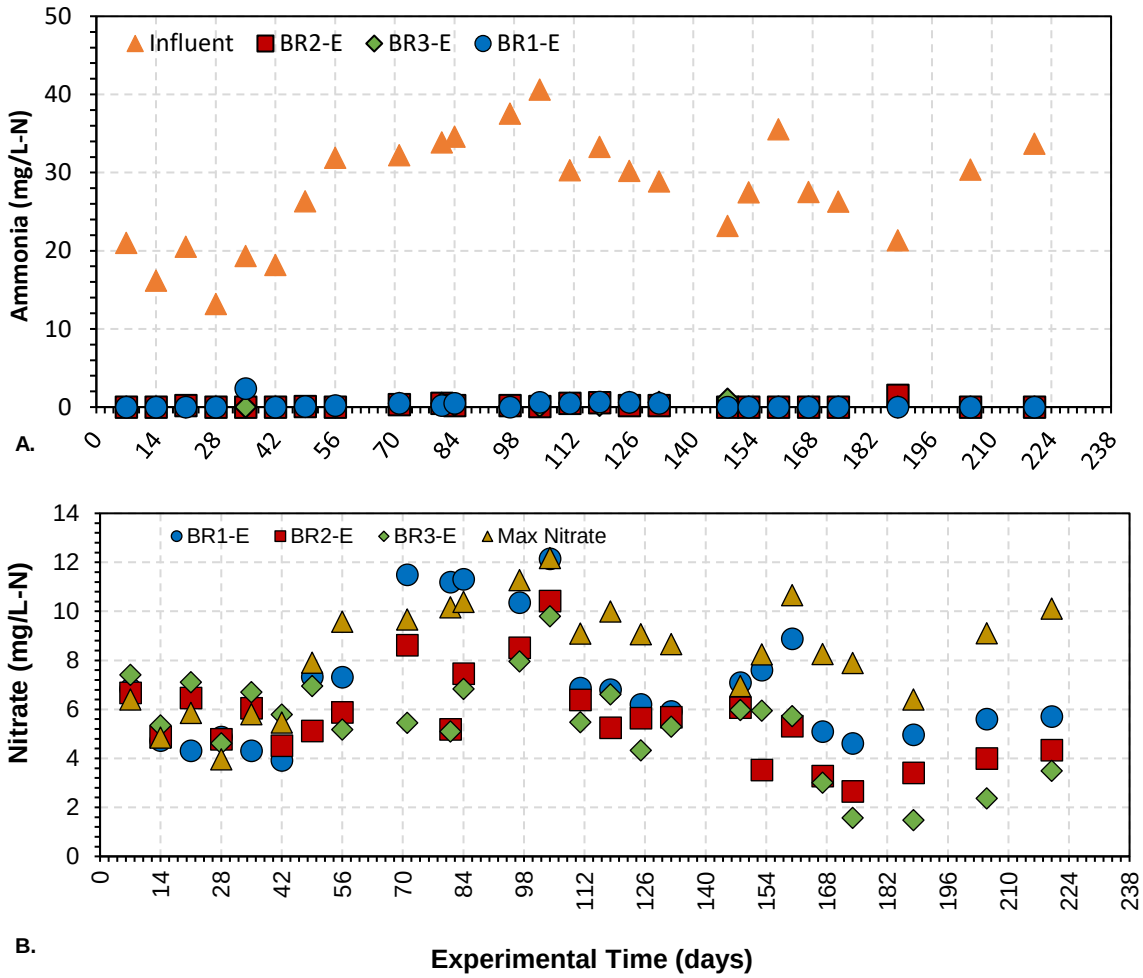

Figure. 4.8. A) Influent ammonia and BRs 1-3 effluent ammonia B) Effluent nitrate for BRs 1-3 and maximum nitrate concentration based on influent ammonia concentration

Effluent ammonia concentrations for all BRs were consistently lower than 1 mg/L, regardless of the varying influent concentration (Fig. 8A). However, during the first 49 days of the study, limited to no denitrification occurred as shown in Fig. 8B. The brown triangles represent the concentration of ammonia nitrogen that may be converted to nitrate; and during the first 49 days, the effluent nitrate values for all BRs were nearly identical to the maximum nitrogen concentration. After day 49 the influent ammonia and thus effluent nitrate potential increased. During this time BR1 effluent nitrate concentration increased while BR2 and BR3 were able to develop simultaneous nitrification/denitrification. The operating conditions of the BR ensured feast/famine; thus, a long aeration phase with a high DO between 4-6 mg/L was required. Even with unfavorable denitrification conditions, BR2 and BR3 were constantly denitrifying. By day 111 BR1 had also gained the ability to denitrify, but it always had higher effluent nitrate concentration compared to BR2 and BR3.

Orthophosphate was also measured periodically in both the influent and BR effluents as shown in Fig. 4.9. Phosphorus has become a highly regulated nutrient, with some wastewater facilities having maximum

discharge concentrations of less than 1 mg/L PO_4-P. Many wastewater facilities have already modified or intend to modify their biological process to accumulate PAOs. Due to the initial low strength of the wastewater, orthophosphate concentration was 6 mg/L-P at the beginning of the study. By day 94, influent orthophosphate reached a maximum concentration of 13 mg/L-P. Orthophosphate then decreased and stabilized at approximately 10 mg/L-P for the remainder of the study. All BRs had excellent phosphorus removal ability with BR2 and BR3 always having an effluent concentration of less than 1 mg/L-P. BR1 also removed phosphorus effectively until day 81, when effluent phosphorus levels spiked, potentially due to increasing influent phosphorus concentration. Effluent phosphorus levels in BR1 remained above 1 mg/L-P until day 160. Although it is evident that all BRs had PAOs, a potential benefit of the AGS in BR2 and BR3 are the greater abundance of PAOs that could manage higher phosphorus loads.

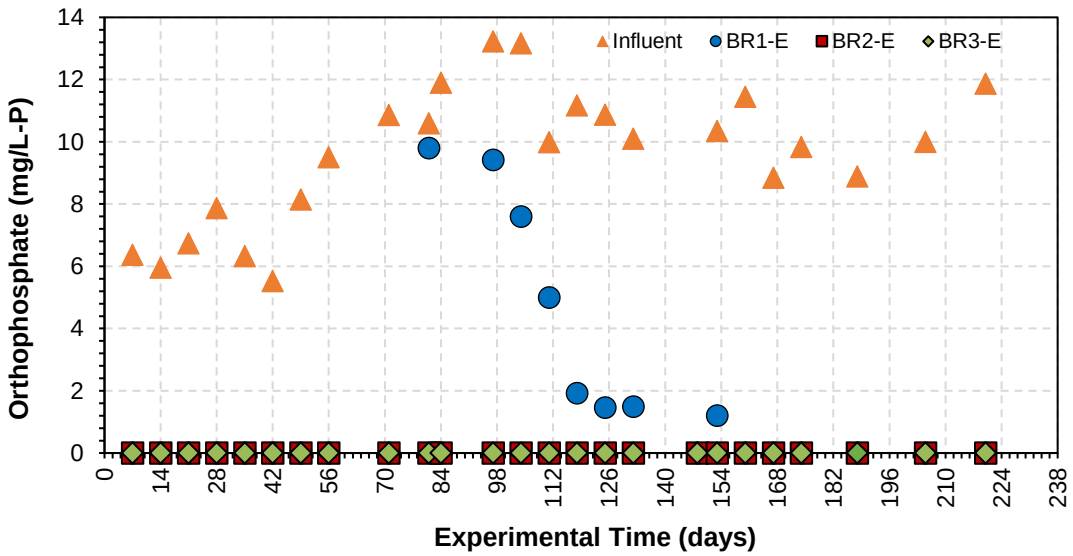

Figure 4.9 Influent and BRs effluent orthophosphate concentration over the duration of the study.

4.4.5 Solids removal

Improved AS settling characteristics are extremely important for increasing wastewater treatment capacity; nevertheless, the priority for the solid/liquid process is to maintain a low decant TSS. A common maximum discharge concentration for secondary treatment facilities is 30 mg/L. BR2 and BR3 had online TSS probes monitoring decant TSS, while grab samples of BR1 were taken twice per stage. TSS as a function of time is shown in Fig. 4.10.

BR1 had a total of 10 decant TSS measurements, which had an average of 15±3 mg/L. Comparisons of BR1 to BR2 and BR3 are difficult to make due to the limited measurements and will not be discussed. BR2 and BR3 maintain low decant TSS values for the first 28 days then both reactors began to increase with BR3 surpassing the 30 mg/L on day 43. This same trend occurred again at the end of the third stage. High effluent TSS values are common for AGS systems [36]—a recent study concluded that the cause for high effluent TSS is purely due to nitrogen gas production [37] and recommend an additional air stripping

step. But the definite cause is still unknown and is potentially influenced by multiple factors. Another plausible reason for the elevated TSS concentration was described in section 4.3.2, when core of granule does not obtain substrate due to its consumption by new biomass. Similar observations have occurred when F:M suddenly drops [17,38]. When comparing BR2 and BR3 decant TSS, BR3 always had a higher. Wasting from the bottom of the reactor reduced TSS outbreaks for BR2, potentially indicating that the larger granules may have been the cause of the higher effluent TSS in BR3. Thus, additional wasting from the bottom of the reactor may be required to reduce the mean floc diameter and stabilize effluent TSS. Future AGS systems may need to consider an alternate biomass retention measurement and relate the mean floc diameter to an SRT.

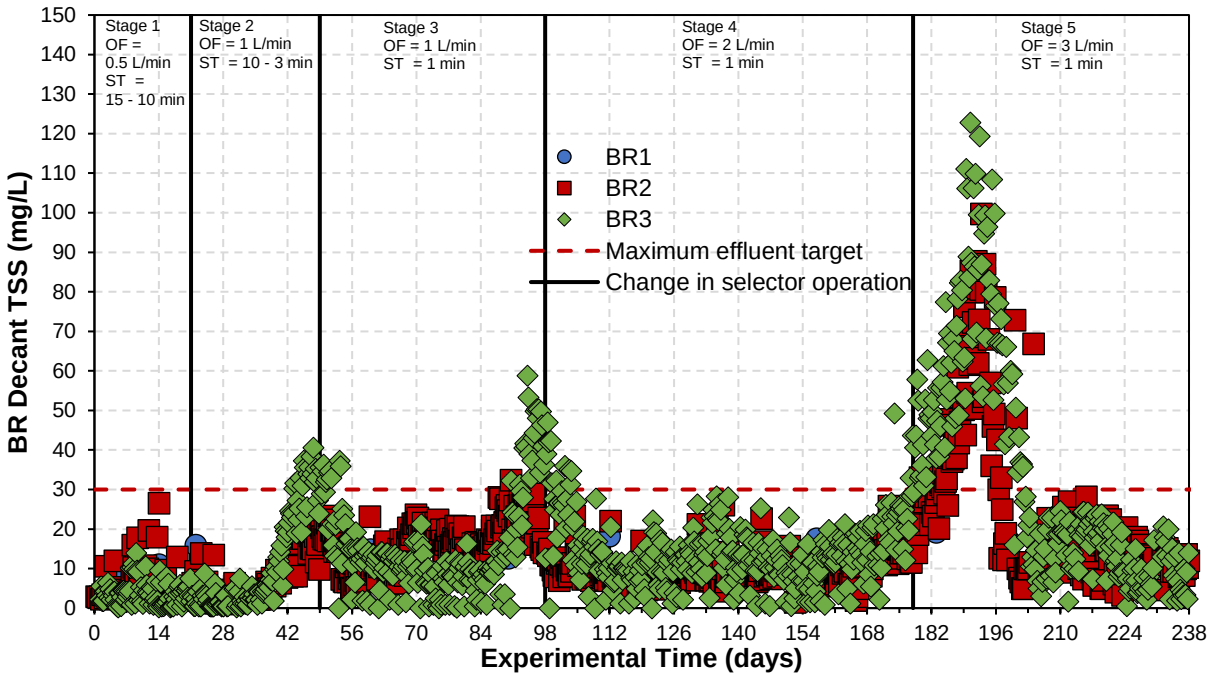

Figure 4.10 BR1 had a total of 10 decant TSS measurements while BR2 and BR3 had online TSS probes. All BRs maintained decant TSS below the maximum effluent discharge value of 30 mg/L for the majority of the study, with the expectations occurring at the end of Stages 2 and 3 and beginning of Stage 5.

4.4.6 DNA sequencing

4.4.6.1 Eukaryotes

Protozoa and metazoa are almost always present in AS, and mainly feed on bacteria that are free floating or bacteria that are not firmly attached to floc. The dominant eukaryote taxa in this study were different in each BR and changed over time. Heatmaps of the Epistylis, Telotrochidium, Rhogostoma, LKM11, and Dipolgasterida taxa are shown in Fig. 4.11. The consortium percentage corresponds to the percentage of eukaryotic tax in relationship to the entire bacteria and archaea communities. Epistylis are a genus of peritrich ciliates, they have a rigid stalk with a collar with a short oral disc at the end of the stalk and often form branched tree-like colonies. Epistylis ingest small particles, which reduces effluent

suspended solids and are associated with high COD removal—they often provide the structure of AGS and can be attached to the outside of AGS [39,40]. Epistylis was not present in a measurable concentration at the beginning of the study in any of the BRs. By day 27 Epistylis was detected in BR3 and by day 55 Epistylis was present in all BRs. Epistylis was present at a higher percentage between days 55 and 150 during the formation of AGS, then it decreased in BR2 and BR3. This decrease may indicate that the development of new AGS was limited.

Telotrochidium is also a peritrich ciliate and is important for the removal of suspended solids; however, unlike the Epistylis, it is stalkless or free swinging [41]. Telotrochidium is often present during the early stages of granulation but is unable to colonize the surface of AGS. Similar to Epistylis, Telotrochidium was not present in any of the BRs at the beginning of the study, but by day 93 was present in all BRs. Fully granulated systems have reported not having Telotrochidium once granules were fully mature [42]; however, both BR2 and BR3 contained Telotrochidium throughout the study.

Rhogostoma is a thecate amoeba and is known to feed on bacteria and eukaryotic taxa [43,44]. BR3 contained the highest percentage of Rhogostoma throughout the study. Rhogostoma may potentially cause the destruction of floc, thus increasing decant TSS concentration.

LKM11 is an uncultured fungal group in the Cryptomycota phylum, and has been detected in in influent sewage and AS. Some members of the LKM11 group are expected to be a parasitic fungi but specific functions within the wastewater treatment are still largely unknown [45]. LKM11 seemed to thrive at the beginning of the experiment, but soon after day 55 the percentage of LKM11 declined, potentially due to the operating conditions of the BRs.

Diplogasterida is an order of nematode, commonly found in AS and increases in abundance with SRT. Nematodes play an important role in the AS community, as they graze on floc and introduce oxygen into biofilms through their burrowing [46]. Nematodes are also known to be destructive to floc at higher abundances leading to the washout of biomass [14]. Diplogasterida was in present all BRs in a low abundance for the first 55 days, BR1 and BR2 continued to maintain the relatively low abundance for the remainder of the study. However, the Diplogasterida abundance in BR3 continued to increase throughout the study. This accumulation was caused by wasting through the hydraulic selector, creating a bias of biosolids wasted to maintain the desired SRT of 10-15 days (Fig. 4.11E). It was clear that the BR operating conditions and hydraulic selection had an impact on the eukaryote community. CAS facilities currently have the potential to tailor their AS process to induce feast/famine. If a WRRF adopts a hydraulic selection technology it will be necessary to incorporate their traditional wasting mechanism to prevent accumulation of grit and nematodes such as the Diplogasterida.

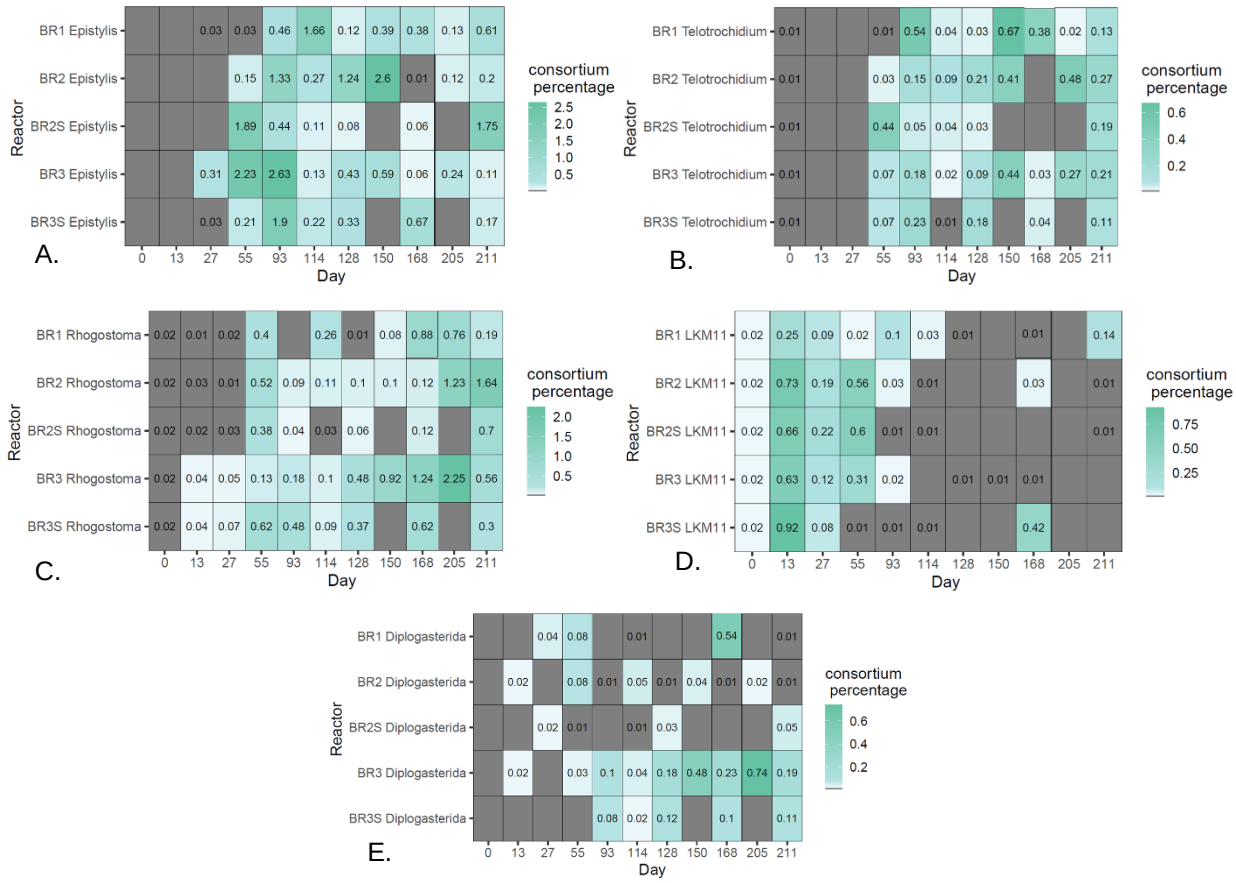

Figure 4.11 Heatmaps of the following eukaryotes: (A) Epistylis, (B) Telotrochidium, (C) Rhogostoma, (D) LKM11, and (E) Diplogasterida over the duration of the study.

4.4.6.2 16S rRNA sequencing

Samples of the BR2 and BR3 AS and hydraulic selector discharge were collected throughout the study and compared using 16S rRNA sequencing. This comparison evaluates the abundance of filamentous bacteria, PAOs, AOBs, and NOBs, results are shown in Fig. 4.12. The 16S rRNA was evaluated through the MIDAS data base and compiled at the genus level. The POS in Fig. 4.12 means that all species of that genus perform the activity, while VAR means that only some species of the genus perform the specified activity, results are compared using the sum of the POS and VAR values. At the beginning of the study both BR2 and BR3 hydraulic selector discharge was 39 and 23%, respectively, higher in filamentous abundance than the BR AS (Fig. 4.12A-B). Filamentous abundance was never an apparent problem in any BR, but the slow removal of filamentous bacteria from the BR2 and BR3 may have assisted in the microbiome transformation that led to improve AS settling velocities. For the remainder of the study, filamentous abundance in the reactor was always less than the initial measurement. The abundance of filamentous bacteria was not always greater in the hydraulic selector discharge. This may have been caused by growth of filamentous bacteria on AGS that was not removed by the hydraulic selector. Measurements with high filamentous abundance in the hydraulic selector discharge may indicate periods of sudden filamentous growth that were captured and removed by the selector.

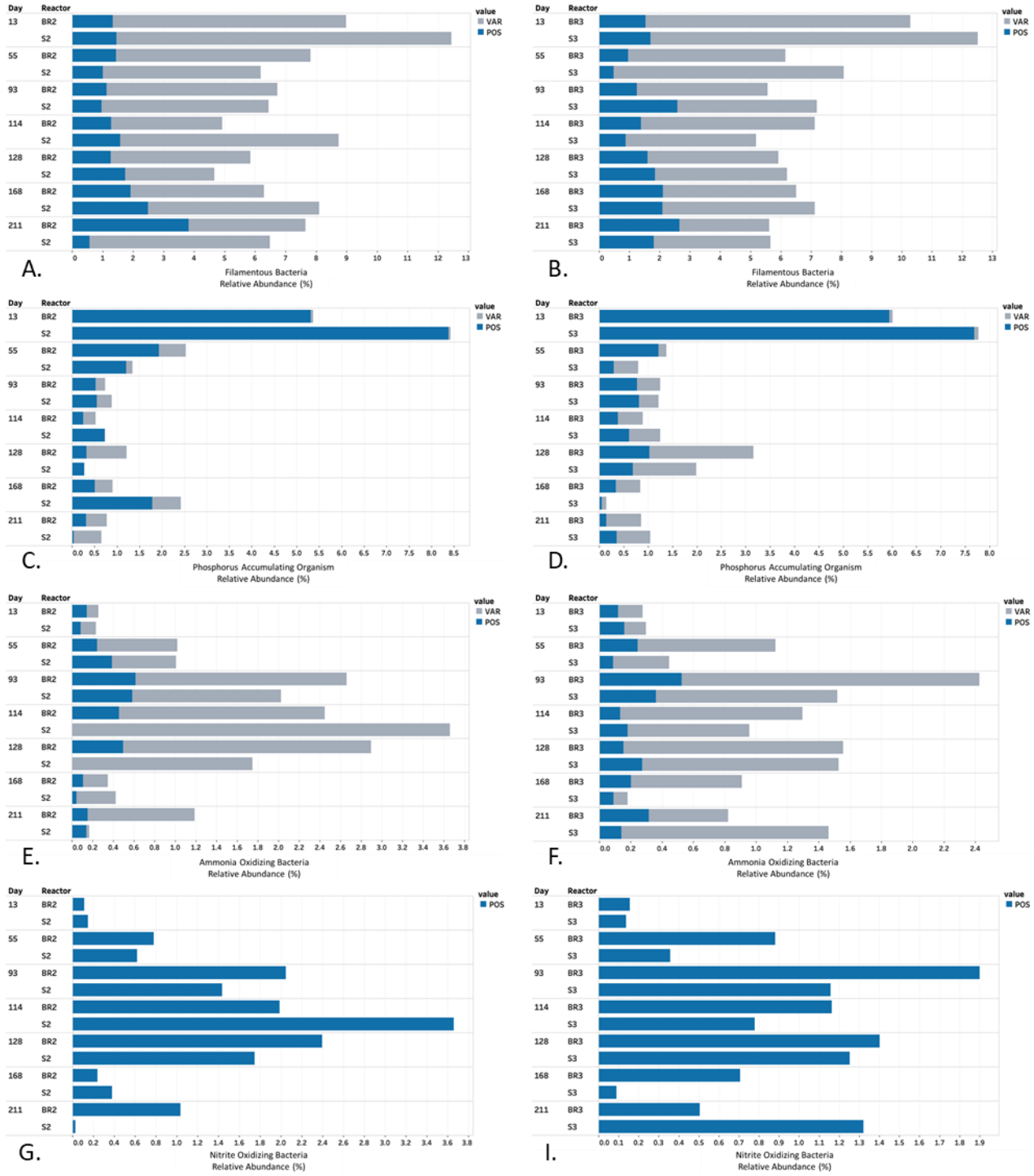

Figure 4.12 Percentage of relative abundance of filamentous bacteria, PAOs, AOBs, and NOBs for BR2, BR2 hydraulic selector (S2), BR3, and BR3 hydraulic selector (S3). The blue POS bars means that all species of that genus perform the activity, while gray VAR bar means that only some species of the genus perform the specified activity

For the remaining microorganisms (PAOs, AOBs, and NOBs), higher abundances were expected in the BR compared to the hydraulic selector discharge. The initial seed sludge contained a high abundance

of PAOs that seemed to be removed by the selection process. PAOs were higher in abundance in the reactor compared to the selector discharge for only 2-3 of the measurements (Fig. 4.12 C-D). For the remainder of the measurements PAO abundance for the reactor and hydraulic selector discharge was similar. The hydraulic selector was operated with the intention to increase floc diameter the mean floc diameter of the selector discharge on average was only 20% smaller than the mean floc diameter of the BR AS. Thus, for PAO abundance, these communities were similar. For AOBs, a greater abundance of the microorganism was found in the BR for 3-4 of the measurements, indicating that a higher percentage of AOB tend to thrive on the larger floc that remain in the BR. For the NOBs, four of the seven measurements had a higher abundance of NOBs in the BRs, indicating the preference of NOB development on faster settling sludge that remained in the BR. In addition to removing poor settling floc, the hydraulic selector continuously removes new developments of filamentous bacteria and allows for the accumulation of AOBs and NOBs.

For the following evaluation, the microbial communities in BRs 1-3 were monitored through 16S rRNA gene sequencing. Before samples were sequenced each BRs AS was separated into four floc diameter categories <250 µm, 250-500 µm, 500-1000 µm, and >1000 µm. This allowed a floc diameter comparison and provided insight on which floc diameter provide the greatest nutrient removal (Fig. 4.13). For the PAOs, both BR2 and BR3 had greater abundance of the bacterium on day 150 for all the floc diameter categories Fig.13A. This may indicate that the selection process allowed the PAO abundance to increase BR2 and BR3 compared to BR1. In general, BR1 PAO abundance increased on day 205 for all floc diameter categories, and floc diameters <500 µm had the highest abundance. BR2 and BR3 PAO abundance was also highest in floc <500 µm. By day 205 BR2 PAO abundance had decreased in all floc diameter categories and abundance values were similar to that of BR1. For BR3 PAO values in the >250 µm, and 500-1000 µm categories increased while all other floc diameter categories decreased but maintained a higher relative abundance when compared to BR1. The decrease in PAO abundance in BR2 may have been caused by traditional BR wasting, while BR3 without BR wasting continued to maintain high PAO abundance values. Additionally, floc in BR2 and BR3 may have continued to increase in diameter due to heterotrophic growth and a PAO biomass that remained the same would have resulted in an abundance decrease. For the AOBs, abundance in the <250 µm category was substantially less compared to all other floc diameter categories and abundance increased in larger floc for all BRs. Similar to the PAOs, on day 150 the AOB abundance was substantially higher for BR2 and BR3 compared to BR1. However, by day 205, the AOB abundance in BR2 decreased but was still on average higher than BR1 while BR3 values were on average less than in BR1. For the NOBs, all floc <250 µm experienced a low NOB abundance, but abundance increased in all larger floc diameters in all BRs. NOB abundance was once again higher in BR2 and BR3 on day 150 but decreased on day 205. With only two sample points it is difficult to assess if the change of PAO, AOB, and NOB abundance from day 150 to 205 occurred suddenly or gradually over time. Future work requires additional AS sampling and sequencing to quantify and maintain high nutrient removing function.

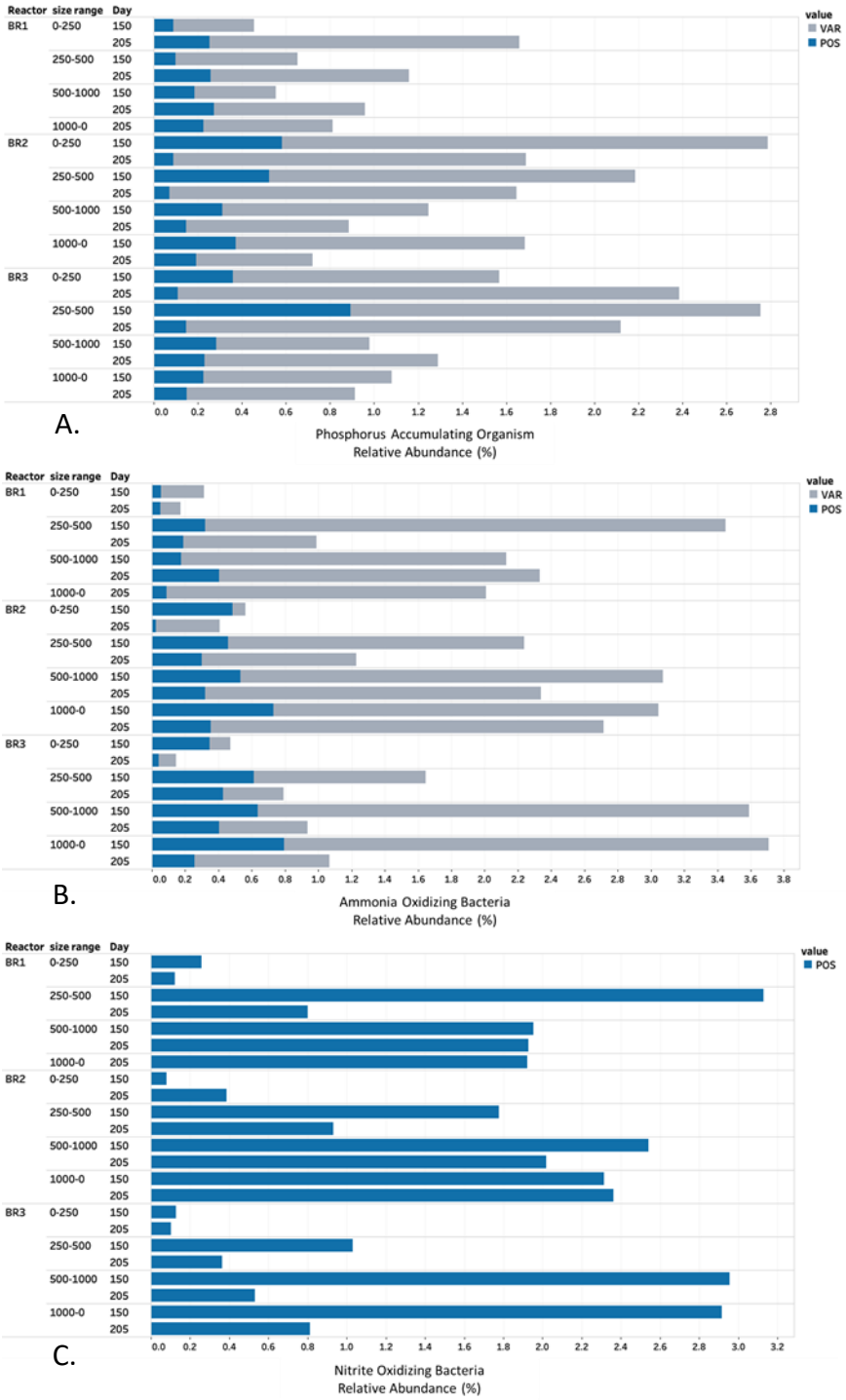

Figure 4.13 Percentage of relative abundance of filamentous bacteria, PAOs, AOBs, and NOBs for BRs 1-3 on days 150 and 205 separated into four floc diameter categories, <250 µm, 250-500 µm, 500-1000 µm, and >1000 µm. The blue POS bars means that all species of that genus perform the activity, while gray VAR bar means that only some species of the genus perform the specified activity

4.5 Conclusion

Over the duration of the 238-day study the feast/famine conditions and the various biomass wasting approaches (traditional BR wasting, hydraulic selection with BR wasting, only hydraulic selection) had a substantial impact on the development of AGS and influenced the AS microbiome. This study shows that feast/famine alone resulted in the improvement of floc diameter without the assistance of any selection technology. However, when hydraulic selection is combined with feast/famine the mean floc diameter is larger than 500 µm and settling velocity is higher than 15 m/h compared to 5 m/h in control reactor. From the phase contrast microscopy, stalked ciliates were observed in all BRs which are vital for the development of AGS. These observations were confirmed with the 18S-rRNA gene sequencing that detected Epistylis, and Telotrochidium a genus of rigid stalked and free-swimming ciliates. Although BR1 had ciliates, most of the AS did not develop into large granules, most likely due to the wasting mechanism of the reactor. On day 224 the abundance of nematodes in BR3 was notable. The 18S-rRNA sequencing detected an order of nematode, Diplogasterida, which was 0.02% of the initial microbiome and increased to 0.74% over the duration of the study, compared to BR1 and BR2, which had an average abundance of 0.03±0.02. Nematodes are known to predatory eukaryotes and can cause floc destruction that may have resulted in high effluent TSS. In regard to the effluent water quality, a sudden spike in influent COD and phosphorus resulted in an increase in the BR1 effluent, reaching 53 mg/L COD and 9.8 mg/L-P compared to the previous average values of 20±5 mg/L COD and <1 mg/L-P. These results may indicate that the granular systems were able to effectively treat a sudden shift in carbon and phosphorus loading. Although the nutrient removal of BR2 and BR3 was excellent, both BRs suffered from higher effluent TSS concentrations. BR3 had three major events when effluent TSS exceed 30 mg/L, this only occurred once for BR2. The exact reason for the higher effluent TSS is still unknown but may possibly be related to the AS wasting mechanism because BR2 always had a lower effluent TSS concentration. The hydraulic selector for BR2 and BR3 removed a higher abundance of filamentous bacteria throughout the study and the PAO, AOB, and NOB abundance increased in all BRs. The highest abundance of these organisms was found in floc with a diameter smaller than 1000 µm. BR2 combined feast/famine, hydraulic selection, and traditional wasting which resulted in the best performance among the three BRs. BR2 provided fast settling AGS, excellent nutrient removal and reasonable effluent TSS quality. Additional research is required to further refine the combined wasting method to maintain an appropriate floc diameter, this would ensure high abundance of PAO, AOBs, and NOBs while minimizing effluent suspended solids.

4.6 References

[1] G. Tchobanoglous, Metcalf, Eddy, Wastewater Engineering Treatment and Resource Recovery, Fith, New York City, 2005.

[2] G. Gaval, J.J. Pernelle, Impact of the repetition of oxygen deficiencies on the filamentous bacteria proliferation in activated sludge, Water Res. 37 (2003) 1991–2000.

https://doi.org/10.1016/S0043-1354(02)00421-9.

[3] D.C. Banti, P.D. Karayannakidis, P. Samaras, M.G. Mitrakas, An innovative bioreactor set-up that reduces membrane fouling by adjusting the filamentous bacterial population, J. Memb. Sci. 542 (2017) 430–438. https://doi.org/10.1016/j.memsci.2017.08.034.

[4] R. Simona, T. Valter, W. Jiri, Activated Sludge Seperation Problems Theory, Control Measures, Practical Experiences, IWA Publishing, London, 2017.

[5] M.K. de Kreuk, M.C.M. van Loosdrecht, Selection of slow growing organisms as a means for improving aerobic granular sludge stability, Water Sci. Technol. 49 (2004) 9–17. https://doi.org/10.2166/wst.2004.0792.

[6] M. Figueroa, A. Val Del Río, J.L. Campos, R. Méndez, A. Mosquera-Corral, Filamentous bacteria existence in aerobic granular reactors, Bioprocess Biosyst. Eng. 38 (2015) 841–851. https://doi.org/10.1007/s00449-014-1327-x.

[7] Z. Li, P. Lu, D. Zhang, G. Chen, S. Zeng, Q. He, Population balance modeling of activated sludge flocculation : Investigating the influence of Extracellular Polymeric Substances (EPS) content and zeta potential on flocculation dynamics, Sep. Purif. Technol. 162 (2016) 91–100. https://doi.org/10.1016/j.seppur.2016.02.011.

[8] G. Sheng, H. Yu, X. Li, Extracellular polymeric substances (EPS) of microbial aggregates in biological wastewater treatment systems : A review, Biotechnol. Adv. 28 (2010) 882–894. https://doi.org/10.1016/j.biotechadv.2010.08.001.

[9] B. Su, Z. Qu, Y. Song, L. Jia, J. Zhu, Journal of Environmental Chemical Engineering Investigation of measurement methods and characterization of zeta potential for aerobic granular sludge, Elsevier. 2 (2014) 1142–1147. https://doi.org/10.1016/j.jece.2014.03.006.

[10] K.R. Pagilla, D. Jenkins, W.H. Kido, Nocardia control in activated sludge by classifying selectors , Water Environ. Res. 68 (1996) 235–239. https://doi.org/10.2175/106143096x127677.

[11] S.D. Weber, W. Ludwig, K.H. Schleifer, J. Fried, Microbial composition and structure of aerobic granular sewage biofilms, Appl. Environ. Microbiol. 73 (2007) 6233–6240. https://doi.org/10.1128/AEM.01002-07.

[12] M.K.H. Winkler, R. Kleerebezem, W.O. Khunjar, B. de Bruin, M.C.M. van Loosdrecht, Evaluating the solid retention time of bacteria in flocculent and granular sludge, Water Res. 46 (2012) 4973–4980. https://doi.org/10.1016/j.watres.2012.06.027.

[13] M. Sepúlveda-Mardones, J.L. Campos, A. Magrí, G. Vidal, Moving forward in the use of aerobic granular sludge for municipal wastewater treatment: an overview, Rev. Environ. Sci. Biotechnol. 18 (2019) 741–769. https://doi.org/10.1007/s11157-019-09518-9.

[14] R.A. Maltos, R.W. Holloway, T.Y. Cath, Enhancement of activated sludge wastewater treatment with hydraulic selection, Sep. Purif. Technol. 250 (2020) 117214. https://doi.org/10.1016/j.seppur.2020.117214.

[15] I. Avila, D. Freedman, J. Johnston, B. Wisdom, J. McQuarrie, Inducing granulation within a full-scale activated sludge system to improve settling, Water Sci. Technol. (2021) 1–12. https://doi.org/10.2166/wst.2021.006.

[16] R.D.G. Franca, H.M. Pinheiro, M.C.M. Van Loosdrecht, N.D. Lourenço, Stability of aerobic granules during long-term bioreactor operation, 36 (2018) 228–246. https://doi.org/10.1016/j.biotechadv.2017.11.005.

[17] R.A. Hamza, Z. Sheng, O.T. Iorhemen, M.S. Zaghloul, J.H. Tay, Impact of food-to-microorganisms ratio on the stability of aerobic granular sludge treating high-strength organic wastewater, Water Res. 147 (2018) 287–298. https://doi.org/10.1016/j.watres.2018.09.061.

[18] J.-H. Tay, S. Pan, Y. He, S.T.L. Tay, Effect of Organic Loading Rate on Aerobic Granulation. II: Characteristics of Aerobic Granules, J. Environ. Eng. 130 (2004) 1102–1109. https://doi.org/10.1061/(asce)0733-9372(2004)130:10(1102).

[19] R. Maltos, A. Waclawski, B. Marten, T. LeClear, F. Bruecken, S. Jonson, T. Cath, R.W. Holloway, G. Rajagopalan, J. Debroux, T.Y. Cath, Minimizing solid retention time through hydraulic selection for the development of aerobic granular sludge, (2021).

[20] American Public Health Association (APHA), Standard Methods for the Examination of Water & Wastewater 21st Edition, Am. Public Heal. Assoc. Am. Water Work. A Ssociation, Water Environ. Fed. (1999) 541. http://www.mwa.co.th/download/file_upload/SMWW_1000-3000.pdf.

[21] D.M. Gohl, P. Vangay, J. Garbe, A. MacLean, A. Hauge, A. Becker, T.J. Gould, J.B. Clayton, T.J. Johnson, R. Hunter, D. Knights, K.B. Beckman, Systematic improvement of amplicon marker gene methods for increased accuracy in microbiome studies, Nat. Biotechnol. 34 (2016) 942–949. https://doi.org/10.1038/nbt.3601.

[22] A.E. Parada, D.M. Needham, J.A. Fuhrman, Every base matters: Assessing small subunit rRNA primers for marine microbiomes with mock communities, time series and global field samples, Environ. Microbiol. 18 (2016) 1403–1414. https://doi.org/10.1111/1462-2920.13023.

[23] B.J. Callahan, P.J. McMurdie, M.J. Rosen, A.W. Han, A.J.A. Johnson, S.P. Holmes, DADA2: High-resolution sample inference from Illumina amplicon data, Nat. Methods. 13 (2016) 581–583. https://doi.org/10.1038/nmeth.3869.

[24] B.J. Callahan, P.J. McMurdie, S.P. Holmes, Exact sequence variants should replace operational taxonomic units in marker-gene data analysis, ISME J. 11 (2017) 2639–2643. https://doi.org/10.1038/ismej.2017.119.

[25] P.J. McMurdie, S. Holmes, Phyloseq: An R Package for Reproducible Interactive Analysis and Graphics of Microbiome Census Data, PLoS One. 8 (2013). https://doi.org/10.1371/journal.pone.0061217.

[26] C. Lozupone, R. Knight, UniFrac: A new phylogenetic method for comparing microbial communities, Appl. Environ. Microbiol. 71 (2005) 8228–8235.

https://doi.org/10.1128/AEM.71.12.8228-8235.2005.

[27] M.I. Love, W. Huber, S. Anders, Moderated estimation of fold change and dispersion for RNA-seq data with DESeq2, Genome Biol. 15 (2014) 1–21. https://doi.org/10.1186/s13059-014-0550-8.

[28] R. Jenné, E.N. Banadda, G. Gins, J. Deurinck, I.Y. Smets, A.H. Geeraerd, J.F. Van Impe, Use of image analysis for sludge characterisation: Studying the relation between floc shape and sludge settleability, Water Sci. Technol. 54 (2006) 167–174. https://doi.org/10.2166/wst.2006.384.

[29] K. Krysiak-Baltyn, S.L. Gras, W. Burger, P.J. Scales, A.D. Stickland, G.J.O. Martin, The influence of protruding filamentous bacteria on floc stability and solid-liquid separation in the activated sludge process, Water Res. 123 (2017) 578–585. https://doi.org/10.1016/j.watres.2017.06.063.

[30] J. Xu, Y. Sun, Y. Liu, W. Yuan, L. Dai, W. Xu, H. Wang, In-situ sludge settleability improvement and carbon reuse in SBR process coupled with hydrocyclone, Sci. Total Environ. 695 (2019). https://doi.org/10.1016/j.scitotenv.2019.133825.

[31] K. Sears, J.E. Alleman, J.L. Barnard, J.A. Oleszkiewicz, Density and Activity Characterization of Activated Sludge Flocs, J. Environ. Eng. 132 (2006) 1235–1242. https://doi.org/10.1061/(asce)0733-9372(2006)132:10(1235).

[32] D.G. Weissbrodt, S. Lochmatter, S. Ebrahimi, P. Rossi, J. Maillard, C. Holliger, Bacterial selection during the formation of early-stage aerobic granules in wastewater treatment systems operated under wash-out dynamics, Front. Microbiol. 3 (2012) 1–22. https://doi.org/10.3389/fmicb.2012.00332.

[33] T.T. Ren, Y. Mu, L. Liu, X.Y. Li, H.Q. Yu, Quantification of the shear stresses in a microbial granular sludge reactor, Water Res. 43 (2009) 4643–4651. https://doi.org/10.1016/j.watres.2009.07.019.

[34] S.S. Adav, D. Lee, K. Show, J. Tay, Aerobic granular sludge : Recent advances, i (2008) 411–423. https://doi.org/10.1016/j.biotechadv.2008.05.002.

[35] Y. V Nancharaiah, G.K. Kumar, Bioresource Technology Aerobic granular sludge technology : Mechanisms of granulation and biotechnological applications, 247 (2018) 1128–1143. https://doi.org/10.1016/j.biortech.2017.09.131.

[36] H. Horn, C. Klarmann, K. Sørensen, T. Rocktäschel, P. Boisson, J. Ochoa, Influence of the granulation grade on the concentration of suspended solids in the effluent of a pilot scale sequencing batch reactor operated with aerobic granular sludge, Sep. Purif. Technol. 142 (2015) 234–241. https://doi.org/10.1016/j.seppur.2015.01.013.

[37] E.J.H. van Dijk, M. Pronk, M.C.M. van Loosdrecht, Controlling effluent suspended solids in the aerobic granular sludge process, Water Res. 147 (2018) 50–59. https://doi.org/10.1016/j.watres.2018.09.052.

[38] A.J. Li, X.Y. Li, H.Q. Yu, Effect of the food-to-microorganism (F/M) ratio on the formation and size of aerobic sludge granules, Process Biochem. 46 (2011) 2269–2276. https://doi.org/10.1016/j.procbio.2011.09.007.

[39] B. Pérez-Uz, L. Arregui, P. Calvo, H. Salvadó, N. Fernández, E. Rodríguez, A. Zornoza, S. Serrano, Assessment of plausible bioindicators for plant performance in advanced wastewater treatment systems, Water Res. 44 (2010) 5059–5069. https://doi.org/10.1016/j.watres.2010.07.024.

[40] J. Liu, J. Li, S. Piché-Choquette, B. Sellamuthu, Roles of bacterial and epistylis populations in aerobic granular SBRs treating domestic and synthetic wastewaters, Chem. Eng. J. 351 (2018) 952–958. https://doi.org/10.1016/j.cej.2018.06.161.

[41] M.L. Barrios-Hernández, C. Bettinelli, K. Mora-Cabrera, M.C. Vanegas-Camero, H. Garcia, J. van de Vossenberg, D. Prats, D. Brdjanovic, M.C.M. van Loosdrecht, C.M. Hooijmans, Unravelling the removal mechanisms of bacterial and viral surrogates in aerobic granular sludge systems, Water Res. 195 (2021). https://doi.org/10.1016/j.watres.2021.116992.

[42] C.S. Herng, Predator-Prey Interactions in Aerobic Granulation Systems, (2018).

[43] K. Dumack, S. Flues, K. Hermanns, M. Bonkowski, Rhogostomidae (Cercozoa) from soils, roots and plant leaves (Arabidopsis thaliana): Description of Rhogostoma epiphylla sp. nov. and R. cylindrica sp. nov., Eur. J. Protistol. 60 (2017) 76–86. https://doi.org/10.1016/j.ejop.2017.06.001.

[44] N. Remmas, P. Melidis, G. Paschos, E. Statiris, S. Ntougias, Protozoan indicators and extracellular polymeric substances alterations in an intermittently aerated membrane bioreactor treating mature landfill leachate, Environ. Technol. (United Kingdom). 38 (2017) 53–64. https://doi.org/10.1080/09593330.2016.1190792.

[45] Y. Hirakata, M. Hatamoto, M. Oshiki, T. Watari, K. Kuroda, N. Araki, T. Yamaguchi, Temporal variation of eukaryotic community structures in UASB reactor treating domestic sewage as revealed by 18S rRNA gene sequencing, Sci. Rep. 9 (2019) 1–11. https://doi.org/10.1038/s41598-019-49290-y.

[46] H. Salvadó, A. Palomo, M. Mas, J. Puigagut, M.D.P. Gracia, Dynamics of nematodes in a high organic loading rotating biological contactors, Water Res. 38 (2004) 2571–2578. https://doi.org/10.1016/j.watres.2004.03.007.

CHAPTER 5

THE DEVELOPMENT OF THE HYDRAULIC SELECTOR THROUGH COMPUTIONAL FLUID DYNAMICS

In preparation for submission to Water Research

Rudy A. Maltos, Gregory E. Bogin Jr., Tzahi Y. Cath

5.1 Abstract

Computational fluid dynamic (CFD) models have allowed wastewater facilities to predict the settling rates of the activated sludge (AS) blanket in secondary clarifiers and effluent total suspended solids concentration associated with a wide range of flows. CFD models provide a visualization of turbulent areas in the secondary clarifier, changes to the hydrodynamics can then be made in these regions to promote laminar flow and often results in improved AS settling. These 2D, steady-state, turbulent models are effective and are relatively low cost to model. However, current improvements to AS settling do not investigate the root cause of poor settling, which is an accumulation of filamentous bacteria or floc with a diameter <100 µm. Hydraulic selection technology has the ability to remove poor settling floc and allow the accumulation of aerobic granular sludge. For hydraulic selector technology to be adopted by the wastewater industry the selection process must be effective in both laminar and turbulent conditions. Thus, a 3D, transient, multiphase, turbulent CFD model of the hydraulic selector was developed, and similar bench-scale experiments were conducted. Results from the bench-scale experiments demonstrated that the settling time before hydraulic selection was the most influential parameter in preventing the removal of both 120 µm and 220 µm particles, considered fast settling particles. For the CFD model, an eddy viscosity of more than 1Pa s and turbulent kinetic energy (TKE) of more than 0.002 $m^2 s^2$ were sufficient to maintain both 60 µm (slow settling) and 120 µm particles in suspension. Unlike the hydraulic selector outflow, TKE and eddy viscosity conditions in the reactor had the largest influence on the particle volume fraction composition removed by the selector. This led to a similar particle distribution for all hydraulic selector outflows.

5.2 Introduction

For the last 100 years, wastewater treatment has relied on activated sludge (AS), a dispersed floc composed of microorganisms, for the removal of carbon, nitrogen (N), and phosphorus (P). A final step of wastewater treatment process is the separation of AS from the decant (clean water), this separation commonly occurs via gravity. A typical AS settling time in a batch reactor may range between 20 and 30 minutes, longer settling times increases hydraulic retention time (HRT) and reduces treatment efficiency. Currently, many of the wastewater facilities in the United States are nearing their maximum capacity. For many of these facilities, expanding the treatment footprint is not an option due to limited land availability. Therefore, to increase treatment capacity, the HRT of these facilities must be reduced. Minimizing the AS

settling time would have a substantial impact on water resource reclamation facilities (WRRFs) operation and reduce HRT.

AS settling is described by four types of settling, discrete, flocculated, hindered, and compression. The AS settling type and duration is determined by floc characteristics, parameters that include zeta potential, floc diameter, floc morphology, and floc density [1]. The average AS zeta potential range is between -20 and -15 mV, this negative charge reduces the flocs ability to aggregate and results in tall sludge blankets in the secondary clarifier [2,3]. Tall sludge blankets in clarifiers requires the clarifier to operate with low flows to ensure that the sludge blanket does not break through the effluent weirs. The morphology of the AS is dependent on the reactors shear forces, developed by the mixing and aeration systems of the AS basins. Strong shear force results in floc deterioration, and weak shear force allows the floc to expand quickly, resulting in long filamentous outgrowth outside of the floc core and increase of drag forces [4,5]. The density of floc is dependent on zeta potential and shear force. A neutral zeta potential allows floc to aggregate, and the proper shear force ensures that a slow and compact floc develops. The majority of traditional AS settling is slow settling of less than 5 m/h [6], best described by hindered and compressed settling [1]. Hindered settling occurs when floc settle together as a zone or blanket, floc maintain the same relative position with respect to each other [1], this settling may occur due to a limited floc diameter distribution and highly negative zeta potential. Compression settling occurs when there is close physical contact among the floc and uniform concentration within the layer.

To address these AS settling deficiencies, many researchers have focused on reducing the electronegativety of floc through the biological production of extracellular polymeric substance (EPS), an electropositive biological polymer composed mainly of polysaccharides, proteins, and DNA. The production of EPS would allow flocculation during settling and reduce settling times. Researchers have studied for over three decades the AS operating conditions that result in maximum EPS production. They found that a short feeding stage containing a high concentration of carbon, followed by an extensive famine stage induces a stress within the microorganism and results in high EPS production. These conditions are known as feast/famine and are further discussed in Chapter 4. Combining EPS production along with high shear forces produces aerobic granular sludge (AGS), which follows a discreet settling pattern. AGS has a diameter range of 150-6,000 μm, a settling velocity of 15-60 m/h, and a density of 1.02-1.08 g/mL [7,8]. However, conventional activated sludge facilities have not adopted this technology. These facilities have the ability to induce feast/famine conditions, and appropriate shear forces but lack the ability to manage their floc diameter distribution through retention of fast settling floc and elimination of poor settling floc.

Currently, facilities continuously remove AS from the bottom of the bioreactor or secondary clarifier to maintain a desired AS concentration. The AS wasted is then dried and delivered to a landfill or further processed for land application. This wasting technique often removes a higher percentage of fast settling floc, resulting in an accumulation of poor settling floc, Fig. 51.

AGS systems maintain a high percent of granular sludge by selectively wasting undesirable biomass. To achieve this separation and selection, an AGS full-scale reactor require a minimum height of 5.5 m (Fig.

5.2), this height allows floc to overcome turbulent conditions after mixing/aerating and to stratify according to their terminal velocities [9,10].

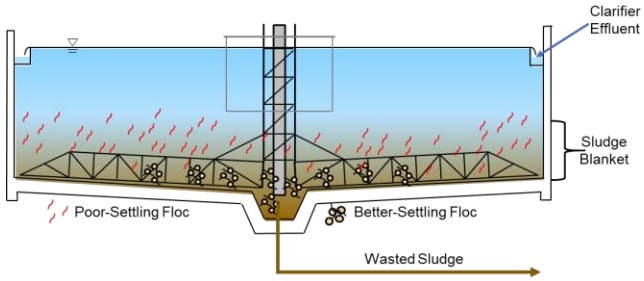

Figure 5.1 A secondary clarifier, traditional activated sludge (AS) wasting only occurs from the bottom of the clarifier, resulting in elimination of dense floc and accumulation of poor settling floc.

A floc that fails to settle a predetermined distance within a specified time, known as the minimum settling velocity, is then discarded. Floc that is retained in the reactor continues to develop and increase in diameter.

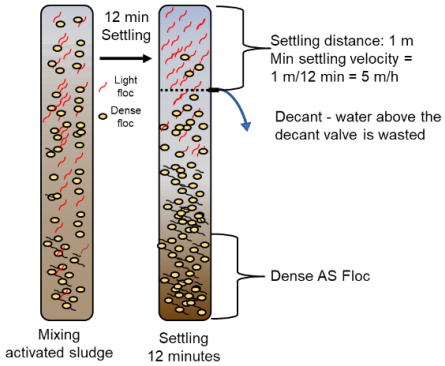

Figure 5.2 The selection process used for tradition AGS development. The column on the left represents the sludge during mixing and on the right after 12 minutes of settling. A particle from the top of the reactor must travel 1 m in 12 minutes to be retained in the reactor. Particles with a minimum settling velocity of less than 5 m/h are wasted through the decant.

A majority of WRRF across the United States have bioreactors with height of less than 5 m, lacking the appropriate height to develop and retain AGS. Therefore, there is a need to develop a technology that can select and remove poor settling floc within current WRRF infrastructure. In the last several years we have developed a Hydraulic Selector (HS), a uniquely designed device that generates a negative pressure at the selector's inlet, hence facilitating the removal of poor settling floc [6,11]. At low flow rates, the lighter flocs (slower-settling) are pulled into the selector and are withdrawn from the system while denser solids settle and retained in the bioreactor. Previous pilot scale studies implementing the hydraulic selector in a batch reactor have demonstrated the effectiveness of the technology, increasing sludge settling velocity from 1 to 28 m/h and reduced the sludge volume index from 250 mL/g to less than 50 mL/g. Pilot scale experiments have proven to be successful; however, activated sludge research is costly, labor intensive, and can take 6–12 months to test a single parameter. The target floc for removal at a WRRF may always be changing

and is dependent on the desired AS settling velocity and abundance of specific microorganisms, as described in Chapter 4. Thus, a new approach such as computational fluid dynamics (CFD) is needed to further comprehend the effects of turbulent kinetic energy (TKE), eddy viscosity conditions and settling time on the solid/liquid separation process. This information can then be used to optimize hydraulic selector operating conditions for the removal of any desired floc.

5.3 CFD and wastewater modeling

CFD uses partial differential equations to solve complex momentum and continuity equations. CFD is a common and reliable tool used in various industries, and over the last two decades environmental engineers have begun to apply this modeling approach to further understand the hydrodynamics in wastewater treatment facilities. Currently, CFD in wastewater treatment processes have been used for flow splitting between unit processes, estimations of complex headloss, grit removal, primary sedimentation, and secondary sedimentation. Secondary sedimentation modeling is the most complex one—it is a multiphase model that must account for the various AS settling characteristic such as flocculation, discrete, hindered, and compression settling. These models are developed to predict the movement and bulk settling of activated sludge within the clarifier. The majority of these models have been 2D, 2 phase, a combination of laminar and turbulent, steady state simulations [12–14]. Although these models have been helpful for predicting sludge blanket heights at various flows, there have been no CFD investigations on the selection process required to change the settling characteristics of the AS. From empirical bench top studies on the hydraulic selector, it was determined that the settling time prior to the selection, the selector outflow rate (pressure difference developed at the entrance of the selector) and the selector depth in the reactor are the most important factors that influence floc selection and removal.

In this work a CFD model was developed to provide an understanding of the solid/liquid separation process, specifically the impacts of settling time and various hydraulic selector outflows were investigated. The settling of AS after turbulent mixing provides insight on the remaining TKE in the reactor and its effects on various AS floc sizes. The effects of the selector geometry on TKE were also evaluated due to the potential of the selector impacting the settling trajectory of AS. Lastly, the hydraulic selectors sphere of influence, the low-pressure environment induced by the operation of hydraulic selector was evaluated at various outflows. This simulation may provide insight on the effectiveness of the hydraulic selector 50 seconds after turbulent mixing and may offer guidance on improvements that would increase selection efficiency of poor settling floc.

The first stage of simulation begins with a 3D circular reactor, particles of various diameter and densities are then patch evenly across the reactor water. Mixing is then conducted along the z-axis via frame motion. Once a homogeneous reactor was achieved, the simulation began its settling phase. Flocculation and hindered settling were not accounted for because the selection process occurred before the development of an activated sludge blanket. In the second stage of the simulation, the hydraulic selector outflow was varied, and the same mixing and settling conditions were used for all outflows. Bench scale experiments

were conducted and used a vacuum gauge, flow meter, and particle distribution to quantify the removal of poor settling floc. However, CFD simulations were not validated, the operation of the hydraulic selector for the experiments ranged between 1.5 and 6 minutes while the various outflows were only simulated for 10 seconds each.

5.4 Materials and methods

5.4.1 Bioreactor and hydraulic selector geometry

The hydraulic selector was designed in SolidsWorks (SolidWorks 2018, Dassault Systemes, Waltham, MA) and 3D printed with polylactic acid filament (Pro2 Plus, Raised 3D, Irvine, CA). Dimensions of the hydraulic selector and reactor for both simulation and bench-scale experiments are shown in Fig. 5.3. The reactor was circular, with a 30 cm diameter and 42 cm height, resulting in a volume of ~30 L. The hydraulic selector was located in the center of the reactor, with the entrance of the selector 20 cm below the reactor top or 22 cm above the reactor bottom. The selector was designed with steep external sides to reduce the accumulation of particles on the selector. Details on the hydraulic selector configuration and development are provided in Appendix A.

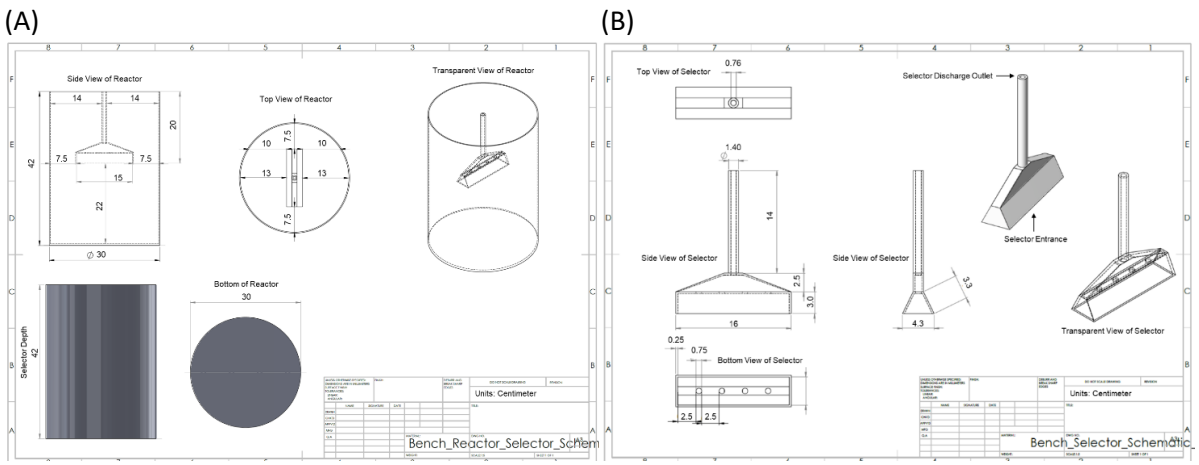

Figure 5.3 (A) Reactor dimensions used in both CFD simulation and bench-scale experiments. The hydraulic selector was located directly in the center of the reactor with the entrance of the selector 22 cm above the bottom of the reactor. (B) The hydraulic selector dimensions, the same selector was used in both CFD simulation and bench-scale experiments, all units are in cm.

5.4.2 Mixed particles simulation

The mixed particle simulation replicates the mixing conditions and volume fraction distribution of activated sludge from the pilot experiment discussed in Chapter 3. Data from day 42 of a 238-day study was used to develop the distribution of particles for the mixed particle simulation. The data set was taken from BR3 and was chosen due to its high percentage of slow settling floc (<60 µm) as well as the presence of medium (>100 µm) and fast settling floc (>200 µm). The data used to develop the mixed particle volume distribution is summarized in Table 1.

The study in Chapter 3 tested various operations of the hydraulic selector and evaluated impact on sludge settleability. This data set was chosen due to variety of floc present in the AS and the difficulty of operating the hydraulic selector during the first two months of the study. By understanding how to effectively remove the highest concentration of poor settling sludge, the start-up time of granulation would be reduced. In Table 5.1, particle diameter percentiles indicate the percentage of the particle volume that is less than the size indicated. For example, 50% of the total particle volume is composed of a floc that has a diameter ≤80 µm or 95 % or the particle have a diameter ≤229 µm. The AS sample is separated into 10 floc diameters—simulating 10 separate volume fraction phases would require an intensive computational effort; therefore, these 10 floc diameters were reduced to 3 categories.

Table 5.1 The particle diameter percentiles from a study conducted in Chapter 3, on day 42. Orange cells represent slow settling floc, yellow cells medium settling floc, and green cells fast settling floc

Particle Diameter Percentiles			
% Tile	Size (µm)	Avg Particle Diameter	% Floc Distribution
10	25		
20	42		
30	54		
40	66		
50	80	53	50
60	97		
70	118		
80	143	119	30
90	185		
95	229	207	20

Thus, the particles were classified as slow, medium, or fast settling categories. Particles between 25 and 80 µm are defined as slow settling and have an average particle diameter of 53 µm, they represent 50% of the AS volume fraction. The medium particle diameter ranges from 97 to 143 µm and have an average of 119 µm and represent 30% of the AS of volume fraction. And the fast particles range between 185 and 229 µm and have an average of 207 µm and represent 20% of the AS volume fraction. For bench scale experiments it would not be feasible to consistently obtain this identical volume fraction distribution from activated sludge; therefore, polyethylene microspheres with similar densities and diameters as the slow, medium, and fast settling particles were used for the CFD model and bench scale experiments. However, only a limited number of particle diameters and densities are available for purchase; thus, a slight modification to the particle distribution in Table 5.1 was made. Characteristics of the particles used in the CFD model and bench experiments are summarized in Table 5.2.

Table 5.2 A description of the particle characteristics and the volume fraction distribution used in the CFD model and bench scale experiments. Approximately 50% of the volume fraction is represented by the slow particles, 30% by the medium particles and 20% by the fast particles

Settling Characteristic	Volume Fraction	Particle Diameter (µm)	Particle Density (g/mL)
Slow	0.001408	60	1.01
Medium	0.000874	120	1.05
Fast	0.000610	220	1.10

5.4.3 Multiphase model

The two approaches for multiphase modeling are the Euler-Lagrange and Euler-Euler approach. The Euler-Lagrange method tracks individual particles, this approach is useful with low amounts of particles, and had been used for tracking air bubbles in reactors [13]. However, this simulation requires millions of particles with various densities and diameters and thus would require a large computational effort. The general Euler-Euler approach may account for both the dispersed-continuous phase and interactions and continuous-continuous phase interactions [13,15,16]. The dispersed-continuous phase can be particles (solids), droplets (liquids), or bubbles (gas) present in the continuous fluid—these dispersed phases are typically in the µm to mm diameter range. The continuous-continuous phase occurs when there is a discrete interface between two phases, they are often immiscible with each other. A mixture model is a simplified version of the full Eulerian model and only accounts for the dispersed-continuous phase interaction, while a volume-of-fluid model is another simplified Eulerian model that only accounts for the continuous-continuous phase interaction. The Eulerian-Eulerian approach was used for this model because it can account for both the various particles in the reactor, water, and an air-water interphase introduced during the hydraulic selector operation, which may be conducted in future simulations.

5.4.4 Viscous modeling

Turbulent flow may be described as an unsteady, three-dimensional, and random flow, or a flow containing eddies of various sizes and vorticities. The operation of the hydraulic selector at the pilot-scale begins after a turbulent mixing/aeration phase followed by a settling phase. Longer settling times result in TKE dissipation. For the CFD simulation, only mixing was used to ensure that all particles were well dispersed. To determine a rotational speed that would result in turbulent conditions for both simulation and experiments, Eq. 1 was used to calculate Reynolds number:

$$Re = \frac{D^2 N \rho}{\mu} \quad (1)$$

where D is the impeller diameter (0.1-0.3 m), N is the impeller's rotational speed (1-3 rps), ρ is the water density (998 kg/m^3), and µ is the Dynamic viscosity of water (1.002*10^{-3} N sec/m^2). An impeller diameter of ≥0.1 m coupled with a minimum rotational speed of 1 rps resulted in turbulent conditions with a Re number >10,000. Various impeller speeds were tested at the bench scale and a final speed of 3 rps, resulting in a

Re >29,000, was chosen for the CFD model due to its ability to quickly suspended and disperse particles, similar to that of the pilot scale aeration and mixing.

The three main turbulent models used in CFD are direct numerical simulation (DNS), Reynolds-averaged Navier-Stokes equations (RANS), and large eddy simulation (LES). A DNS solves for the Navier-Stokes equations numerically, without any turbulence model. This provides the greatest eddy resolution [13,17]; however, this approach is not commonly used due to the intensive computational requirements. RANS turbulent models are based on eddy viscosity and differential transport equation to evaluate Reynolds stress [18]. RANS models are a common way to introduce turbulent effects on transportation and momentum equations and require the least amount of computational resources. LES simulation is a combination of the DNS and RANS in which spatially filtered Navier-Stokes equations are used to solve for large scale eddies directly, while smaller eddies are solved through the RANS approach. For this study, an RANS turbulent model was chosen due to the low computational requirements and sufficient accuracy.

The most widely used turbulent model by the CFD community is the *k*-ε model, a two-equation RANS model which was developed to improve the mixing-length model by account for convection and diffusion of turbulent energy. This model is also the most common when simulating turbulent flow in a secondary clarifier and batch reactors [19–22]. However, the standard *k*-ε turbulence model has been considered insufficient for modeling flows with strong swirling components due to large pressure gradients developed, while the realizable *k*-ε model, the Re-Normalisation Group (RNG) *k*-ε model, and the k-ω model have increased accuracy for such flows [23,24]. The k-ω model incorporates specific dissipation (ω) instead of turbulent dissipation rate. This allows the scale of the turbulence to be determined. The k-ω model has not traditionally been used for secondary clarifier simulations due to the model producing large turbulence levels in regions with large normal strain such as regions with stagnation or strong acceleration. RNG *k*-ε model was developed to account for the effects of smaller scales of motion. Few studies have claimed that the model improves accuracy in rotating flows, however, most common application for this model is indoor air simulations [13,24]. The realizable *k*-ε model predicts turbulent stresses for flows involving rotation and recirculation. Thus, the realizable *k*-ε turbulent model was chosen for the selector CFD simulation because both rotation and recirculation were expected to occur during and after mixing.

5.4.5 Mesh independence

Mesh independence was determined by evaluating and comparing the velocity profile of water (phase one) after 15 seconds of mixing along various lines (Fig. 5.4). The maximum desired difference in water velocity difference between meshes was 10%. Mixing was conducted with frame motion, the reactor water (water outside the hydraulic selector) rotated along the z-axis at 60 RPM.

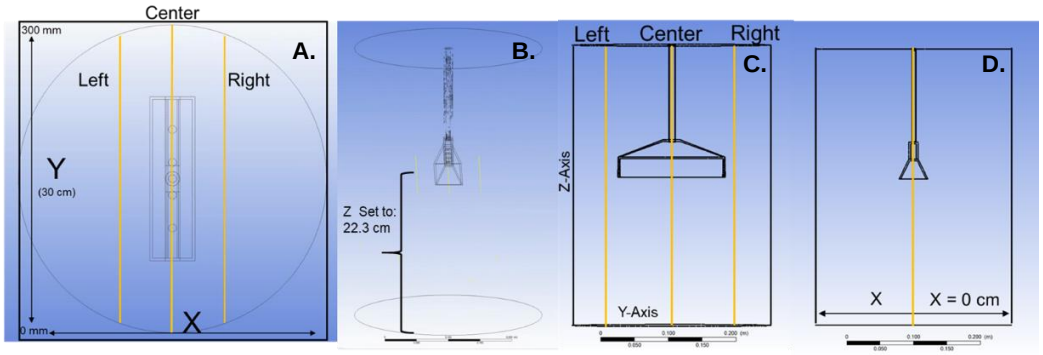

Figure 5.4 Three lines from each XY and YZ planes were used for mesh independence. (A) the XY plane, (B) the z-axis was set to 22.3 cm for the XY plane, (C) the YZ plane, and (D) the x-axis was set to 0 cm for the YZ plane.

A total of six lines, three from an XY and three from a YZ plane were used to make the water velocity comparison, planes and sampling lines are shown in Fig. 4. For the XY plane, the z-axis was set to 22.3 cm, just below the entrance of the hydraulic selector. The center line was set directly in the center of the selector, the left and right lines were offset by 5 cm respectively. For the YZ plane, the x-axis was set to 0 cm, both left and right lines were located 3 cm from the end of the hydraulic selector.

A tetrahedral structured mesh was used for both reactor and selector water (water inside the hydraulic selector), the default element size was set to 2.025 mm and maximum element size was 4.0 mm. Face meshing was used at the entrance of the hydraulic selector. A contact sizing of 1.5 mm was also applied to the selector entrance along with the external and internal faces of the selector. This ensured a smooth mesh transition from the reactor water into the selector water, images of the mesh are shown in Fig. 5.5.

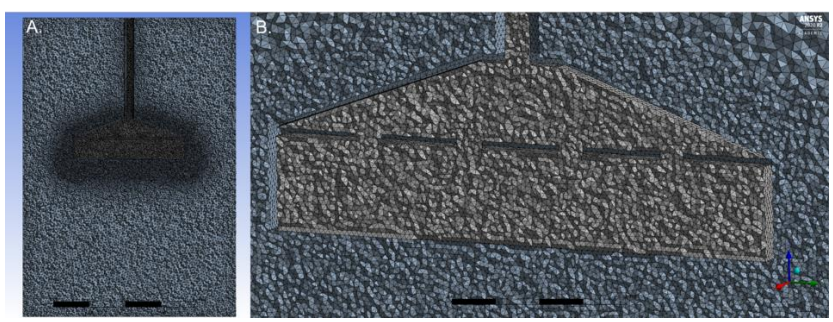

Figure 5.5 A tetrahedral structured mesh with the reactor water shown in gray and selector water in brown. (A) a sliced image of the reactor and selector, and (B) a zoomed in image of the selector.

A total of four different meshes were developed and tested, each mesh maintained the same face and contact sizing, but the default element size was varied to increase or decrease element count. The characteristic of each mesh and quality of the mesh are summarized in Table 5.3.

Table 5.3. Four meshes were developed and simulated. Each mesh varied in quantity of elements and quality of mesh. Mesh quality was determined by the element quality, aspect ratio and skewness

Mesh	Nodes	Elements	Element Quality				Aspect Ratio				Skewness			
			Avg	STD	Min	Max	Avg	STD	Min	Max	Avg	STD	Min	Max
1	1.469,063	8,474,298	0.854	0.009	0.003	1	1.782	0.435	1.158	45.49	0.202	0.11	1.3E-6	0.987
2	1,875,000	10,770,242	0.854	0.009	0.003	1	1.786	0.436	1.158	45.58	0.203	0.11	1.8E-6	0.987
3	2,231,558	12,782,940	0.853	0.009	0.003	1	1.788	0.436	1.157	45.51	0.204	0.11	4.4E-10	0.987
4	3,000,000	17,232,000	0.852	0.009	0.003	1	1.790	0.436	1.157	45.54	0.204	0.11	9.7E-10	0.988

The mesh elements varied between 8.4 and 17.2 million. An average element quality for a high-quality mesh is ≥0.8, all meshes were above this minimum value. The aspect ratio measures the element's deviation from having all sides of equal length, all four meshes had an aspect ratio of less than 2.5, common for a high-quality mesh. Lastly, skewness, the difference between the shape of the cell and the shape of an equilateral cell of equal volume, skewness for all mesh were less than 0.5, indicating that all meshes were between an excellent and very good quality. A comparison of the velocity profiles for all the meshes after 15 seconds of mixing are presented in Fig. 5.6.

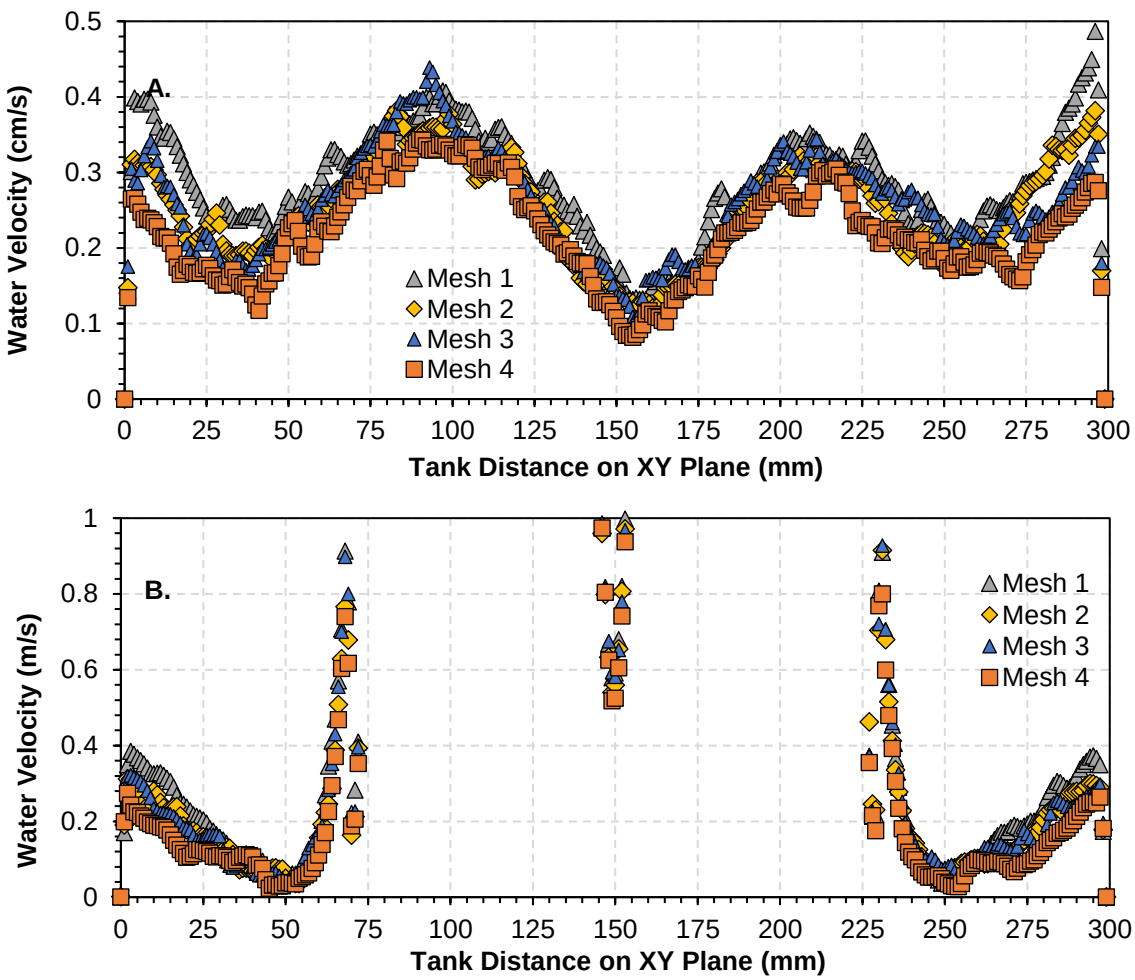

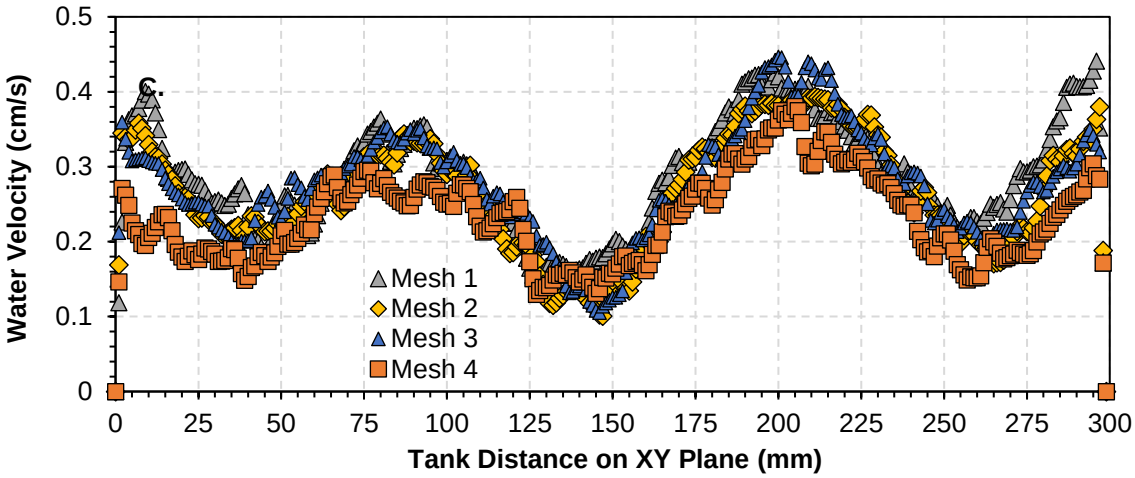

Figure 5.6 Water velocity profiles on the XY plane for Meshes 1-4 for the (A) Left, (B) Center, and (C) Right lines.

All meshes in the left line profile have a similar velocity between 50 and 250 mm on the XY plane, while in the initial 50 mm, Mesh 1 was higher than mesh 2-3, and this trend reoccurred between 275 and 300 mm. For the center line profile, all meshes had nearly identical profiles, with the expectation occurring between 0-25 mm and 275-300 mm, when the water velocity is <0.4 cm/s. For the Right line, mesh 2 and 3 are nearly identical, while mesh 1 and 4 have larger difference near the edges of the reactor. Table 5.4 was used to compare the average and median percent difference between meshes for the left, center, and right lines. For all lines mesh 2 and 3 had the lowest percent difference.

Table 5.4**.** Comparing water velocity profiles for meshes 1-4, on lines across the XY plane (left, center, and right)

Water Velocity Comparison	**Left**			**Center**			**Right**		
Mesh Comparison	1/2	2/3	3/4	1/2	2/3	3/4	1/2	2/3	3/4
Avg % Difference	12.3	10.7	15.7	13.8	8.9	13.7	12.2	9.6	17.8
Med % Difference	11.2	6.8	15.0	2.9	2.3	4.6	10.1	6.7	17.2

In addition to the water velocity profiles, the volume fraction of the slow and fast settling particles were also used for the mesh independence study. A total of six planes were used, 3 XY planes (bottom, middle and top of the reactor) and 3 ZY planes (positive, center, negative), as shown in Fig. 5.7.

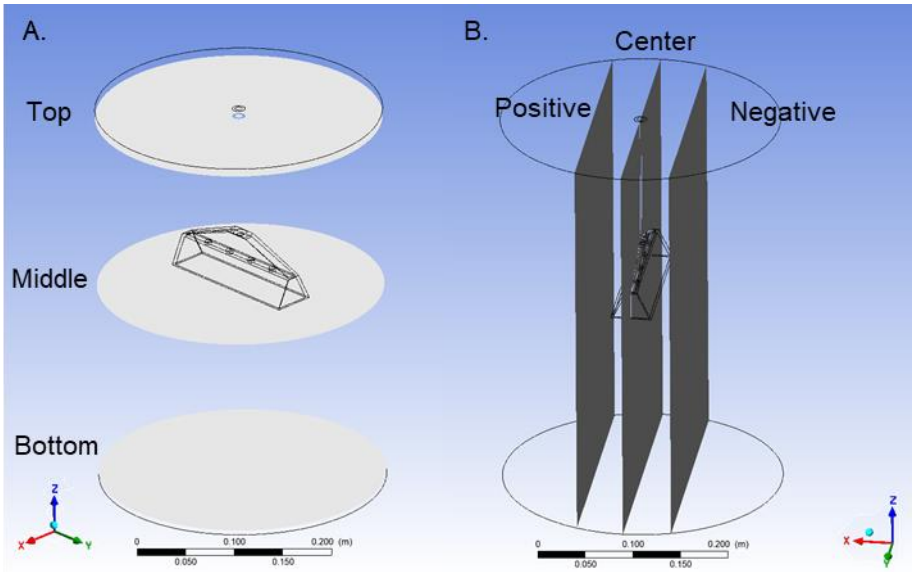

Figure 5.7 (A) XY planes at three locations along the z-axis labeled top, middle, and bottom. (B) ZY planes with three locations along the x-axis labeled, positive, center, and negative. The average volume fraction of fast and slow settling particles was taken from each plane after 15 seconds of mixing at 60 RPM.

To compare the average volume fraction on the various XY and ZY planes Table 5.5 was developed. Mesh 2 and 3 had the lowest percent volume fraction difference (<10%) for both slow and fast particles on all planes (top, middle, and bottom). For the ZY plane, all meshes for each plane had a similar volume fraction distribution. From this mesh independent study, it was found that mesh 2 or 3 would be an acceptable and mesh 3 was used for the remainder of the CFD simulation.

Table 5.5**.** Comparing average volume fraction distribution for meshes 1-4, on various XY (top, middle, and bottom) and ZY (positive, center, negative) planes.

XY Plane – Avg Volume Fraction/Cell Area						
	Slow Particles (% Difference)			Fast Particles (% Difference)		
Mesh	1/2	2/3	3/4	1/2	2/3	3/4
Top Plane	29.9	7.8	10.9	24.5	4.8	20.9
Mid Plane	8.7	6.2	4.1	0.8	1.3	0.2
Bot Plane	11.8	8.6	4.2	17.6	0.3	0.1
ZY Plane – Avg Volume Fraction/Cell Area						
	Slow Particles (% Difference)			Fast Particles (% Difference)		
Mesh	1/2	2/3	3/4	1/2	2/3	3/4
Pos Plane	4.2	3.3	3.8	8.1	1.3	1.1
Center Plane	3.5	3.8	4.2	8.4	2.6	1.8
Neg Plane	4.4	3.7	4.2	8.3	1.9	1.1

5.4.6 Simulation setup - mixing, settling, and hydraulic selector operation

The mixing stage of the simulation imitates the conditions that occur in AS reactors before the hydraulic selection process. To provide the particles a similar condition in the least amount of time the CFD simulation is initialized with all particle phases evenly distributed in the reactor water, then particles are rotated around the center of the reactor (z-axis). As in the mesh independence study, the mixing in the reactor was conducted through frame motion. For the first 2 seconds the reactor water rotated at 60 RPM, then increased to 120 RPM for an additional 2 seconds and for the remainder 6 seconds mixing was increased to 180 RPM. After 10 seconds, mixing was reduced to 0 RPM and the settling phase of the simulation began. After a settling time of 50 seconds the hydraulic selection process followed. During the hydraulic selection process flow through the hydraulic selector was controlled by increasing the mass flow of water through the reactor inlet, top of the reactor. It was assumed that the density of the solution displaced was equal to water, thus a flow of 1L/min is equal to 0.0167 kg/sec. Water entering from the inlet would then displace water and force flow through the hydraulic selector. Using this method reduce the need of an additional air/water interface. A total of three hydraulic selector outflow were simulated, 0.5, 1, and 2 L/min and each outflow was simulated for 10 seconds. This CFD model is pressure based, with a transient time step, and gravity enacted in the Z direction at -9.81 m/s^2. A multiphase approach was used to simulate the three different particle sizes, in total there were four phases including water. For near wall treatment a scalable wall function was used with curvature correction and standard model constants were not altered.

5.4.7 Boundary conditions

During the mixing and settling phases of the simulation, all zones were defined as interfaces, walls, or interiors. During the hydraulic selection phase the top of the reactor water was changed to a mass flow inlet and the hydraulic selector discharge was changed to a pressure outlet. For the first 50% of the simulation, all the spatial discretization including pressure, momentum, volume fraction, TKE, and turbulent dissipation rate were a second order or second order upwind model. For the remainder of the simulation, spatial discretization was changed to first order models. The gradient spatial discretization was always the least squares cell based and the transient formulation was always first order.

5.4.8 Experimental setup

Polyethylene particles (Cospheric, Santa Barbara, CA) were used to validate the CFD simulation. At the same volume fraction described in Table 2, particles were added to an acrylic reactor with identical conditions as in the simulation. Particles were coated with a 0.1% Tween solution to improve the hydrophilicity. A difference between the CFD simulation and bench reactor experiments were the mixing conditions. In the bench scale experiment all particles were added to the reactor and allowed to settle. Once the particles settled, the mixing in the reactor was conducted with a 10 cm stir-bar for a total of four minutes. For the first minute, mixing was set to 60-RPM, for the second minute, mixing was set to 120 RPM, and for the final two minutes mixing was set to 180 RPM. After mixing was complete particles were allowed to settle

for the desired amount of time. Once settling was complete the positive displacement rotary vane pump was turned on and set to the required hydraulic selector discharge flow, flow was measured with an inline flow meter. The vacuum developed by the hydraulic selector was also measured inline, 2.5 cm above the initial water level. The discharge of the hydraulic selector was collected in a separate acrylic tank. The three different particle sizes were then separated using a 200 µm, 100 µm, and 50 µm sieves. The discharge of the hydraulic selector was poured through all sieves and particles retained on each sieve were washed with DI to ensure only appropriate particles were retained. Particles were then removed by backwashing the sieve with DI water. The particles were collected in a plastic weigh boat and allowed to air dry for 48 hrs. The mass of the particles was then weighted on an analytical scale. Images of the experimental set-up conducted at the Mines Park Laboratory are shown in Fig. 5.8.

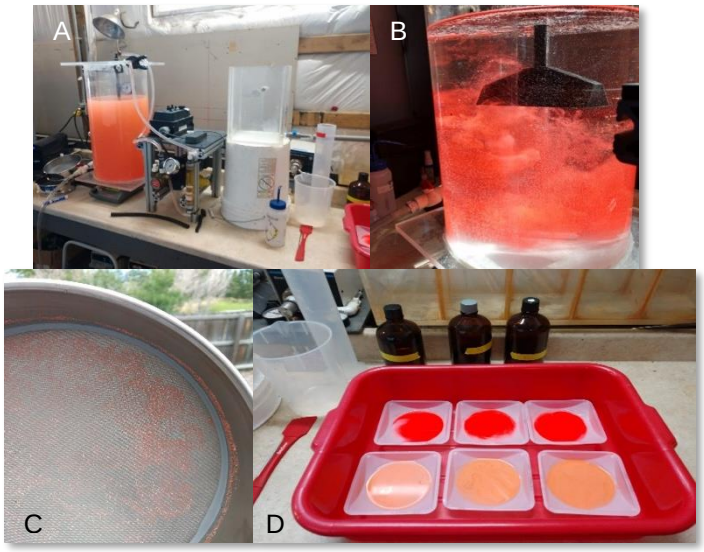

Figure 5.8 The experimental setup, experiments were conducted at the Mines Park laboratory. (A) the entire bench scale setup, with the acrylic reactor in the far left, the positive displacement, rotary vane pump in the middle, and the collection tank the far right. (B) The addition of the 120 µm particles (red) to the acrylic reactor. (C) particles collected on a sieve. (D) particles collected in plastic weigh boats, red is 120 µm and orange is 60 µm.

The experiments conducted varied the settling time prior to the hydraulic selection process and the hydraulic selector outflow. The mixing prior to settling and the location of the selector remained constant. The various operating conditions of the bench scale experiments are summarized in Table 5.6. The mixing time of 4 minutes was constant for all experiments, the settling time varied between 1 and 4 minutes, this affected the minimum settling velocity. The hydraulic selector outflow varied between 0.5 and 2 L/min. The total volume discharged for all experiments were the same, 3 L, this affected the total operation time of each experiment.

Table. 5.6 Operating conditions of experiments. Settling time and hydraulic selector outflows were varied and effected the minimum settling velocity and total operation time.

Mixing Time Bench (min)	Settling Time (min)	Min Settling Velocity (m/h)	HS Outflow (L/min)	HS Entrance Velocity (m/h)	Volume Discharged (L)	Total Operation Time (min)
4	1	12	0.5	4.4	3	11
4	1	12	1	8.5	3	8
4	1	12	2	17	3	6.5
4	2	6	0.5	4.4	3	12
4	2	6	1	8.5	3	9
4	2	6	2	17	3	7.5
4	4	3	0.5	4.4	3	14
4	4	3	1	8.5	3	11
4	4	3	2	17	3	9.5

5.5 Results and discussion

5.5.1 Bench scale result – particle distribution

Each of the operating condition described in Table 5.6 was only tested once. The experimental error was calculated by placing a known mass of particles in a 3 L solution, the particles were then collected as described in section 5.3.8 and weighed. For the 60 and 120 µm particles, the experimental error (underestimation of particle mass) was between 4-9% while the error of the 220 µm was 3-5%. The higher error for the particles <120 µm was due to their small diameter, making them difficult to retrieve from the sieves. The results of the bench scale experiments are presented in Fig. 5.9. Figs. 9A-C represent the mass fraction of particles (60 µm, 120 µm, 220 µm) relative to the total particle mass removed by the hydraulic selector under the various operating conditions. Figs. 5.9D-F present the mass fraction of particles (60 µm, 120 µm, 220 µm) relative to the total mass of particle contained in the reactor at various operating conditions.

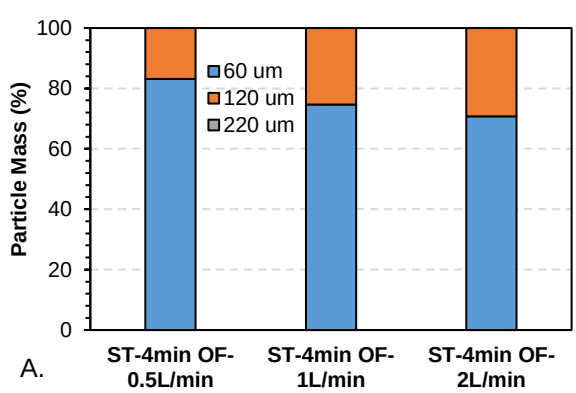

A.

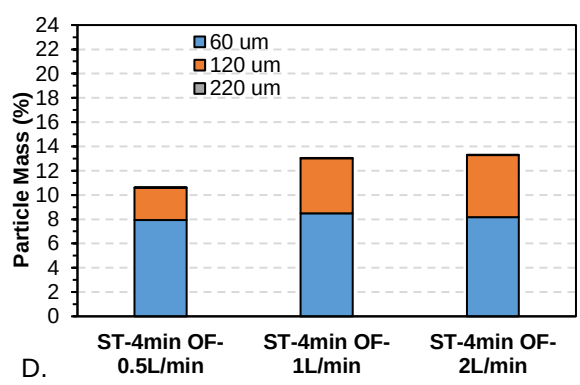

D.

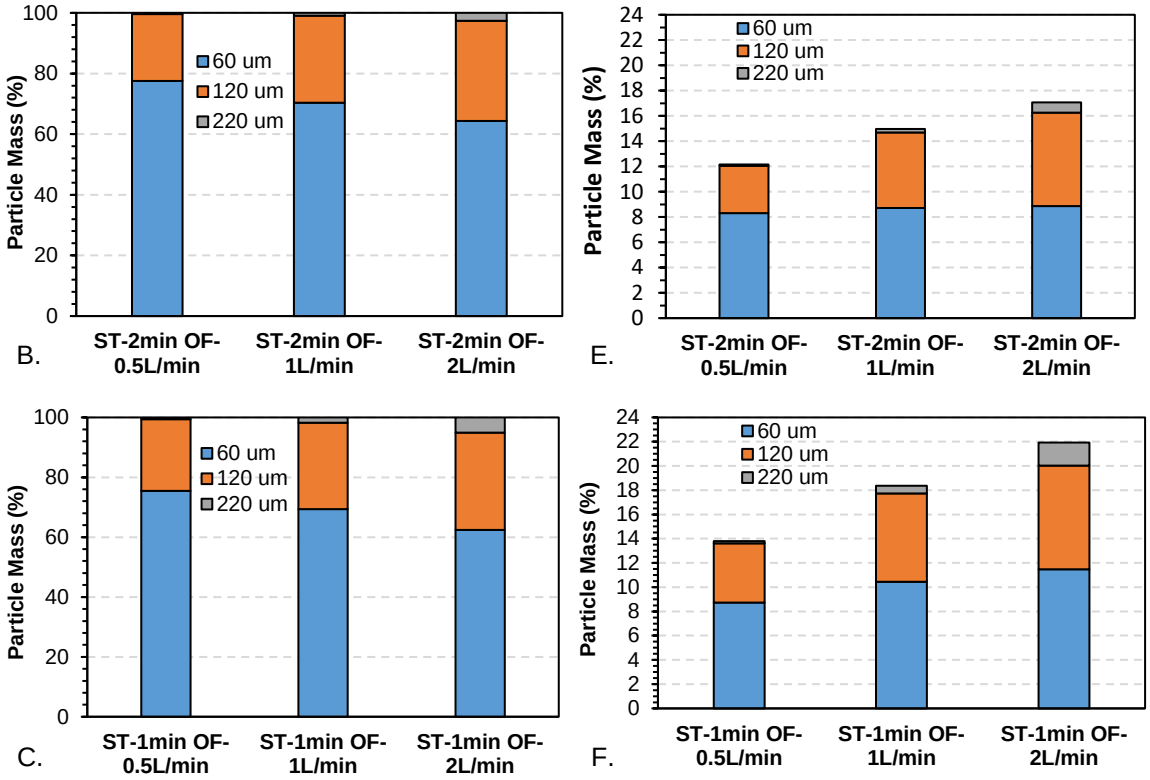

Figure 5.9 Particle distribution for bench scale experiments, A-C) the x-axis describes the experimental operating conditions, and the y-axis represents the mass fraction of particles relative to the total particle mass removed by the hydraulic selector. D-F) the x-axis described the experimental operating conditions, and the y-axis represents the mass fraction of particles relative to the total mass of particle contained in the reactor.

With the longest settling time of 4 minutes, Fig. 9A demonstrates the ability of the hydraulics selector to influence the removal of particles in what appeared to be laminar conditions in the reactor. At the slowest outflow of 0.5 L/min, the selector discharge was dominated by poor settling floc at 83%, compared to the initial solution composition of 50%. The remainder of the selector discharge was composed of medium settling floc and there was no measurable amount of fast settling floc. As the selector increased outflow from 1 to 2 L/min, the medium size particle fraction slightly increased, and due to the experimental error, this difference may not be substantial. Fig. 9D shows data obtained under the same operating conditions as Fig. 9A, but compared particle mass removed to the entire mass of the particles in the reactor. This distribution shows that once the hydraulic selector outflow increases above 1 L/min, the selector discharge had a similar particle distribution.

To increase the total biomass removed, the settling time was reduced to 2 minutes. Results are shown in Figs. 9B and 9E. Compared to the 4-minutes settling time at 0.5 L/m, the medium particle mass fraction removed increased by 22%. With each increase in selector outflow the fraction of medium settling floc increased, reaching a maximum of 33%, greater than the initial conditions of 30%. Also, at the 2 L/min discharge the first measurable amount of fast settling particle mass was detected at 3% of the particle mass. With respect to total particle mass in the reactor, as the hydraulic selector outflow increased so did

the percentage of the medium and fast settling particles while the slow settling particles remained constant. This indicates that a higher abundance of medium and fast settling particles were still in suspension at the 2 minute settling time and the ability of the selector to remove more particles at higher dischargers. Data collected for Figs. 9C and 9F was from operation with the shortest settling time of 1 minute. At the slowest outflow of 0.5 L/min, <1 % of the particle mass removed was composed of the fastest settling floc. This indicates that even though fast settling particles were present, the entrance velocity of the selector (0.0012 m/s) was not sufficient to remove the particles. As the outflow of the hydraulic selector increased so did the fractions of fast settling particles. At 2 L/min the fasting settling fraction had increased to 5% compared to 2.6% at a 1-minute settling time and same outflow. However, even at a 1-minute settling time, the majority of the fast-settling floc remained in the reactor outside the hydraulic selector's sphere of influence. For both the slow and medium settling particles the reduced settling time maintained the particles in suspension and increased outflow, resulted in higher particle mass removal. At longer settling time, the selector can effectively remove a higher percentage of poor settling floc; comparing Figs. 9D and 9F, both removed 8% of the slow settling particle mass from the reactor while the longer settling time only remove 2.6% of the medium particle mass and the 1-minute settling time removed 4.9%. Although the difference in medium floc removal may not seem substantial, this selection process occurs multiple times a day and may help control the mean particle diameter of a reactor.

5.5.2 Mixing and settling simulation

After 10 seconds of mixing, the simulation then settled for approximately 50 seconds. Contours of the water velocity after mixing and settling are presented in Fig. 5.10. The velocity profile in the reactor water developed a uniform gradient after the mixing phase, as shown in Fig. 5.10A, with the highest velocities along the reactor wall and slowest velocities in the middle of the reactor. This velocity profile was expected due to the initialization conditions of the model. After 50 seconds of settling, the velocities in the reactor were greatly reduced, with the majority of the water velocity lower than 0.3 m/sec (Fig 5.10B). The highest velocities in the reactor remained along the reactor and selector walls, the majority of these velocities were still substantially higher than the expected hydraulic selector entrance velocity of 0.0048 m/s at a 2 L/min discharge. Zooming onto the hydraulic selector, Fig. 5.10D, there are patches of high velocity water in the hydraulic selector. These initial conditions may have affected the initial particles removal by the hydraulic selector.

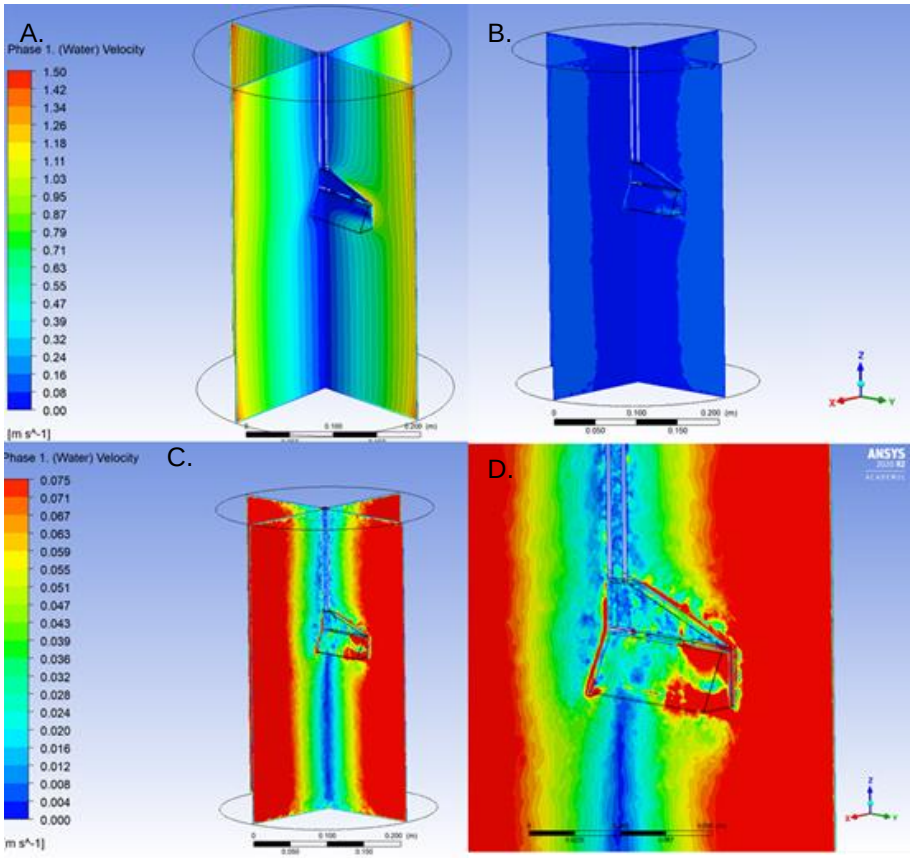

Figure 5.10 Water velocity contours of the reactor and selector water. (A) after 10 seconds of mixing, 0-1.5 m/s scale, (B) after 50 seconds of settling, 0-1.5 m/s scale, (C) after 50 seconds of settling, 0-0.075 m/s scale, and (D) velocity field around the hydraulic selector, 0-0.075 m/s.

In addition to water velocity profiles, TKE, the mean kinetic energy per unit mass associated with eddies in turbulent floc [25], is presented for both after mixing and settling in Fig. 5.11. TKE had the potential to influence the movement and distribution of all the particles in the reactor, understanding how much TKE along with eddy viscosity is required to maintain certain particles in suspension is crucial for selecting and remove target floc in real activated sludge. Additionally, understanding how TKE dissipates with time is important for choosing the settling time prior to the selection process.

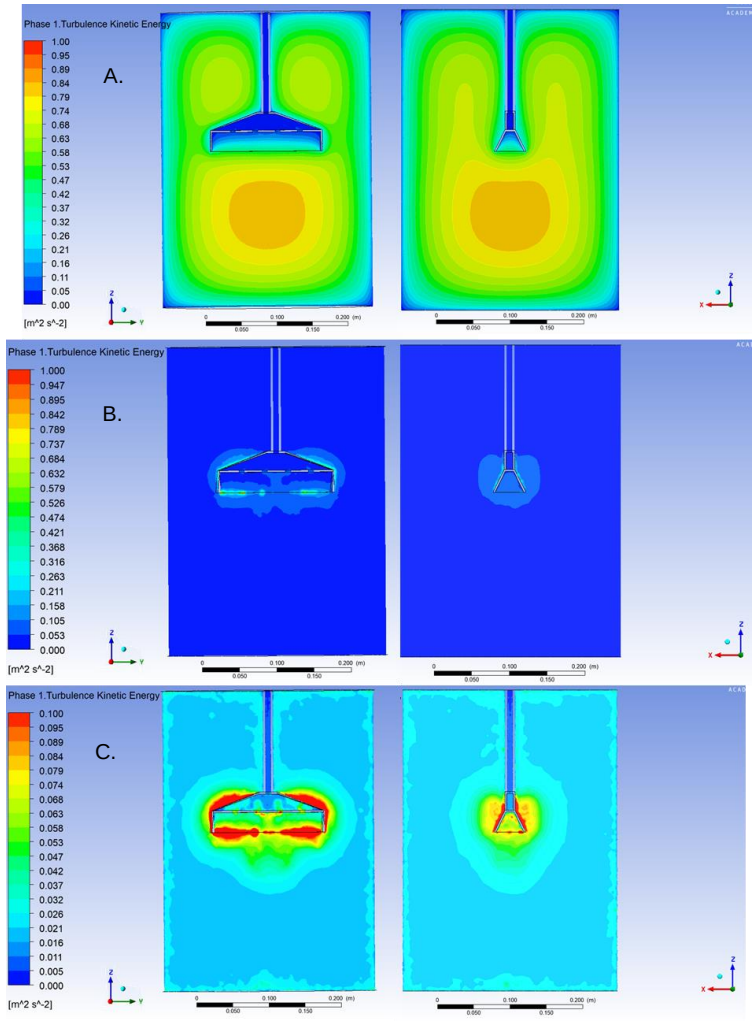

Figure 5.11 Turbulent kinetic energy of water, contours on the left are slices from the ZY plane and contours on the right are slices from the XZ plane. (A) after 10 seconds of mixing, 0-1 m^2 s^{-2} scale, (B) after 50 seconds of settling, 0-1 m^2 s^{-2} scale, and (C) after 50 seconds of settling, 0-0.1 m^2 s^{-2}.

After mixing, various areas developed with a high TKE, including directly below the hydraulic selector and above the selector, as shown in Fig. 5.11A. After 50 seconds of settling, the majority of the activated sludge has dissipated, only within 5 cm of the selector was the TKE greater than 0.2 m^2/s^2. The scale of TKE was reduced to a maximum of 0.1 m^2/s^2, as shown in Fig 5.11C. The larger eddy zones observed at the end of mixing were no longer present; new eddy zones were concentrated around the hydraulic selector, potentially impacting the resuspension of particles. Future designs of the selector could use selector geometry to further enhance or minizine these zones depending on the selection process. Fig. 5.12 was generated to visualize the effects of TKE on the various particle volume distributions.

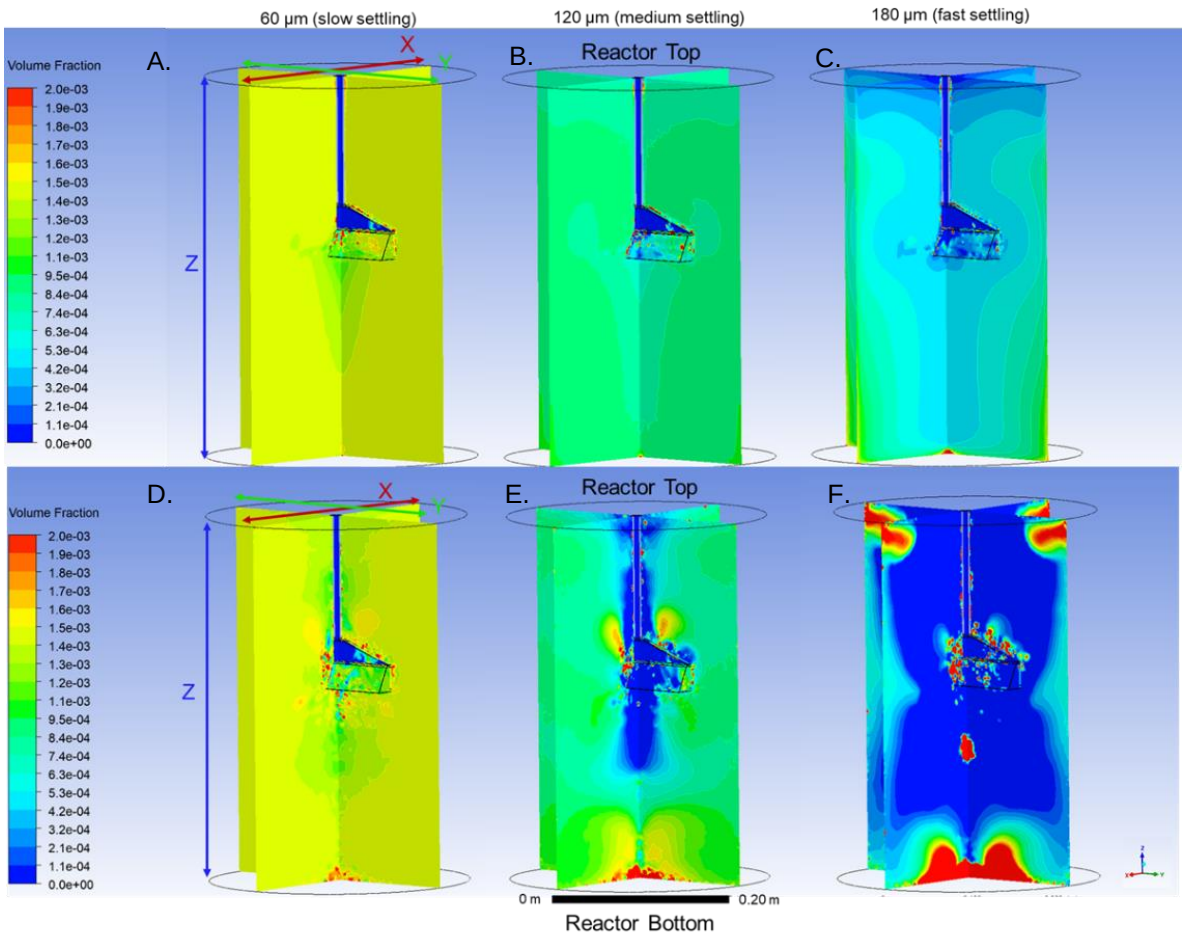

Figure 5.12. Volume fraction contours in the XZ and ZY planes, A-C) after mixing, D-F) after settling, A/D) 60 µm particles, B/E) 120 µm particles, and C/F) 220 µm particles

At the end of the mixing phase, the 60 µm particles were uniformly distributed. The contours are dominated by bright yellow, similar to initial volume fraction of 1.41e-03, as shown in Fig. 5.12A. In Fig. 5.12B the 120 µm particles are displayed, initial volume fraction was 8.7e-4, unlike the 60 µm particles there is a slightly lower volume fraction at the top of the reactor. For the 220 µm particles, Fig. 5.12C, the initial volume fraction was 6.1e-04, after mixing higher volume fractions are concentrated near the selector wall and above the hydraulic selector where the TKE is highest, ≈0.65 m^2/s^2. After settling, the majority of the 60 µm particles remained suspended, while the both the 120 and 220 µm particles both experience some settling. The settling on the bottom of the reactor corresponds with the velocity of water shown in Fig. 5.10C. Additionally, the 220 µm particles had also settled on top of the reactor and began sliding off and into the middle of the reactor. To quantify the change in volume fraction along the z-axis Fig. 5.13 was developed to provide an average volume fraction distribution. A total of four lines, two from the XZ plane and two from YZ, were averaged along the z-axis after mixing and after the settling phase. The bottom of the reactor begins at the 0 mm mark and the top of the reactor is at 420 mm.

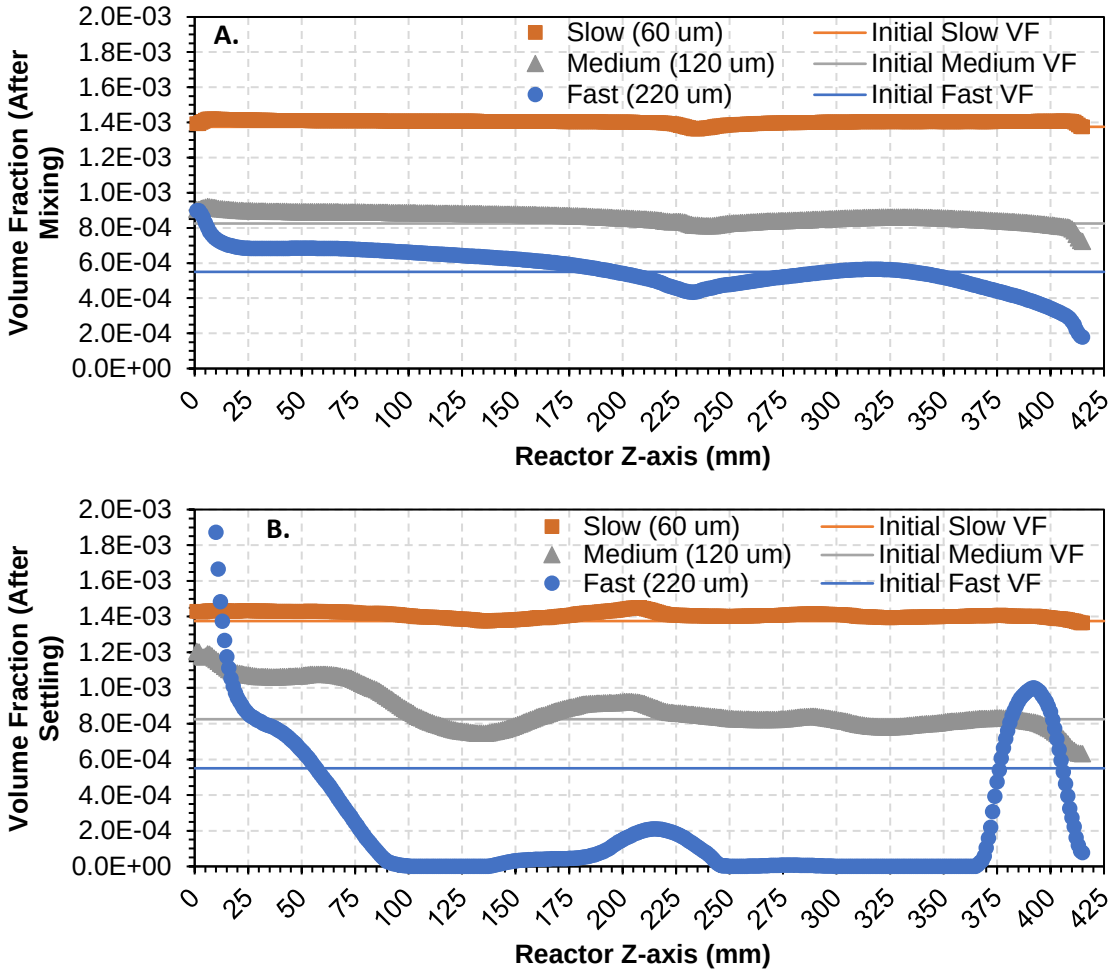

Figure 5.13 The average volume fraction of the 60 µm, 120 µm, and 220 µm particles after A) mixing and B) after settling. The average was taken along the z-axis of the reactor, 0 mm being the bottom of the reactor and 420 mm being the top. The average was taken from a total of four points from both XZ and YZ planes. The thin orange lines across the graphs represent the initial slow, medium, and fast volume fractions.

As can be observed in Fig. 5.12A, the volume fraction of the slow and medium particles after mixing were nearly identical to their initial volume fraction values (Fig. 5.13A). However, the 220 µm particles were already beginning to settle at the bottom of the reactor, with the volume fraction increasing by 51% and decreasing by 67% at the top of the reactor. This indicates that future bench scale experiment and AGS system may need to reconsider their traditional mixing technologies. Also, aeration was not included in this simulation but will be required in future simulation to determine if current reactor configuration would provide enough mixing for AGS. Interestingly, all particle volume fraction slightly decreased at the height of the hydraulic selector beginning at 223 mm and ending at 270 mm. This decrease in particle volume fraction maybe caused by the higher velocity induce in the smaller area between the hydraulic selector and reactor wall. After the settling phase, the 60 µm particles along the z-axis continued to be evenly distributed (Fig 5.13B). Although by the end the mixing phase the velocity of water and TKE had greatly decreased, the

conditions were enough to maintain the 60 µm completely suspended. The 120 and 220 µm particles began to settle, and had a substantial increase in volume fraction at the bottom of the reactor. Also, volume fractions of all particles increased at the hydraulic selector height along the z-axis. This increase in particle volume fraction may have been caused by settled particles on the selector or a resuspension of particle due to the higher TKE surrounding the hydraulic selector.

5.5.3 Hydraulic selector results

The velocity profile of water and all three-particle phase in the reactor were nearly identical after operating the hydraulic selector at the three different discharge rates, 0.5, 1, and 2 L/min, for a total of 10 seconds each. Contours of the velocity profiles for the 2 L/min hydraulic selector discharge are presented in Fig. 5.14.

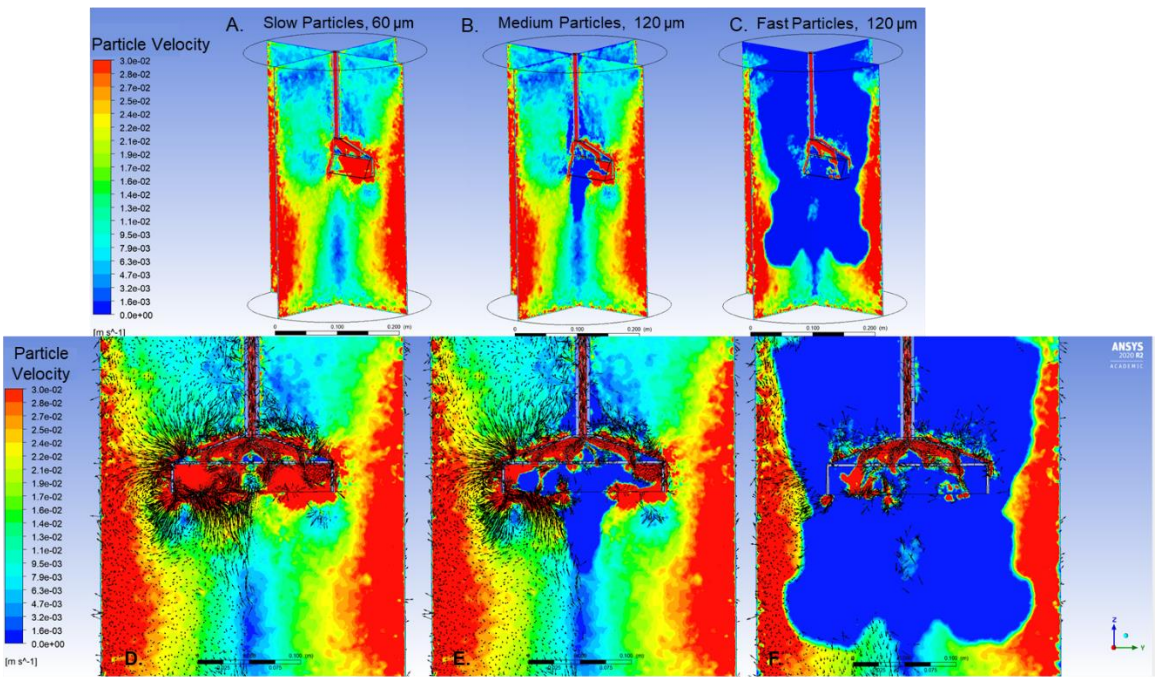

Figure 5.14 Velocity contours of the reactor and selector water on the XZ and YZ planes after operating the hydraulic selector at 2 L/min for 10 seconds. (A) slow particles (60 µm), (B) medium particles (120 µm), (C) fast particles (220 µm), (D-F) YZ plane, velocity contours of 60, 120, or 220 µm particles, respectively, with vectors indicating flow direction.

For all particle sizes, the highest velocities continued to occur along the reactor wall. The 60 µm particle velocity, Fig. 5.14A, showed that a high velocity of the particle entering the selector are higher than 0.01 m/s while the entrance velocity to the selector due to hydraulic selector discharge was calculated to be 0.0048, indicating that the high velocity of the water and particle phases were influencing the external volume fraction distributions. By overlaying the velocity contours with vectors, the 60 µm flow direction can be visualized (Fig. 5.14D). Particles above the selector seemed to be rotating in place, trapped by eddies—eddy viscosity in this region varied between 1 and 2 Pa s (Fig. 5.15A). Below these eddies, particles flow

toward the hydraulic selector, and results in a high TKE (Fig. 5.15B). For the 120 µm particles, the velocity profiles and vectors look similar to 60 µm particles (Figs. 5.14B and 5.14E). For the 220 µm particles, the suspended particles contain a velocity of higher than 0.01 m/s. Fast settling particles along the reactor wall and near the hydraulic selector were drawn towards the hydraulic selector (Fig. 5.14F). However, by comparing the 220 µm velocity with the hydraulic selector operation of 0.5 L/min, effects of the hydraulic selector and TKE conditions can be assessed. At 0.5 L/min hydraulic selector discharge, the 220 µm particles had nearly the same velocities and direction as the 2.0 L/min discharge, the only difference was within the selector, where few particles settled out of the selector. Thus, the velocity of the fast particles outside the reactor continued to be influenced by the TKE and eddy viscosity conditions.

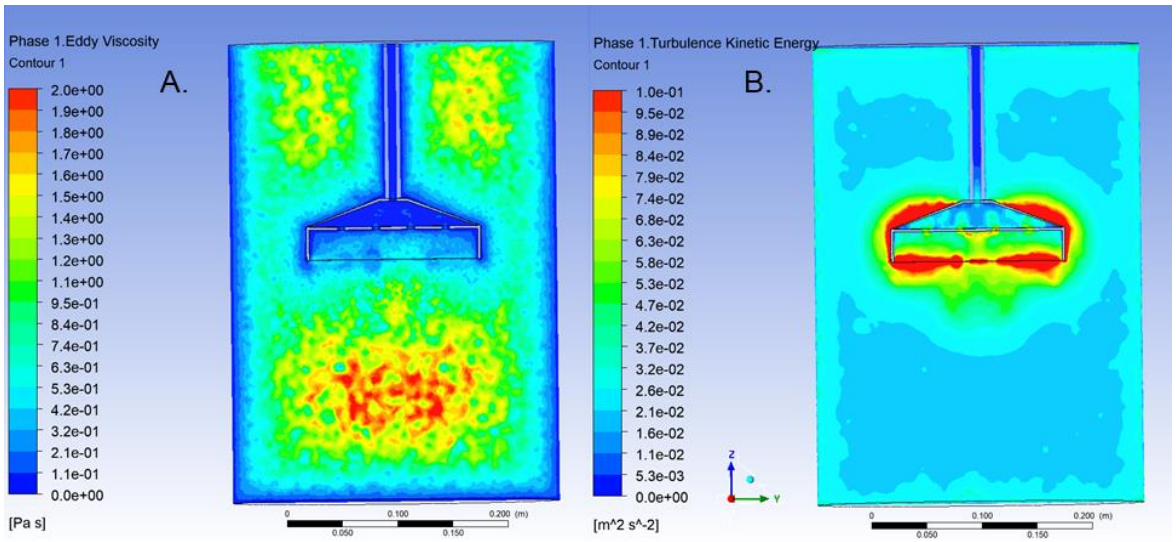

Figure 5.15. (A) The eddy viscosity and (B) the turbulent kinetic energy in the YZ plane after 10 second of hydraulic selector discharge at 2 L/min.

The volume fractions of the various particles are presented in Fig. 5.16. For the 60 µm particles (Fig. 5.16A), although the particles along the reactor wall contained the highest velocity, the volume fraction of these particles seems to be evenly distributed as shown in Fig. 5.17. The 60 µm particle mass was between 32 and 33% for all three regions of the reactor. This was similar for the medium size particles, although there was slightly higher particle settling, with the bottom region containing 39% of the particle mass while the top region had 29% particle mass (Fig. 5.17). The small 60 µm particle surround the inside and outside of the selector. The 120 µm particle were further away from the selector due to what seemed to be the development of large eddies. Still, there were particles that encounter higher velocities along the edges of the selector and being removed by the selector (Fig. 5.14E). For the fast settling 220 µm particles, a high-volume fraction accumulated around and on top of the hydraulic selector, which resulted in particles sliding off the sides of the selector. A cluster of particles below the selector seem be trapped due to the eddy viscosity presence and hydraulic selection at 2L/min. 65% of the volume fraction was located at the third of

the reactor and the final volume fraction was suspended in high along the walls and seemed to be settling or caught in turbulence hear the hydraulic selector entrance (Fig. 5.16D and Fig. 5.14F).

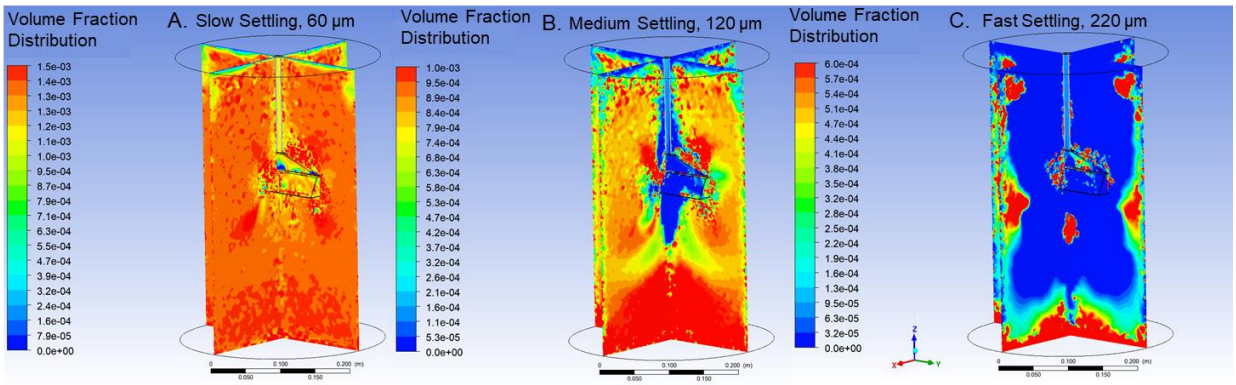

Figure 5.16 Volume fraction distribution across XZ and YZ planes after operating the hydraulic selector at 2 L/min for 10 seconds. A) slow particles (60 µm) B) medium particles (120 µm), C) fast particles (220 µm)

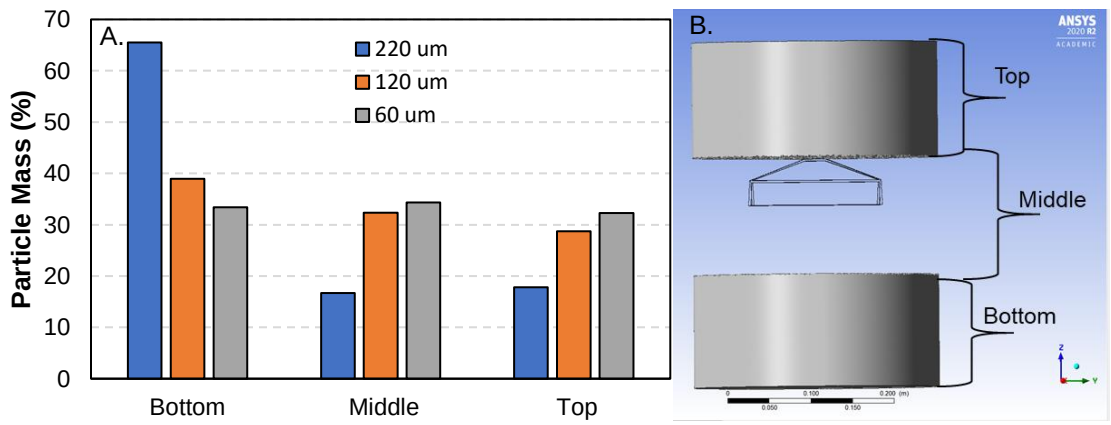

Figure 5.17 The distribution of the particle mass in the reactor after 10 second of selector operation at 2 L/min. The reactor water was split into three regions bottom, middle and top, each region approximately 1/3 of the reactor volume.

After settling, the hydraulic selector operated at three different hydraulic selector outflow (0.5, 1, and 2 L/min) for 10 seconds each, the hydraulic selector discharge particle composition is presented in Fig. 5.18. During this time an eddy viscosity of higher than 1 Pa s and TKE of higher than 0.002 m^2/s^2 were sufficient to maintain the majority of the 60 µm and 120 µm in suspension. This resulted in the turbulent conditions around the selector and had a large influence on particle volume fractions removed. This resulted in a similar particle distribution for all hydraulic selector outflows, with the majority of the distribution being composed of the 60 µm particles. If the model were to continue to run, an additional 30 to 60 seconds of hydraulic selector operation may have resulted in reduced TKE and eddy viscosity values. This reduction may have allowed for the hydraulic selector entrance velocity to influence the removal of the poorly settling floc from the reactor.

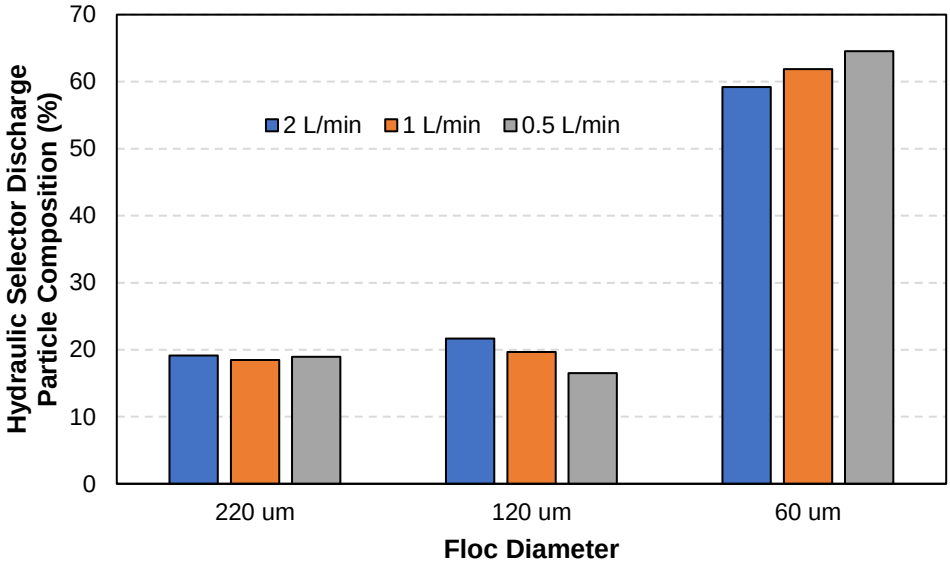

Figure 5.18 The particle composition for all hydraulic selector discharges (0.5, 1, and 2 L/min) after 10 second of operation.

5.6 Conclusion

For hydraulic selection technologies to be adopted by conventional activated sludge facilities, these technologies must be able to operate in a range of conditions, including in high turbulence. Bench scale experiments demonstrated the effects of particle settling and the hydraulic selector discharge rate on the particle size distribution and particle mass removed. Results demonstrated that the settling time before hydraulic selection was the most influential parameter in preventing the removal of both 120 µm and 220 µm particles. Future experiments could potentially use lower hydraulic selector outflow to further reduce medium and larger particle removal under turbulent conditions. For the CFD model, after mixing it was evident that the 220 µm was not evenly distributed, while this was not the case for the 60 and 120 µm particles. Both CFD model and bench scale experiments did not operate with aeration, which occurs in aeration basins; however, there are anoxic and anerobic tanks that only rely on mixing, and problems with floc settling may occur in the basin if granules become too large. Thus, additional research is required to ensure granules of various sizes and densities are retained in suspension. After 50 second of settling, both the 60 and 120 µm particles remained suspended in the reactor while over 60% of the 220 µm particles had already settled to the bottom third of the reactor. During this time, an eddy viscosity of more than 1Pa s and a TKE greater than 0.002 m^2/s^2 was sufficient to maintain both 60 and 120 µm in suspension. This resulted in the turbulent conditions around the selector and had a large influence on particle volume fractions compared to the hydraulic selector discharge. This led to the particle distribution of all hydraulic selector outflow to be similar, with the majority of the particle being composed of the 60 µm particles. This work provides insight on TKE and eddy viscosity conditions that develop around the hydraulic selector and impacts on volume fraction distribution. Reducing the TKE around the selector, potentially caused by

selector geometry, would reduce the removal of medium particles and increase the removal of slow settling particles.

5.7 References

[1] G. Tchobanoglous, Metcalf, Eddy, Wastewater Engineering Treatment and Resource Recovery, Fith, New York City, 2005.

[2] Z. Li, P. Lu, D. Zhang, G. Chen, S. Zeng, Q. He, Population balance modeling of activated sludge flocculation : Investigating the influence of Extracellular Polymeric Substances (EPS) content and zeta potential on flocculation dynamics, Sep. Purif. Technol. 162 (2016) 91–100. https://doi.org/10.1016/j.seppur.2016.02.011.

[3] G. Sheng, H. Yu, X. Li, Extracellular polymeric substances (EPS) of microbial aggregates in biological wastewater treatment systems : A review, Biotechnol. Adv. 28 (2010) 882–894. https://doi.org/10.1016/j.biotechadv.2010.08.001.

[4] A. Sharaf, B. Guo, Y. Liu, Impact of the filamentous fungi overgrowth on the aerobic granular sludge process, Bioresour. Technol. Reports. 7 (2019). https://doi.org/10.1016/j.biteb.2019.100272.

[5] K. Krysiak-Baltyn, S.L. Gras, W. Burger, P.J. Scales, A.D. Stickland, G.J.O. Martin, The influence of protruding filamentous bacteria on floc stability and solid-liquid separation in the activated sludge process, Water Res. 123 (2017) 578–585. https://doi.org/10.1016/j.watres.2017.06.063.

[6] R.A. Maltos, R.W. Holloway, T.Y. Cath, Enhancement of activated sludge wastewater treatment with hydraulic selection, Sep. Purif. Technol. 250 (2020) 117214. https://doi.org/10.1016/j.seppur.2020.117214.

[7] R.D.G. Franca, H.M. Pinheiro, M.C.M. Van Loosdrecht, N.D. Lourenço, Stability of aerobic granules during long-term bioreactor operation, 36 (2018) 228–246. https://doi.org/10.1016/j.biotechadv.2017.11.005.

[8] S.S. Adav, D. Lee, K. Show, J. Tay, Aerobic granular sludge : Recent advances, i (2008) 411–423. https://doi.org/10.1016/j.biotechadv.2008.05.002.

[9] M. Winkler, C. Meunier, O. Henriet, J. Mahillon, M. Suarez-Ojeda, G. Del Moro, M. De Sanctis, C. Di Iaconi, D. Weissbrodt, An integrative review of granular sludge for the biological removal of nutrients and recalcitrant organic matter from wastewater, Chem. Eng. J. 336 (n.d.) 489–502. https://doi.org/10.1016/j.cej.2017.12.026.

[10] M. Pronk, M.K. De Kreuk, B. De Bruin, P. Kamminga, R. Kleerebezem, M.C.M. Van Loosdrecht, Full scale performance of the aerobic granular sludge process for sewage treatment, Water Res. 84 (2015) 207–217. https://doi.org/10.1016/j.watres.2015.07.011.

[11] R. Maltos, A. Waclawski, B. Marten, T. LeClear, F. Bruecken, S. Jonson, T. Cath, R.W. Holloway, G. Rajagopalan, J. Debroux, T.Y. Cath, Minimizing solid retention time through

hydraulic selection for the development of aerobic granular sludge, (2021).

[12] M. Patziger, Chemical Engineering Research and Design Computational fluid dynamics investigation of shallow circular secondary settling tanks : Inlet geometry and performance indicators, Chem. Eng. Res. Des. 112 (2016) 122–131. https://doi.org/10.1016/j.cherd.2016.06.018.

[13] A.M. Karpinska, J. Bridgeman, CFD-aided modelling of activated sludge systems e A critical review Standard Method of Moments, Water Res. 88 (2016) 861–879. https://doi.org/10.1016/j.watres.2015.11.008.

[14] R.W. Samstag, J.J. Ducoste, A. Griborio, I. Nopens, D.J. Batstone, J.D. Wicks, S. Saunders, E.A. Wicklein, G. Kenny, J. Laurent, CFD for wastewater treatment : an overview, (2018) 549–563. https://doi.org/10.2166/wst.2016.249.

[15] R. Hreiz, O. Potier, J. Wicks, J.M. Commenge, CFD Investigation of the effects of bubble aerator layouts on hydrodynamics of an activated sludge channel reactor, Environ. Technol. (United Kingdom). 40 (2019) 2657–2670. https://doi.org/10.1080/09593330.2018.1448001.

[16] J. Laurent, R.W. Samstag, J.M. Ducoste, A. Griborio, I. Nopens, D.J. Batstone, J.D. Wicks, S. Saunders, O. Potier, A protocol for the use of computational fl uid dynamics as a supportive tool for wastewater treatment plant modelling, (2014) 1575–1584. https://doi.org/10.2166/wst.2014.425.

[17] E.R. Hawkes, R. Sankaran, J.C. Sutherland, J.H. Chen, Direct numerical simulation of turbulent combustion: Fundamental insights towards predictive models, J. Phys. Conf. Ser. 16 (2005) 65–79. https://doi.org/10.1088/1742-6596/16/1/009.

[18] C.L. Jiyuan Tu, Guan-Heng Yeoh, Computational Fluid Dynamics, First, Elsevier Ltd, Oxford, UK, 2013.

[19] A. Griborio, Secondary Clarifier Modeling : A Multi-Process Approach, (2004).

[20] M. Meister, M. Rezavand, C. Ebner, T. Pümpel, W. Rauch, Mixing non-Newtonian flows in anaerobic digesters by impellers and pumped recirculation, Adv. Eng. Softw. 115 (2018) 194–203. https://doi.org/10.1016/j.advengsoft.2017.09.015.

[21] L. Yde, P.J. Binning, E. Ramin, S.W. Dorottya, M.R. Rasmussen, P. Steen, B. Gy, ScienceDirect A new settling velocity model to describe secondary sedimentation, 6 (2014). https://doi.org/10.1016/j.watres.2014.08.034.

[22] Y. Le Moullec, C. Gentric, O. Potier, J.P. Leclerc, Comparison of systemic , compartmental and CFD modelling approaches : Application to the simulation of a biological reactor of wastewater treatment, Chem. Eng. Sci. 65 (2010) 343–350. https://doi.org/10.1016/j.ces.2009.06.035.

[23] S. Das, H. Bai, C. Wu, J. Kao, B. Barney, M. Kidd, M. Kuettel, Mechanics Improving the performance of industrial clarifiers using three-dimensional computational fluid dynamics, 2060 (2016). https://doi.org/10.1080/19942060.2015.1121518.

[24] J. Bridgeman, B. Jefferson, S.A. Parsons, Computational Fluid Dynamics Modelling of Flocculation in Water Treatment : A Review OF FLOCCULATION IN WATER TREATMENT : A REVIEW, 2060 (2014). https://doi.org/10.1080/19942060.2009.11015267.

[25] R. Absi, Analytical Solutions for the Modeled k Equation, J. Appl. Mech. 75 (2008). https://doi.org/10.1115/1.2912722.

CHAPTER 6.
CONCLUSION

6.1 Research synopsis

The selection and removal of poorly settling floc from activated sludge systems have been proven possible through alternative technologies such as AGS, hydrocyclones, and now the hydraulic selector. These alternative selection processes now allow conventional activated sludge facilities to take advantage of fast settling floc. When compared to the traditional AGS technology, the hydraulic selector did not experience washout and maintained low effluent carbon and nitrogen levels. When the hydraulic selector operated as the sole wasting mechanism, activated sludge settling velocity exceeded 25 m/h, but also had several phases in the experiment where effluent TSS exceeded target concentration. A second BR compared a combination of wasting technologies, traditional wasting with hydraulic selection. This resulted in AS that settled at 18 m/h and did not have as many spikes in effluent TSS concentration. For the microbiology aspect of the research, the detection of ciliates using 18S-rRNA in all BRs indicated that the feast/famine conditions were responsible for the ciliate abundance, which provide the foundation for AGS development. However, without the selection process, the AS settling velocity stagnated at 5.0 m/h. Also, nematodes accumulated in the BR with only hydraulic selection; these predatory eukaryotes can destroy floc and may have resulted in high effluent TSS concentration. Lastly, CFD modeling and bench-scale experiments show that high turbulence conditions continued to exist after 1 minute of settling and solid/liquid separation improved once the settling time reached 4 minutes.

6.1.1 Enhancement of activated sludge wastewater treatment with hydraulic selection

This study began with the development of the hydraulic selector, this included modifying selector geometries, selector scale, and activated sludge settling time prior to selection process. For 112 days a pilot reactor with a H:D ratio <2.5 used only hydraulic selector for AS wasting. This led to the improvement of the AS settling characteristics. Additionally, a traditional AGS reactor operated only for 56 days due to BR complications that resulted in the biomass washout. The results from this study demonstrate the hydraulic selector's ability to prevent biomass wash out, while improving the AS settling properties. The floc diameter of the AS increased throughout the experiment and contributed to a maximum settling velocity of 20 m/h. Zeta potential measurements taken throughout the study showed that the AS became more positive, potentially due to feast/famine conditions. These conditions force bacteria to produce EPS, which may be utilized as a future carbon source. EPS is also positively charged and helped neutralize the negative floc charge which then allow flocculation and improve settling velocity.

6.1.2 Reducing solids retention time through hydraulic selection for the development of aerobic granular sludge

Continuing the favorable performance of the initial research, this study further assessed the long-term effects of the hydraulic selector operation on AS settling velocity. This study also evaluated effects of

various AS wasting schemes to control solid retention time and mean floc diameter. When hydraulic selection was only used for AS wasting, the settling velocity of the AS matched the entrance velocity of the hydraulic selector, indicating that hydraulic selection can be the driving parameter for controlling AS settling velocity. However, only wasting through the hydraulic selector resulted in a large volume of water that was discharged by the hydraulic selector. It was also believed that the granules became too large for the F:M ratio and was potentially the cause of the high effluent TSS concentration. The second AS wasting approach was a combination of the hydraulic selector and traditional AS wasting. The AS settling was only 18 m/h compared to 28 m/h with only hydraulic selection. However, this approach led to a stable effluent TSS concentration and reduced total volume discharge by the selector. The final BR operated without hydraulic selection and only wasted from the bottom of the reactor. The feast/famine conditions present in the reactor allowed the AS to increase in diameter but settling velocity only reached 5 m/h, indicating that the hydraulic selector also improved the density of the AGS developed.

6.1.3 Shifts in activated sludge microbiology due to feast/famine conditions and the operations of a hydraulic selector

Aerobic granular sludge studies often focus on the develop of granules with the fastest settling sludge. While improved AS settling is beneficial, many full-scale WRRF would not be able to operate with such fast-settling sludge. This chapter evaluates the microbial communities and abundances of bacteria such as filamentous, PAOs, AOBs, NOBs and eukaryotes through 16S-rRNA and 18S-rRNA gene sequencing. Through this study, wastewater facilities can select a mean floc diameter that balances fast settling velocity and enhanced nutrient removal. Results from this study showed that stalked and free-swimming ciliates (fundamental for the development of AGS) were abundant in all three BRs, identical to the BRs operated in Chapter 3, and led to AGS development in all BRs. However, without hydraulic selection, the settling velocity of AS blanket never exceed 5 m/h. The BR*s* operating with hydraulic selection removed a high abundance of filamentous bacteria throughout the study while the abundance of PAO, AOB, and NOB increased. The highest abundance of these nutrient removing organisms was found in floc with a diameter smaller than 1000 µm. The 18S-rRNA sequencing detected an order of nematode, Diplogasterida, was approximately 0.02% of the initial microbiome for all three BRs. Wasting from the bottom of the BRs maintained a low Diplogasterida abundance in BR1 and BR2 while abundance in BR3 continued to increase-and reached 0.74% by the end of the study. Nematodes are predatory eukaryotes and can cause floc destruction. Thus, for this study, the ideal floc diameter range was between 500 and 1000 µm, providing fast settling and a high abundance of nutrient removing bacteria.

6.1.4 Development of the hydraulic selector through computational fluid dynamics

CFD is often used in wastewater to model the settling of the AS blanket in the secondary clarifier. These models are often 2-D, steady-state, laminar models. While they are effective for their purpose, modeling the hydraulic selector requires 3-D, transient, multiphase, and turbulent conditions. Improving the hydraulic selector's ability to remove poorly settling floc in turbulent conditions would make adopting the technology

easier for wastewater facilities, which would require the removal of poor settling floc in plug-flow system. Results from this study show that the volume fraction of particles outside the hydraulic selector are determined by TKE and eddy viscosity conditions and not the hydraulic selector discharge rate. Also, the geometry of the selector may increase TKE conditions. By changing the external or internal geometry of the selector, the removal efficiency of poorly settling particles may be increase while preventing the removal of particles larger than 100 µm.

6.2 Future work

Currently, wastewater facilities use controls such as DO, SRT, and redox potential to ensure that the appropriate conditions are present to achieve their treatment objectives. As influent flows to municipal wastewater treatment plants increase, an additional control such as AS mean floc diameter will be important for maximizing AS settling velocity and abundance of nutrient removing bacteria. Technologies like the hydraulic selector allow facilities to determine their mean floc diameter and effectively waste poor settling AS. Moving forward, researchers must continue to investigate the minimum biomass required to be wasted through the hydraulic selector to achieve granulation. Lower biomasses wasted through the hydraulic selector reduces cost of operation while maximizing AS settleability. This dissertation provides insight on an ideal mean floc diameter for a system that maintains feast/famine conditions and a constant F:M ratio range between 0.1 and 0.2. Additional research must determine how to maintain this floc distribution so that new granulation is encouraged while floc greater than the desired mean floc diameter is removed. Controlling the floc diameter distribution in such a manner may require an additional selection and wasting process from the bottom of the BR.

Regardless of the selection process, a new waste stream will be generated and will require treatment. This stream will have a lower MLSS concentration compared to traditional AS wasting and cannot be recycled to beginning of the AS process. This stream will most likely require dewatering, a new technology such as the cloth media filter, which provides rapid solid/liquid separation, may provide an ideal treatment system. Additionally, effects of the dewatered stream on the anaerobic digestion process will need to be quantified to ensure that methane production is maintained or improved. This technology would also need to be compared to similar selection technologies such as hydrocyclone. A techno-economic assessment (TEA) evaluates the costs, benefits, risk, and uncertainties of a technology, this assessment would be useful in comparing both selection technologies. Both technologies can be incorporated into current wastewater infrastructure and result in the development of AGS. However, no study on the hydrocyclone has shown a correlation between hydrocyclone operating parameters and AS settling velocity. From the various studies conducted in this dissertation, a relationship between the hydraulic selector entrance velocity and the AS settling velocity has been developed. However, the selector has not been tested at a demonstration or full-scale facility. Thus, to complete a TEA of the hydraulic selector and hydrocyclone both systems will require further research. Lastly, to continue to improve the hydraulic selection's ability to remove poorly settling floc the CFD model must be validated with bench scale results and then be scaled to a full-size BR.

APPENDIX A

HYDRAULIC SELECTOR DESIGN CRITERIA

To determine the discharge rate and entrance area of the hydraulic selector area, the desired solid retention time (SRT) and targeted floc for removal must be determined. If the hydraulic selector is the only mechanism used to remove biomass from the bioreactor, then it is crucial that the selector remove enough biomass to achieve the appropriate SRT, for further details refer to chapter 3. The SRT for a bioreactor is dependent on bioreactor size, biomass concentration, and concentration and volume of biomass wasted. Various scenarios for required biomass removal for a desired SRT at different biomass concentrations is presented in Table 1. The calculation for Table 1 assumed a reactor volume of 28 L. SRT for a typical wastewater facility is kept as low as possible, between 7 and 14 days, but for facilities trying to grow granules an SRT between 10 and 21 days is preferred but the higher the SRT the higher the demand for oxygen and increases energy consumption at the WRRF. MLSS concentration is related to SRT and may vary between 1000 and 5000 mg/L.

Table A1. Mass of activated sludge removed by the hydraulic selector each day, dependent on the desired SRT and MLSS concentration of the activated sludge

Desired SRT (days)	MLSS Concentration (mg/L)								
	1000	1500	2000	2500	3000	3500	4000	4500	5000
	Solids Wasting (g/day)								
7	4	6	8	10	12	14	16	18	20
14	2	3	4	5	6	7	8	9	10
21	1.3	2.0	2.7	3.3	4.0	4.7	5.3	6.0	6.7
28	1	1.5	2	2.5	3	3.5	4	4.5	5

At a low MLSS concentration of 1000 mg/L and long SRT of 28 days only 1 g of biomass must be wasted, as the SRT is reduced the required biomass wasting increases to 4 g. As MLSS concentration increases so does the daily biomass wasting. This table assumes that only the hydraulic selector is the only mechanism for biomass wasting; however, pilot scale experiments have demonstrated that the hydraulic selector may operate at a reduced capacity, wasting only 25-50% of the total biomass, and still provide substantial benefits to the activated sludge settling characteristics. For this chapter, the hydraulic selector is the sole wasting mechanism, the design and operation of the selector must be able to achieve the minimum (1 g) and maximum (20 g) biomass wasting per day.

Mass of solids discharged by the selector is dependent on the outflow rate and MLSS concentration. Lower MLSS concentrations results in larger hydraulic selector discharge volumes, this is an important consideration when selecting and sizing the pump and motor size connected to the selector. Using a 28 L

bioreactor, a range of volumes displaced by the hydraulic selector per day based on selector discharge MLSS concentration are presented in Table 2. The range of volume varies between 4 and 20 L's, this corresponds to 15 to 4 % percent of the reactor volume.

Table A2. Volume of water displaced by the hydraulic selector each day

AS MLSS (mg/L)	Selector Discharge TSS (mg/L)	Biomass of Activated Sludge Discharged (g/day)				
		40	30	20	10	4
		Volume Discharged by Selector (L/day)				
5000	2500	16	12	8		
4000	2000		15	10		
3000	1500		20	13	7	
2000	1000			20	10	4
1000	500				20	8

While the discharge of biomass and displaced volumes are important to the operation of the selector the flowrate and quality of the sludge that is discharged is of higher importance. Floc with a diameter less than 50 μm is typically non-settable and remains in suspension, thus, floc between 50 and 100 μm are targeted for removal. This removal is dependent on entrance velocity of the hydraulic selector, a combination of selector outflow rate and selector geometry. While basic force calculations, shown in the materials and methods, provide estimates on the selector entrance area and discharge rate a CFD model will provide an in-depth evaluation of the flow-fields developed around the selector. The CFD simulation will also be able to compare various selector geometries based on the percentage of poor settling floc removed.